OkTC

OKLAHOMA TRANSPORTATION CENTER

ECONOMIC ENHANCEMENT THROUGH INFRASTRUCTURE STEWARDSHIP

WMA PAVEMENTS IN OKLAHOMA: MOISTURE DAMAGE AND PERFORMANCE ISSUES

ROUZBEH GHABCHI, PH.D. CANDIDATE
MUSHARRAF ZAMAN, PH.D., P.E.
RIFAT BULUT, PH.D.
MURAT KOC, M.SC.
DHARAMVEER SINGH, PH.D.

OTCREOS10.1-06-F

DISCLAIMER

The contents of this report reflect the views of the authors, who are responsible for the facts and accuracy of the information presented herein. This document is disseminated under the sponsorship of the Department of Transportation University Transportation Centers Program, in the interest of information exchange. The U.S. Government assumes no liability for the contents or use thereof.

TECHNICAL REPORT DOCUMENTATION PAGE

1. REPORT NO. OTCREOS10.1-06-F	2. GOVERNMENT ACCESSION NO.	3. RECIPIENTS CATALOG NO.	
4. TITLE AND SUBTITLE WMA Pavements in Oklahoma: Moisture Damage and Performance Issues		5. REPORT DATE August 6, 2013	
		6. PERFORMING ORGANIZATION CODE	
7. AUTHOR(S) Rouzbeh Ghabchi, Musharraf Zaman, Rifat Bulut, Murat Koc, and Dharamveer Singh		8. PERFORMING ORGANIZATION REPORT	
9. PERFORMING ORGANIZATION NAME AND ADDRESS Oklahoma State University, School of Civil & Environmental Engineering, 207 Engineering South, Stillwater, OK 74078 University of Oklahoma, College of Engineering, Norman, OK 73019		10. WORK UNIT NO.	
		11. CONTRACT OR GRANT NO. DTRT06-G-0016	
12. SPONSORING AGENCY NAME AND ADDRESS Oklahoma Transportation Center (Fiscal) 201 ATRC Stillwater, OK 74078 (Technical) 2601 Liberty Parkway, Suite 110 Midwest City, OK 73110		13. TYPE OF REPORT AND PERIOD COVERED Final January 2010- July 2013	
		14. SPONSORING AGENCY CODE	
15. SUPPLEMENTARY NOTES University Transportation Center			

16. ABSTRACT

This study explored the potential effects of using different Warm Mix Asphalt (WMA) technologies on the rut, fatigue and moisture-induced damage potential of WMA pavements. This task was pursued in two levels: (i) performance evaluation of WMA and control Hot Mix Asphalt (HMA) mixes in laboratory; and (ii) mechanistic evaluation of the moisture-induced damage potential of asphalt binders with different types of WMA additives and aggregates. For performance evaluation of asphalt mixes, a total of six Superpave mixes (three WMA plant mixes and three control HMA mixes produced in laboratory) were tested. WMA mixes consisted of one Advera® and one Evotherm® surface course mixes each and one Evotherm® base course mix. WMA mixes were collected from different projects in Texas. HMA control mixes corresponding to the collected WMAs were produced in the laboratory. The performance characteristics of mixes were evaluated by conducting Hamburg Wheel Tracking (HWT), retained indirect Tensile Strength Ratio (TSR) and Four-Point Bending Beam Fatigue (FTG) tests. Furthermore, in order to mechanistically evaluate the moisture-induced damage potential of different WMA additives combined with aggregates, Surface Free Energy (SFE) approach was applied. The SFE components of a PG 64-22 OK asphalt binder mixed with different percentages of Sasobit®, Advera®, Evotherm® and Permatac Plus® were measured using a Wilhelmy Pate (WP) and a Sessile Drop (SD) device. Moreover, the SFE components of a Dolese limestone and Snyder granite from Oklahoma were evaluated using a Universal Sorption Device (USD) and a SD device. The HWT test results showed that all of the tested WMA and HMA control mixes, except the Evotherm® mix with lime as anti-stripping agent, performed almost equally well against rutting and moisture-induced damage with no detectable stripping inflection point. The TSR test results provided no correlation between TSR values and the results from HWT test. However, indirect tensile strength values of mixes tested under dry condition in a TSR test were found to be well correlated with the inverse rutting rate obtained from a HWT test. The FTG test results revealed that all of the HMA control mixes showed a higher number of cycles to fatigue failure, compared to those of WMA mixes. The SFE test results showed that Sasobit® and Advera® do not significantly increase or decrease the moisture-induced damage potential of the asphalt binder, over different aggregates. However, use of Advera®-modified asphalt binder with basalt resulted in a measurable decrease in moisture-induced damage potential of the mix. Evotherm® was observed to have the maximum effect on the reduction of moisture-induced damage potential over different aggregates. Also it was observed that Perma-tac® Plus increased the resistance to the moisture-induced damage in almost all cases. Furthermore, through this study it was shown that the SD device, besides WP and USD, is capable of performing direct contact angle measurements on flat surfaces such as aggregate and asphalt binder. Findings of this study are expected to be useful to pavement professionals in understanding the moisture-induced damage mechanisms and designing WMA mixes.

17. KEY WORDS WMA, Moisture Damage, Surface Free Energy, USD, Wilhelmy Plate, Sessile Drop, Tensile strength	18. DISTRIBUTION STATEMENT No restrictions. This publication is available at www.oktc.org and from the NTIS.		
19. SECURITY CLASSIF. (OF THIS REPORT) Unclassified	20. SECURITY CLASSIF. (OF THIS PAGE) Unclassified	21. NO. OF PAGES 160 + covers	22. PRICE

SI (METRIC) CONVERSION FACTORS

Approximate Conversions to SI Units

Symbol	When you know	Multiply by	To Find	Symbol
LENGTH				
in	inches	25.40	millimeters	mm
ft	feet	0.3048	meters	m
yd	yards	0.9144	meters	m
mi	miles	1.609	kilometers	km
AREA				
in²	square inches	645.2	square millimeters	mm
ft²	square feet	0.0929	square meters	m²
yd²	square yards	0.8361	square meters	m²
ac	acres	0.4047	hectares	ha
mi²	square miles	2.590	square kilometers	km²
VOLUME				
fl oz	fluid ounces	29.57	milliliters	mL
gal	gallons	3.785	liters	L
ft³	cubic feet	0.0283	cubic meters	m³
yd³	cubic yards	0.7645	cubic meters	m³
MASS				
oz	ounces	28.35	grams	g
lb	pounds	0.4536	kilograms	kg
T	short tons (2000 lb)	0.907	megagrams	Mg
TEMPERATURE (exact)				
°F	degrees Fahrenheit	(°F-32)/1.8	degrees Celsius	°C
FORCE and PRESSURE or STRESS				
lbf	poundforce	4.448	Newtons	N
lbf/in²	poundforce per square inch	6.895	kilopascals	kPa

Approximate Conversions from SI Units

Symbol	When you know	Multiply by	To Find	Symbol
LENGTH				
mm	millimeters	0.0394	inches	in
m	meters	3.281	feet	ft
m	meters	1.094	yards	yd
km	kilometers	0.6214	miles	mi
AREA				
mm²	square millimeters	0.00155	square inches	in²
m²	square meters	10.764	square feet	ft²
m²	square meters	1.196	square yards	yd²
ha	hectares	2.471	acres	ac
km²	square kilometers	0.3861	square miles	mi²
VOLUME				
mL	milliliters	0.0338	fluid ounces	fl oz
L	liters	0.2642	gallons	gal
m³	cubic meters	35.315	cubic feet	ft³
m³	cubic meters	1.308	cubic yards	yd³
MASS				
g	grams	0.0353	ounces	oz
kg	kilograms	2.205	pounds	lb
Mg	megagrams	1.1023	short tons (2000 lb)	T
TEMPERATURE (exact)				
°C	degrees Celsius	9/5+32	degrees Fahrenheit	°F
FORCE and PRESSURE or STRESS				
N	Newtons	0.2248	poundforce	lbf
kPa	kilopascals	0.1450	poundforce per square inch	lbf/in²

ACKNOWLEDMENTS

WMA PAVEMENTS IN OKLAHOMA: MOISTURE DAMAGE AND PERFORMANCE ISSUES

Final Report
OTCREOS10.1-06
August 6, 2013

Prepared by:

Rouzbeh Ghabchi, Ph.D. Candidate[1]
Musharraf Zaman, Ph.D., P.E.[1]
Rifat Bulut, Ph.D.[2]
Murat Koc, M.Sc.[2]
Dharamveer Singh, Ph.D.[1]

[1]College of Engineering
The University of Oklahoma
202 W. Boyd, Street, CEC 106
Norman, OK 73019

[2]School of Civil and Environmental Engineering
Oklahoma State University
Stillwater, OK 74078

TABLE OF CONTENTS

LIST OF FIGURES

LIST OF TABLES

EXECUTIVE SUMMARY

This study explored the potential effects of using different Warm Mix Asphalt (WMA) technologies on the rut, fatigue and moisture-induced damage potential of WMA pavements. This task was pursued in two levels: (i) performance evaluation of WMA and control Hot Mix Asphalt (HMA) mixes in laboratory; and (ii) mechanistic evaluation of the moisture-induced damage potential of asphalt binders with different types of WMA additives and aggregates. For performance evaluation of asphalt mixes, a total of six Superpave mixes (three WMA plant mixes and three control HMA mixes produced in laboratory) were tested. WMA mixes consisted of one Advera® and one Evotherm® surface course mixes each and one Evotherm® base course mix. WMA mixes were collected from different projects in Texas. HMA control mixes corresponding to the collected WMAs were produced in the laboratory. The performance characteristics of mixes were evaluated by conducting Hamburg Wheel Tracking (HWT), retained indirect Tensile Strength Ratio (TSR) and Four-Point Bending Beam Fatigue (FTG) tests. Furthermore, in order to mechanistically evaluate the moisture-induced damage potential of different WMA additives combined with aggregates, Surface Free Energy (SFE) approach was applied. The SFE components of a PG 64-22 OK asphalt binder mixed with different percentages of Sasobit®, Advera®, Evotherm® and Permatac Plus® were measured using a Wilhelmy Pate (WP) and a Sessile Drop (SD) device. Moreover, the SFE components of a Dolese limestone and Snyder granite from Oklahoma were evaluated using a Universal Sorption Device (USD) and a SD device. The HWT test results showed that all of the tested WMA and HMA control mixes, except the Evotherm® mix with lime as anti-stripping agent, performed almost equally well against rutting and moisture-induced damage with no detectable stripping inflection point. The TSR test results provided no correlation between TSR values and the results from HWT test. However, indirect tensile strength values of mixes tested under dry condition in a TSR test were found to be well correlated with the inverse rutting rate obtained from a HWT test. The FTG test results revealed that all of the HMA control mixes showed a higher number of cycles to fatigue failure, compared to those of WMA mixes. The SFE test results showed that Sasobit® and Advera® do not significantly increase or decrease the moisture-induced damage potential of the asphalt binder, over different aggregates.

However, use of Advera®-modified asphalt binder with basalt resulted in a measurable decrease in moisture-induced damage potential of the mix. Evotherm® was observed to have the maximum effect on the reduction of moisture-induced damage potential over different aggregates. Also it was observed that Perma-tac® Plus increased the resistance to the moisture-induced damage in almost all cases. Furthermore, through this study it was shown that the SD device, besides WP and USD, is capable of performing direct contact angle measurements on flat surfaces such as aggregate and asphalt binder. Findings of this study are expected to be useful to pavement professionals in understanding the moisture-induced damage mechanisms and designing WMA mixes.

1

1.1   General

Over the past two decades, many transportation agencies, asphalt producers and pavement construction companies have taken major initiatives to implement green paving technologies (NAPA, 2011; NAPA, 2007). Saving energy during asphalt production is an important element of such initiatives. Many studies have been conducted in the United States and elsewhere around the world to find innovative ways to design and construct sustainable, environmental friendly and durable pavements. Consequently, the asphalt mix producers and paving contractors are trying to implement the new technologies in their material characterization, mix designs, construction, and maintenance of pavements. The new characterization and test methods are more rigorous, mechanistic and performance-based.

According to the National Asphalt Pavement Association (NAPA), the United States has more than 2.7 million miles of paved roads and 94% percent of the paved roads are surfaced with asphalt (U.S. Department of Transportation, 2008). The federal government invested $58 billion in transportation improvements through the core federal transportation improvement programs during the fiscal year 2011 (American Road & Transportation Builders Association, 2012).

In 2002, NAPA identified a new promising technology, Warm Mix Asphalt (WMA), which was originally developed in Europe, but quickly entered the U.S. market. WMA technologies allow a reduction in production and placement temperatures. The range of reduction in asphalt temperature may vary from 20° to 55°C, depending upon the type of technology. Lower production and construction temperatures lead to reduced energy costs and greenhouse gas emissions.

WMA technologies show significant promise for reduced energy consumption and emission associated with the production of conventional Hot Mix Asphalt (HMA). WMA technology is gaining rapid acceptance and many Departments of Transportations (DOTs) are engaged in evaluating the performance of WMA mixes and developing

permissive specifications that can allow the use of WMA technologies at the contractor's option. In fact, Asphalt Institute expects that in less than five years, 80% of all the mixes placed on the roads will be WMA. However, as a new technology, there are concerns both on the local and national levels. National concerns focus on durability and performance issues of WMA mixes overtime, particularly with respect to its ability to resist moisture-induced damage. Moisture-induced damage in asphalt pavements has been a major problem in many states across the U.S., including Oklahoma.

This research aimed to evaluate some of the national and local issues associated with the implementation of WMA technologies in Oklahoma. The main focus areas of this study are on evaluating moisture-induced damage potential, rutting potential and fatigue life of WMA pavements. Substantial efforts were made to evaluate the moisture-induced damage potential of WMA mixes. Specifically, implementation of recent advancements in fundamental understanding of the moisture-induced damage process was targeted. This was made possible by carefully considering the mechanisms that influence the bonding energy of interface between aggregate and asphalt binder.

During the course of this comprehensive and fundamental study, large amounts of data were produced and analyzed. Specifically, in this study, we were able to evaluate the durability and rutting potential, fatigue cracking and moisture-induced damage potential of WMA asphalt mixes compared to conventional HMA mixes. The experimental data generated in this study are expected to advance the strategic plan of Oklahoma Transportation Center (OkTC).

1.2   Problem Statement

As a new and emerging technology, there are concerns about the performance of WMA on the local, national and international levels. The national and international concerns focus on durability and performance issues of WMA mixes over time, particularly with respect to its ability to resist moisture-induced damage. Even for hot mix asphalt (HMA) pavements, moisture-induced damage has been a major problem in many states across the U.S., including Oklahoma. Some recent studies suggest that WMA mixes can lead to increased moisture-induced damage in pavements (Wasiuddin et al., 2007; WSDOT, 2008).

The performance of asphalt pavement is closely related to adhesive bonding, which is the interaction energy and strength between asphalt binder and aggregate (Curtis et al., 1991). A good adhesion bonding is essential to ensure good performance of asphalt mixes, such as resistance to moisture-induced damage and fatigue (Kanitpong and Bahia, 2005; Hefer et al., 2006; Masad et al., 2006; Lu and Harvey, 2008; Wasiuddin et al., 2008; Pinto et al., 2009).

The loss of strength and durability in asphalt mixtures due to the effects of moisture is referred as moisture-induced damage (Masad et al., 2006; Bhasin and Little, 2007; Lu and Harvey, 2008). Moisture weakens the surface bonds between the asphalt binder and aggregate (Cheng et al., 2002). It is therefore crucial to identify those binders and aggregates that can form mixes that are susceptible to moisture-induced damage.

The moisture-induced damege potential of a mix is generally evaluated using the retained indirect Tensile Strength Ratio (TSR), according to the AASHTO T283 specifications. It is also determined from the inflection point in Hamburg Wheel Tracking (HWT) tests according to OHD L-55 test method. Although useful indicators, neither of these tests directly addresses the failure mechanisms (namely, loss of adhesion bonding and cohesive bonding) that govern the moisture-induced damage in asphalt pavements. Recent studies show that surface free energy (SFE) characteristics of binders and aggregates can be used in a mechanics-based approach to quantify moisture-induced damage potential of asphalt mixes (Lytton et al., 2005; Hossain et al.,

3

2009). In order to define the best binder-aggregate pair in terms of moisture-induced damage and adhesive/cohesive bonding, surface free energy analysis can be used. The level of interface bonding is predictable when the wet adhesive bond strength (i.e., surface energy under wet condition) is compared with the dry adhesive bond strength (i.e., surface energy under dry condition) between the binder and aggregate (Lytton et al., 2005).

Other WMA mixture performance issues include a concern over increased rut depth and a possible increase in fatigue life (potential benefit), both associated with reduced oxidation of the binder due to reduced mix temperatures. On the local level, WMA technologies must either fit into the local DOT's specifications or the specifications must be modified before they can be successfully implemented.

Different WMA technologies introduced to the pavement industry utilize different physicochemical means to lower the shear resistance of the mix at production and placement temperatures, while maintaining or enhancing the pavement performance. However, some conflicting observations associated with the performance of WMA were reported by Kvasnak et al. (2009) and Button et al. (2007). Therefore, there is a need to develop an approval system and comprehensive specifications, both at the local and national levels.

1.3   Purpose

The main purpose of this study was to evaluate the moisture-induced damage potential of WMA asphalt mixes compared to their HMA counterparts. This evaluation includes the study of the micro scale interaction of the binder-aggregate systems using SFE approach. This research is expected to benefit Oklahoma DOT (ODOT) with the implementation of WMA technologies in Oklahoma.

1.4   Scope and Objectives

Although there is a wealth of information available in the literature on constructability, material properties and environmental effects of different WMA technologies, the available literature on the effect of WMA technologies on the QC/QA-

related properties is limited (Prowell and Hurley, 2007; Bistor, 2009; Hossain et al., 2009).

The specific objectives of this study are as follows:

1. To evaluate the moisture-induced damage potential of WMA mixes using both traditional and mechanistic-based approaches using available and innovative techniques.

2. To evaluate the rutting and fatigue behavior of WMA specimens.

This study is an effort to advance the fundamental understanding of the moisture-induced damage process by carefully considering the mechanisms that influence the bonding of interface between aggregate and asphalt binder.

The specific objectives of the study were pursued through two major laboratory activities: (i) performance tests conducted on asphalt mixes (ii) SFE Testing on the WMA-additive modified and neat asphalt binders and SFE tests on aggregates.

Laboratory testing on the WMA asphalt mixes include Hamburg Wheel Tracking (HWT), TSR, and four point bending beam fatigue test (FTG). WMA mixes include one type of surface course mix with Advera® additive, two types of surface and base course mix with Evotherm® additive. Also, control HMA mixes for each WMA were produced in the laboratory and tested. A total of six types of asphalt mixes were tested in this study.

SFE components of the of the aggregates and asphalt binders in this research study were evaluated using a Universal Sorption Device (USD) (SGA-100), a Sessile Drop (SD) device (FTA 1000 series from Firsttenangstroms), and a Wilhelmy Plate (WP) device (from CAHN). In this study, a new testing protocol for sample preparation and for using the Sessile Drop device was developed and is presented herein. A summary of the SFE tests during the course of this study is given as below.

- Two aggregates (Davis limestone and Snyder granite) and one asphalt binder (Muskogee, PG 64-22) from Oklahoma with and without WMA additives were tested.

- The results of SD and USD measurements were compared with each other. Also, these results were compared with those obtained from similar aggregates and other geological materials available in the literature.

- Similarly, the SD results on PG 64-22 asphalt binder were compared with the WP measurements on similar grade asphalt binders.

1.5   Organization of Report

This report consists of seven major chapters, with descriptive subsections in each chapter. A short description on the content of each chapter is given below.

Chapter One- Introduction: This chapter provides general information and problem statement about WMA and moisture-induced damage in asphalt pavement materials. The scope of the work and objectives are also discussed in this chapter.

Chapter Two- Background: This chapter discusses and reviews the available open literature about WMA and its moisture-induced damage, rutting and fatigue performance. Also, recent advances on the use of mechanistic methods for assessment of moisture-induced damage are discussed in this chapter. A brief background on contact angle and surface energy measurement techniques and comparison of their advantages/disadvantages are given and discussed in this chapter. In particular, the following items are discussed:

1. Sessile Drop (SD) Device,

2. Universal Sorption Device (USD),

3. Wilhelmy Plate (WP) Method,

4. Column Wicking and Thin Layer Wicking Methods, and

5. Heat of Immersion Method.

The theoretical background of surface energy, adhesion and cohesion concepts, energy ratio, wettability, and Good–Van Oss–Chaudhury (GVOC) approach in the calculation of surface free energy components are discussed in chapter two.

Chapter Three- Materials and Methods: This chapter covers the sources of materials and their collection details. Also, details of methodologies used for testing asphalt mixes including rutting, fatigue and moisture-induced damage potential are discussed in this chapter. Furthermore, this chapter covers the details of the SFE method used for mechanistic evaluation of moisture-induced damage for aggregate-asphalt binder systems. The sample preparation and USD and WP testing and protocols developed for SD for direct measurements of contact angles on aggregate and asphalt binder are discussed in this chapter.

Chapter Four- Results and Discussions: Test results from the Hamburg Wheel Tracking (HWT), four point bending beam fatigue (FTG), and retained indirect Tensile Strength Ratio (TSR) tests are presented in this section. Moreover, the surface energy test results on the aggregates using the Sessile Drop (SD) and the Universal Sorption Device (USD) as well as test results on the asphalt binder using dynamic Wilhelmy Plate (WP) and Sessile Drop (SD) methods are presented in this chapter. Finally, discussions of the test results on asphalt mixes, aggregates and asphalt binders are presented in this chapter.

Chapter Five- Conclusions and Recommendations: Conclusions of this study, based on the analyses and discussions of the test results are presented in this chapter. Also, recommendations are provided for future research and the limitations of the testing equipment and methods are outlined in this chapter.

Chapter Six- Implementation and Technology Transfer: This chapter presents a summary of the cooperation with industry, publications and presentations as a result of this study.

Chapter Six- References: This chapter presents a list of the published materials and other sources of literature cited in this report.

Appendices: Supplemental information and materials are presented in Appendices.

2.1   General

There is a wealth of available literature on the Warm Mix Asphalt (WMA) technologies. Many studies have been conducted nationwide with a focus on moisture-induced damage and performance issues related to WMA. The literature review for the present study has focused on the WMA technologies used in the asphalt industry, the concerns pertaining to performance-measures of WMA, specifically rutting, moisture-induced damage potential, and fatigue life. Furthermore, recent advances in the mechanistic evaluation of moisture-induced damage of WMA using the Surface Free Energy (SFE) approach are included in the literature review.

2.2   Warm Mix Asphalt Technology

Hot mix asphalt (HMA) is typically produced at temperatures ranging from 280°F to 325°F. It has been necessary to use these elevated temperatures to dry the aggregates, coat them with the asphalt binder, achieve the desired workability, and provide sufficient time to compact the HMA in the field. WMA technologies consist of different materials (i.e., chemical additives) and apply various production methods which allow a reduction in asphalt mix production and placement temperatures. This temperature reduction is achieved by reducing the viscosity of the asphalt binder using different WMA technologies. Hence, the aggregate coating by asphalt binder can occur at lower temperatures. Based on type of the WMA technology, a reduction of 35° to 100°F in asphalt mix production temperature can be achieved as reported by Prowell et al. (2007). Low production and compaction temperatures result in a significant cut in fuel consumption and emissions leading to several economical and environmental benefits. Furthermore, using WMA in place of HMA will result in reduced plant odor, reduced smoke, and improved working conditions at the paving site. Also, the WMA technologies provide the ability to haul the mix longer distances, while maintaining the mixture workability during construction including placement and compaction. Due to its lower viscosity at reduced temperatures, the mix can be compacted with less effort and provide the possibility of incorporating higher percentages of RAP at lower temperatures

(D'Angelo et al., 2008). The WMA technology is currently being used in all types of asphalt pavements, including dense-graded, stone matrix, porous, and mastic asphalt (D'Angelo et al., 2008).

WMA is generally classified based on the technologies and methods used for its production. In general, WMA is produced in two major technology categories: (i) the technologies that use additives such as water vapor releasing admixtures like zeolites, organic additives or waxes and surfactants, and (ii) the process driven technologies which tend to be foaming processes including Double Barrel Green plants, Low Energy Asphalt and WMA-Foam.

This study has focused on the WMA technologies classified in the first category. For this purpose, one type of additive from each group, namely Advera® (water releasing zeolite), Sasobit® (organic additives or wax) and Evotherm® (surfactant) was selected for this study, as discussed below.

2.3 Rutting, Moisture-Induced Damage Potential and Fatigue Life of WMA

Although there is wealth of information available in the literature from different studies that have focused on material, constructability and environmental effects of various warm mix asphalt (WMA) technologies, the available literature on the effects of WMA technologies on asphalt mix properties is rather limited (Bistor, 2009; Hossain et al., 2009; Prowell and Hurley, 2007). An overview of some of these studies is presented herein.

In a study by Goh and You (2012), the rutting potential and fatigue life of Sasobit® and Advera® WMA mixes were evaluated. The WMA mixes were produced at different dosages and temperatures. Dynamic modulus and four-point bending beam fatigue tests were used to evaluate the rutting and fatigue characteristics of selected mixes. It was found that dynamic modulus increases with an increase in the compaction effort. Based on the four-point bending beam fatigue test results it was concluded that WMA's fatigue life in most cases were similar to (or in some cases higher than) those of the control HMA.

Bonaquist (2010) reported that, with the exception of Sasobit®, the mixes with the WMA technologies perform poorly as compared to the performance of the equivalent HMA mixes relative to rutting. Also, it was concluded that WMA and the equivalent HMA mixes can have similar TSR values using the AASHTO T 283 test method. However, both dry and conditioned indirect tensile strengths are lower for the WMA mixes as compared to the equivalent HMA mixes.

Hurley et al. (2010) evaluated two types of WMA mixtures produced using Sasobit® and Evotherm® in a field project located in Milwaukee, Wisconsin. Performance of WMA and conventional HMA test sections was compared after these sections were subjected to four months of traffic. Specifically, field performance was compared in terms of volumetric properties of the mixes, rutting susceptibility, resistance to moisture-induced damage, and dynamic modulus. It was reported that the WMA mixes with Sasobit® and control HMA mixes exhibited very similar performance in laboratory testing. Comparatively, Evotherm® mixes resulted in higher rut depths, lower tensile strengths, and lower moduli than the control HMA. Field performance of all three types of test sections, constructed using Sasobit®, Evotherm® and control HMA were comparable, and no major differences were noticed.

In a recent study, Xiao et al. (2010) conducted laboratory tests to compare rutting performance of five different types of WMA mixes containing moist aggregates. They used two aggregate moisture contents of 0 and 0.5 percent, two lime contents of 1 and 2 percent, three WMA additives, namely Aspha-Min®, Sasobit® and Evotherm®, and three aggregate sources. It was concluded that the WMA mixes with Sasobit® additive exhibit the best rutting resistance. Comparatively, the WMA mixes with Aspha-Min® and Evotherm® additives generally showed a similar rutting resistance as compared to the control HMA mixes.

In a laboratory study, Kvasnak et al. (2009) evaluated the moisture-induced damage potential of both laboratory and plant produced WMA and HMA mixes. A total of three properties namely, TSR, absorbed energy ratio and stripping inflection point were used to assess the moisture-induced damage potential of the mixes. The results indicated that the laboratory produced WMA was more prone to moisture-induced

damage than the plant produced mix. Also, it was observed that WMA specimens are more prone to moisture-induced damage than those of the HMA. Most of the WMA samples, however, passed the resistance to moisture-induced damage criteria, namely TSR, absorbed energy ratio, and stripping inflection point.

A combined field and laboratory study was conducted by Prowell et al. (2007) to evaluate the performance of a WMA mix containing Evotherm®. For this purpose, accelerated test track at the National Center for Asphalt Technology (NCAT) and laboratory rutting-susceptibility tests were conducted using an Asphalt Pavement Analyzer (APA). It was observed that field densities of WMA surface layers were equal or better than those of HMA layers. TSR tests revealed an increase in moisture-induced damage potential of WMA compared to HMA mixes. However, field WMA and HMA sections showed excellent rutting performance. The APA rutting tests showed similar performance for both mixes.

In a similar combined field and laboratory study by Button et al. (2007), a test section was constructed using an Evotherm® mix. Hamburg Wheel Tracking (HWT) tests were conducted on the cores extracted from the WMA pavement section after one month from the end of the construction. It was observed that all of the WMA cores failed the HWT test requirements. However, the control HMA samples generally passed the HWT test requirements.

In a laboratory study, Hurley and Prowel (2006) concluded that stiffness, as measured by resilient modulus, of WMA mixes containing Evotherm® does not show any significant difference compared to the control HMA mixes. In an earlier laboratory study by Hurley and Prowell (2005), the performance of the Sasobit®, Sasoflex® and Aspha-min® additives was evaluated. It was found that the use of WMA additives generally improves the rheological properties of modified binders, but the performance and moisture-induced damage potential tests on the WMA mixes did not produce any consistent results. The APA rut tests did not exhibit any significant increase in the rutting potential of the WMA mixes. However, two other performance tests, namely HWT and TSR, showed an increase in moisture-induced damage potential.

11

The National Asphalt Pavement Association (NAPA), in cooperation with the Federal Highway Administration (FHWA), investigated the feasibility of using WMA technologies in the U.S. Three different WMA technologies namely, Evotherm®, Sasobit® and Aspha-Min® were studied. The findings of this study, summarized by Hurley and Prowell (2006), were published in three different reports that are available on their website. It was found that the use of aforementioned WMA technologies lowers the measured air voids volume in gyratory compactor. However, no significant differences between the resilient modulus of the WMA and control HMA mixes were reported. Furthermore, the study by Hurley and Prowell (2006) showed that Evotherm®, Sasobit® and Aspha-Min® did not increase the rutting potential of the asphalt mixes. However, reduced mixing and compaction temperatures resulted in a higher rutting potential. This was attributed to less asphalt binder aging resulting from lower mixing temperatures. Hurley and Prowell (2006) also reported a higher moisture-induced damage potential in WMA mixes from partial drying of the aggregate at reduced mixing temperatures. It was stated that the entrapped water in the aggregate was the source for the increase in the moisture-induced damage potential.

The specific advantages and disadvantages of WMA are dependent on the specific WMA technologies and processes considered. Therefore, it may be somewhat misleading to assemble all the WMA processes into one group and elucidate their features that are superior or inferior to HMA. The extent of these potential benefits and how to optimize them needs to be studied in a strategically coordinated research program at national and international levels. In the U.S., several state DOTs, NCHRP, NCAT, and other agencies have initiated studies of WMA, but these studies do not specifically address implementation aspects of WMA technologies pertaining to Oklahoma.

The TSR testing method lacks the mechanics-based component to quantify the moisture-induced damage potential of asphalt mixes. It is evident from the literature that TSR tests alone cannot predict the moisture-induced damage potential of asphalt mixes. Therefore, the surface free energy (SFE) approach, which gives a mechanistic understanding of moisture-induced damage, has been applied recently to study adhesion and cohesion mechanisms of HMA and WMA mixes (Ghabchi et al., 2013a;

Ghabchi et al., 2013b; Arabani et al., 2012; Kanitpong et al., 2012; Hossain et al., 2011; Kvasnak et al., 2009; Xiao et al., 2009; Wasiuddin et al., 2008; Bhasin and Little, 2007; Bhasin et al., 2007 and 2006; Kim et al., 2004; Cheng et al., 2002).

Promising results have been reported in the literature about the application of SFE approach to evaluate moisture-induced damage potential of asphalt mixes. For example, Wasiuddin et al. (2008), using the SFE method, observed that Sasobit[®] increases the wettability of the aggregates by asphalt binder and reduces the adhesion between aggregates and asphalt binder. Similarly, Bhasin et al. (2006 and 2007) suggested different applications of the SFE approach including work of adhesion, work of debonding, work of cohesion, and specific surface area of aggregates to describe the moisture-induced damage potential of an asphalt binder-aggregate system. They used fatigue and resilient modulus test results in wet and dry conditions as a measure for describing the moisture-induced damage potential, and developed statistically significant correlations between the abovementioned energy parameters and moisture-induced damage potential indices of the mix. In another study, Cheng et al. (2002) utilized the SFE approach to calculate the work of adhesion and free energy of cohesion for different asphalt binders and aggregates with and without the presence of water. Their results were consistent with those obtained from the accelerated moisture-induced damage tests on mixes. In a recent study, Arabani et al. (2012) reported a significant correlation between moisture-induced damage potential of WMA mixes based on SFE and ratio of conditioned to unconditioned dynamic modulus of asphalt mixes. Similarly, Kim et al. (2004) used the SFE approach and dynamic mechanical analysis (DMA) test to characterize the fracture properties of asphalt binders and mastic, and reported that both methods showed consistent results. According to these studies, it is evident that the SFE approach can be used as a reliable mechanistic tool to assess the moisture-induced damage potential of HMA and WMA mixes.

Studies involving moisture-induced damage potential of Evotherm[®] and Advera[®] WMA mixes based on the surface mechanics using the SFE approach are limited. In addition, the capability of the current practice of the moisture-induced damage assessment of asphalt mixes, like TSR testing according to AASHTO T283 (AASHTO, 2010) and its comparison with the SFE-based methods, has not been studied in detail.

The present study was undertaken to evaluate the effect of three different WMA-additives (i.e., Sasobit®, Advera® and Evotherm®) on the wettability and moisture-induced damage potential using the SFE method. For this purpose, the wettability, the work of adhesion and the work of debonding of two types of aggregates and a neat PG 64-22 asphalt binder, and the same binder modified with different percentages of WMA additives were evaluated. In addition, TSR tests on control HMA and WMA mixes produced with the PG 64-22 asphalt binder modified by Advera® and Evotherm® were conducted and the results were compared with the SFE parameters.

2.4 Surface Free Energy and Its Components

2.4.1 Surface Energy Concept

The molecules in the bulk of a solid material are surrounded by the same type of molecules and thus have force balance. However, if the solid material is cut, the molecules on the surface become unbalanced and therefore have a certain amount of excess energy compared with the molecules in the bulk of the material. The surface energy may, therefore, be defined as the excess energy at the surface of a material compared to the energy in the bulk material.

As first described by Thomas Young (1805), it is the interaction between the forces of cohesion and the forces of adhesion which determines whether wetting (the spreading of a liquid over a solid surface) will occur or not. If complete wetting does not occur, then a bead of liquid will form with a contact angle which is a function of the surface energies of the system.

Surface energy is most commonly quantified using a contact angle goniometer (Shang et al., 2008; van Oss, 2002; Giese and van Oss, 2002). In this research project, a FTA 1000B contact angle goniometer was used as a Sessile Drop (SD) device to measure the contact angles on the surfaces of aggregates and asphalt binders. Detailed information about the FTA 1000B goniometer and the testing protocol is given in following sections.

The theory of surface free energy has been developed in industrial surface science and chemical engineering, and is used reliably in many areas of engineering

disciplines, such as mining, pharmaceutical, petroleum, coating, painting, and printing industries. Recent studies show that surface free energy (SFE) characteristics of binders and aggregates can be used in a mechanics-based approach to quantify moisture-induced damage potential of asphalt mixes (Lytton et al., 2005; Wasiuddin et al., 2008).

For a liquid, the surface tension (force per unit length) and the surface energy density are identical. Water has a surface energy density of 0.072 J/m^2 and a surface tension of 0.072 N/m. As for solids, surface tension is typically measured in dynes/cm (i.e., the force in dynes required to break a film of length 1 cm). It can also be stated as surface energy in ergs per square centimeter.

2.4.1.1 Interfacial Lifshitz-van der Waals interactions

The Gibbs free energy of cohesion (ΔG^c) of a liquid is the formation of a cohesive area of the union of two bodies of the same material under the vacuum condition (Good, 1966).

$$\Delta G^c = -2\gamma^{Total} \tag{2.1}$$

Equation 2.1 is also valid for solids where, ΔG^c is the free energy of the solid to interact with liquids and γ^{Total} is the total surface energy of the solid material (Giese, 1996). Fowkes (1964) stated that the surface free energy of materials could be considered to be a sum of components resulting from each class of intermolecular interaction.

Using the Lifshitz approach for van der Waals interactions in condensed media, Chaudhury (1984) showed that the dispersion, induction and dipole contributions to the Lifshitz-van der Waals (or apolar) component of the surface tension, γ^{LW}, are additive (van Oss, 2002).

In colloid and surface science, the interfacial tension (γ_{ij}) between two different materials i and j is one of the most important parameters since it is directly related to a

quantitative expression for the free energy of interparticle or intermolecular interactions in condensed phase systems (Girifalco and Good, 1957). However, the interfacial tension between a solid and a liquid material and between two solid materials is not feasible to determine directly (Girifalco and Good, 1957). Hence, the interfacial tension ($γ_{ij}$) between these materials must be determined using the surface tensions of each material individually ($γ_i$ and $γ_j$).

According to the experimental works of Girifalco and Good (1957) and Fowkes (1964), if only dispersion interaction forces are available between two condensed phase materials, e.g., a solid and a liquid, the interfacial tension between them ($γ_{ij}^{LW}$) is given by the following equation:

$$\gamma_{ij}^{LW} = \left(\sqrt{\gamma_i^{LW}} + \sqrt{\gamma_j^{LW}} \right)^2 \qquad (2.2)$$

Recalling Equation 2.1, the apolar component of the free energy of cohesion of material i, is given by:

$$\Delta G_i^{cLW} = -2\gamma_i^{LW} \qquad (2.3)$$

The free energy of interaction between materials i and j in vacuum is related to the surface tensions of these materials by the Dupré equation (Giese and van Oss, 2002):

$$\Delta G_{ij}^{LW} = \gamma_{ij}^{LW} - \gamma_i^{LW} - \gamma_j^{LW} \qquad (2.4)$$

Substituting Equation 2.2 into Equation 2.4, the following equation is obtained:

$$\Delta G_{ij}^{LW} = -2 \ \overline{\gamma_i^{LW}\gamma_j^{LW}} \tag{2.5}$$

This equation states that the atoms at an interface are pulled by those in the neighboring phase. Since the Lifshitz-van der Waals forces are always available at the surface, Equation 2.5 also suggests that the energy of interaction is negative, i.e., the interaction energy between two purely polar condensed phases is always attractive (Lobato, 2004).

2.4.1.2   Polar or Lewis acid-base interactions

Chaudhury (1984) showed that the dispersion, induction and dipole force components of the surface tension are simply additive, and should be treated as a single entity as the LW interactions. After this development, it became possible to examine the polar (Lewis acid-base) properties of surfaces separate from the electrodynamic (Lifshitz van der Waals) apolar properties. Moreover, the polar concept has been extended to include all electron donating and electron accepting phenomena, as encompassed in the more general acid-base framework of Lewis (van Oss et al. 1988). To emphasize the (Lewis) acid-base character of the pair interactions, the designation AB has been used.

Since the polar and apolar components of the surface tension are additive, we can write (van Oss et al., 1988):

$$\Delta G_i = \Delta G_i^{LW} + \Delta G_i^{AB} \tag{2.6}$$

where ΔG_i^{LW} is the free energy change due to Lifshitz-van der Waals interaction, and ΔG_i^{AB} is the same due to acid-base interactions. From Equation (2.1),

$$\gamma_i^{Total} = \gamma_i^{LW} + \gamma_i^{AB} \tag{2.7}$$

17

where, γ_i^{LW} and γ_i^{AB} refer to the apolar (Lifshitz-van der Waals) and polar (acid-base) components of surface tension of material i, respectively.

Fowkes (1987) demonstrated the presence and importance of acid-base interactions between two interacting surfaces. He determined the values of acid-base (W_{ij}^{AB}) and Lifshitz-van der Waals (W_{ij}^{LW}) components of work of adhesion for various acidic and basic liquids on polymer surfaces as a function of acidity or basicity of polymer. Fowkes (1987) showed that the contribution of acid-base (or polar) component to the work of adhesion (W_{ij}^{a}) is strictly dependent on the acidity or basicity of the solid (polymer) of interest.

Based on Fowkes's acid-base interaction approach, van Oss and co-workers (1987) suggested that electron-acceptor (Lewis acid) and electron-donor (Lewis base) interactions are essentially asymmetrical meaning that of a given polar substance i the electron-acceptor and the electron-donor parameters are usually quite different hence they must be described by two distinct parameters. For the AB interactions, the free energy of interaction between two materials, i and j is defined as:

$$\Delta G_{ij}^{AB} = -2\left(\sqrt{\gamma_i^+ \gamma_j^-} + \sqrt{\gamma_i^- \gamma_j^+}\right)$$
(2.8)

where the electron donor parameter is designated as γ^- (basic component) and the electron acceptor parameter is designated as γ^+ (acidic component). The polar (AB) free energy of cohesion of material is then defined as:

$$\Delta G_i^{AB} = -4\sqrt{\gamma_i^+ \gamma_i^-}$$
(2.9)

From Equation 2.1, the polar component of the surface tension of material i is then defined as:

$$\gamma_i^{AB} = 2 \; \overline{\gamma_i^+ \gamma_i^-} \tag{2.10}$$

From Dupré equation (2.4), which is applicable to any type of interaction, the following equation can be defined (van Oss, 2002):

$$\Delta G_{ij}^{AB} = \gamma_{ij}^{AB} - \gamma_i^{AB} - \gamma_j^{AB} \tag{2.11}$$

Hence, the interfacial tension, γ_{ij}^{AB}, between substances i and j can be expressed as follows:

$$\gamma_{ij}^{AB} = \Delta G_{ij}^{AB} + \gamma_i^{AB} + \gamma_j^{AB} \tag{2.12}$$

Substituting the value for ΔG_{ij}^{AB} from Equation 2.8 and the values of γ_i^{AB} and γ_j^{AB} from Equation 2.10, gives:

$$\gamma_{ij}^{AB} = 2 \; \overline{\gamma_i^- \gamma_i^+} + \overline{\gamma_j^- \gamma_j^+} - \overline{\gamma_i^- \gamma_j^+} - \overline{\gamma_i^+ \gamma_j^-} \tag{2.13}$$

This can also be written as follows:

$$\gamma_{ij}^{AB} = 2 \; \overline{\gamma_i^+} - \overline{\gamma_j^+} \quad \overline{\gamma_i^-} - \overline{\gamma_j^-} \tag{2.14}$$

Equation 2.14 shows that γ_{ij}^{AB} is not restricted to positive values or zero, as is the case for γ_{ij}^{LW}. Rather, γ_{ij}^{AB} will be negative when either (van Oss, 1994):

$$\gamma_i^+ > \gamma_j^+ \qquad \text{and } \gamma_i^- < \gamma_j^- \tag{2.15}$$

or

$$\gamma_i^+ < \gamma_j^+ \qquad \text{and } \gamma_i^- > \gamma_j^- \tag{2.16}$$

The surface tension components approach by Fowkes (1963) can be applied to interfacial tensions as follows:

$$\gamma_{ij} = \gamma_{ij}^{LW} + \gamma_{ij}^{AB} \tag{2.17}$$

Therefore, since the AB and LW components of the interfacial tension are additive, the total expression for the interfacial tension between two condensed phases can be rewritten as:

$$\gamma_{ij} = \gamma_i^{Total} + \gamma_j^{Total} - 2\sqrt{\gamma_i^{LW}\gamma_j^{LW}} - 2\sqrt{\gamma_i^+\gamma_j^-} - 2\sqrt{\gamma_i^-\gamma_j^+} \tag{2.18}$$

2.4.1.3   The Young's Equation

Thomas Young, in 1805, described the equilibrium (or the interaction energy) between a liquid drop and a solid material in terms of their individual surface forces (or energy) and the interaction forces between them as given in Equation 2.19 (van Oss, 1994) and shown in Figure 2.1. Contact angle (θ) measurement, as described by Young, remains at present the most accurate method for determining the interaction energy (or the work of adhesion) between a liquid (L) and a solid (S) (van Oss, 2002):

$$\gamma_L cos\theta = \gamma_S - \gamma_{SL} \tag{2.19}$$

where γ_S is the surface energy of the solid; γ_L is the surface energy (or surface tension) of the liquid; and γ_{SL} is the interfacial tension (or energy) between the liquid and the solid.

The derivation of the Young's equation assumes that the solid surface is smooth, rigid and homogeneous. Also, it should not react both chemically and physically with the liquid that will be used for contact angle measurements.

In Equation 2.19, γ_L and $cos\theta$ are known and γ_S and γ_{SL} are the unknown parameters. Using two different liquids gives rise to two equations with three unknowns. Thus, Equation 2.19, in the form given above, is not practically usable. However, Dupré equation along with Equation 2.19 can be used to determine contact angles (van Oss, 2002). Dupré equation represents the free energy of interaction between a solid and a liquid (Fowkes, 1963):

$$\Delta G_{SL} = \gamma_{SL} - \gamma_S - \gamma_L \tag{2.20}$$

where, ΔG_{SL} represents the free energy of interaction between the solid and the liquid. Combining Equation 2.19 and Equation 2.20 results in the Young-Dupré equation (Chaudhury, 1984), we get the following equation:

$$1 + cos\theta \ \gamma_L = -\Delta G_{SL} \tag{2.21}$$

The total interaction energy consists of Lifshitz-van der Waals and Lewis acid-base interaction components (van Oss et al., 1987). And can be expressed as:

$$\Delta G_{SL} = \Delta G_{SL}^{LW} + \Delta G_{SL}^{AB} \tag{2.22}$$

In terms of individual surface energy components, Equation 2.22 takes the following form (van Oss, 2002):

$$\Delta G_{SL} = -2 \left[\sqrt{\gamma_S^{LW} \gamma_L^{LW}} + \sqrt{\gamma_S^+ \gamma_L^-} + \sqrt{\gamma_S^- \gamma_L^+} \right] \qquad (2.23)$$

where, γ_L^{LW} is the Lifshitz-van der Waals component of liquid; γ_S^{LW} is the Lifshitz-van der Waals component of solid; γ_L^+ is the Lewis acid component of liquid; γ_S^+ is the Lewis acid component of solid; γ_L^- is the Lewis base component of liquid; and γ_S^- is the Lewis base component of solid. The combination of Equation 2.21 and Equation 2.23 gives the complete Young-Dupré equation that is widely used in determining the surface energy components of solid materials using contact angle measurements (van Oss, 2002). It can be expressed as follows:

$$(1 + cos\theta) \, \gamma_L = 2 \left[\sqrt{\gamma_S^{LW} \gamma_L^{LW}} + \sqrt{\gamma_S^+ \gamma_L^-} + \sqrt{\gamma_S^- \gamma_L^+} \right] \qquad (2.24)$$

Equation 2.24 contains three unknowns (i.e., γ_S^{LW}, γ_S^+, and γ_S^-). In order to calculate the SFE of a sample (aggregate or binder), it is necessary to measure contact angles with three different liquid probes. However, selection of the three probe liquids is crucial. Van Oss (2002) strongly recommends that two of the probe liquids must be polar and one of them must be apolar. It is stated that two polar liquids must be significantly different with regard to their polarities. The calculated surface energy components will vary significantly with minor changes in contact angle measurements if the appropriate combination of the liquid probes is not selected (van Oss, 2002; Lytton et al., 2005; Bhasin, 2006). Based on the guidelines provided by van Oss (2002), diiodomethane (DIM), n-Hexane and Glycerin were selected as the apolar liquids, while ethylene glycol, methyl propyl ketone (MPK), and water were selected as polar liquids in the present study.

2.4.2 Adhesion and Cohesion

Adhesion and cohesion are two main components that affect surface tension. Molecules in liquid state experience strong intermolecular attractive forces. When those forces are between the same molecules, they are referred to as cohesive forces (i.e., molecules of a water droplet are held together by cohesive forces). Cohesive forces at the surface constitute surface tension. When the attractive forces are between different molecules, they are said to be adhesive forces (Adamson and Gast, 1997). The adhesive forces between water molecules and the walls of a glass tube are stronger than the cohesive forces leading to an upward turning meniscus at the walls of the vessel and contribute to capillary action.

The cohesive forces between liquid molecules are responsible for the phenomenon known as surface tension. The molecules at the liquid surface are in a different state of energy equilibrium than the molecules below the surface. This condition forms a surface "film" which makes it more difficult to move an object through the surface than to move it when it is completely submersed (Petrucci et al., 2007).

The cohesive forces between molecules down below a liquid surface are shared by all neighboring atoms. Those on the surface have no neighboring atoms above and exhibit stronger attractive forces upon their nearest neighbors on the surface. This enhancement of the intermolecular attractive forces at the surface is called surface tension (Figure 2.1) (Petrucci et al., 2007).
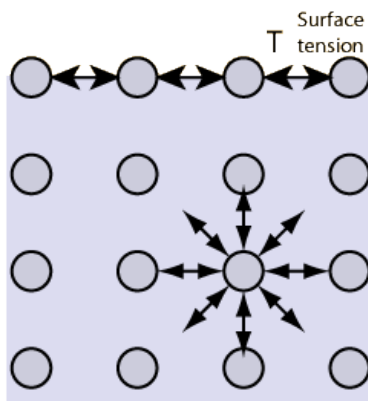
Figure 2.1 An Illustration of the Surface Tension (source: http://www.phy-astr.gsu.edu)

Adhesion is the tendency of liquid molecules to create an attraction to a different substance (Figure 2.2). However, cohesion causes the liquid drop to create the minimum possible surface area which is a sphere under the influence of the gravitational force (Gugliotti, 2004). This is the lowest energy state for a liquid drop (Adamson and Gast, 1997; Gugliotti, 2004). On the other hand, adhesion causes the drop to adhere to other substances.
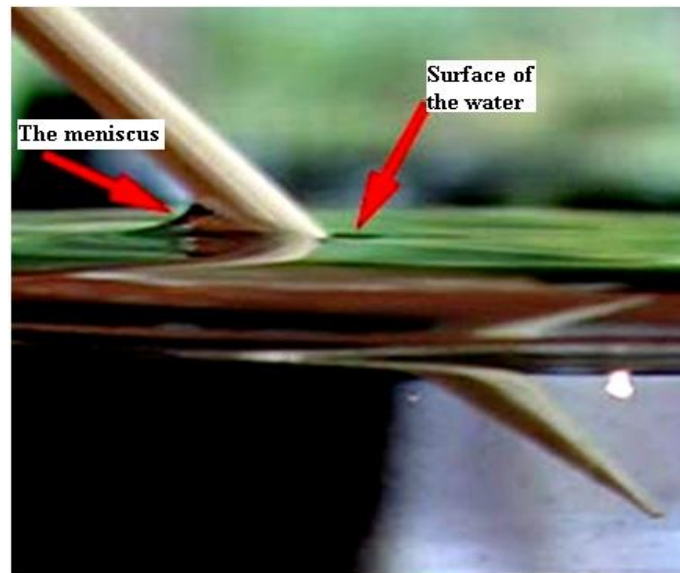
Figure 2.2 Adhesion between Water and Wood (source: http://www.phy-astr.gsu.edu)

2.4.2.1 Work of Adhesion and Cohesion

The most common failure types in asphalt pavements are fatigue cracking and rutting. Since the aggregates are a lot stronger than the asphalt binder, the fatigue cracks usually occur at two regions, namely; aggregate-asphalt interface or within asphalt binder. The interfacial force that holds two different types of molecules together is the force of adhesion. On the other hand, the strength of cohesion keeps the same types of molecules together. In other words, a strong adhesion between aggregate-asphalt interface and a strong cohesion within asphalt binder are very important in terms of fatigue cracking.

According to the principles of thermodynamics, the changes in the surface free energies (SFE) of adhesion and cohesion are related to the bond strength in asphalt-aggregate interface or within asphalt binder itself, respectively.

Hence, it is essential to determine the SFE of aggregates and asphalt binder in order to calculate the work of adhesion and cohesion. By knowing the adhesion/cohesion characteristics of an asphalt mix, water susceptibility, healing, and fatigue cracking properties of asphalt materials can be evaluated (Cheng, 2002).

2.4.2.2   Cohesion of Asphalt Binder

The Gibbs free energy of cohesion (ΔG^c) is the formation of a cohesive area of the union of two bodies of the same material under the vacuum condition (Good and van Oss, 1991).

The Gibbs free energy of cohesion has two components, the Liftshitz-van der Waals component (ΔG_i^{cLW}) and Acid-Base component (ΔG_i^{cAB}).

$$\Delta G^c = -2\gamma^{Total} \tag{2.25}$$

$$\gamma^{Total} = \gamma^{LW} + \gamma^{AB} \tag{2.26}$$

$$\Delta G^c = -2\gamma^{Total} = -2(\gamma^{LW} + 2\ \overline{\gamma^+\gamma^-}) \tag{2.27}$$

If the value of the free energy of cohesion or adhesion is positive, it means that the two phases of the material tend to bind together; and the lower magnitude of surface energy (adhesion or cohesion) dictates the likely mode of fracture.

2.4.2.3   Adhesion of Asphalt-Aggregate Mixture under Dry Condition

The Gibbs free energy of adhesion without the presence of water corresponds to the creation of a unit crack area at the interface between two dissimilar bodies in a vacuum condition.

The Gibbs free energy of adhesion in dry condition is given by Equation 2.4, where, γ_{ij} is the interfacial SFE between i and j. For instance, asphalt binder is represented by subscript i, and aggregate is designated by j, in the following equations:

$$\Delta G_{ij}^a = -\gamma_i - \gamma_j + \gamma_{ij} \tag{2.28}$$

$$\gamma_{ij} = \gamma_{ij}^{LW} + \gamma_{ij}^{AB} \tag{2.29}$$

$$\Delta G_{ij}^a = \Delta G_{ij}^{aLW} + \Delta G_{ij}^{aAB} \tag{2.30}$$

The Berthelot geometric mean is used to calculate the Lifshitz-van der Waals component of SFE as follows (Good, 1992).

$$\Delta G_{ij}^{aLW} = -2\ \overline{\gamma_i^{LW}\gamma_j^{LW}} \tag{2.31}$$

The following equation defines the acid-base component of surface free energy due to the complementarity nature of the acid-base interaction (van Oss et al., 1988).

$$\Delta G_{ij}^{aAB} = -2\ \left[\overline{\gamma_i^+\gamma_j^-} + \overline{\gamma_i^-\gamma_j^+} \right] \tag{2.32}$$

$$\Delta G_{ij}^a = -2\ \overline{\gamma_i^{LW}\gamma_j^{LW}} + -2\ \left[\overline{\gamma_i^+\gamma_j^-} + \overline{\gamma_i^-\gamma_j^+} \right] \tag{2.33}$$

The free energy of adhesion reflects the adhesive bond between asphalt binder and aggregate. The higher the free of adhesion means stronger the bond between the asphalt binder and aggregate.

2.4.2.4   Adhesion under Wet Condition

The moisture-induced damage is very deteriorative to asphalt mixtures. In order to estimate the moisture-induced damage potential of an asphalt pavement material, the adhesive bond energy (the Gibbs free energy of adhesion) between asphalt binder and aggregate in the presence of water should also be calculated. Adhesive bond energy for two different materials in contact within a third medium, ΔG^a_{ikj}, is given by the following equation:

$$\Delta G^a_{ikj} = \gamma_{ij} - \gamma_{ik} - \gamma_{jk} \tag{2.34}$$

Equation 2.34 can be used for calculation of the adhesive bond energy of asphalt pavements under wet condition. In this case the subscripts i, j, and k refer to asphalt binder, aggregate, and water, respectively. In this case Equation 2.34 may be re-written as below:

$$\Delta G^a_{ikj} = \Delta G^{aLW}_{ikj} + \Delta G^{aAB}_{ikj} \tag{2.35}$$

According to van Oss et. al (1988) and van Oss and Good (1991), the final version of formula for adhesive bond energy under wet condition can be expressed as follows:

$$\Delta G^a_{ikj} = -2 \left[\begin{array}{c} \overline{\gamma^{LW}_i \gamma^{LW}_k} + \overline{\gamma^{LW}_j \gamma^{LW}_k} - \overline{\gamma^{LW}_i \gamma^{LW}_j} - \gamma^{LW}_k + \\ \overline{\gamma^+_k} \left(\overline{\gamma^-_i} + \overline{\gamma^-_j} - \overline{\gamma^-_k} \right) + \overline{\gamma^-_k} \left(\overline{\gamma^+_i} + \overline{\gamma^+_j} - \overline{\gamma^+_k} \right) \\ - \overline{\gamma^+_i \gamma^-_j} - \overline{\gamma^-_i \gamma^+_j} \end{array} \right] \tag{2.36}$$

The negative work of adhesion means that if the asphalt-coated surface of the aggregate is replaced by water, the system will release energy. Since the liquid phase is water, the interaction between these three phases is called hydrophobic which means that the presence of water is going to force the aggregate and the asphalt to repel each other (van Oss et. al, 1988). Therefore, stripping will happen whenever the three phases (water, asphalt, and aggregate) meet together.

2.4.2.5　Energy Ratio

Energy ratio (ER) is a parameter related to the moisture-induced damage potential of asphalt pavements (Little and Bhasin, 2006). The ER is calculated as follows:

- Work of adhesion between the asphalt binder and the aggregate,

- Work of cohesion within the asphalt binder, and

- Work of debonding when asphalt-aggregate interface meets water.

The works of adhesion (W^a_{ij}), cohesion (W^c_i), and debonding (W^a_{ikj}), are equal to the negatives of Gibbs free energy of adhesion in dry condition (ΔG^a_{ij}), cohesion (ΔG^c_i), and adhesion under wet condition (ΔG^a_{ikj}), respectively.

$$W^a_{ij} = -\Delta G^a_{ij} \tag{2.37}$$

$$W^c_i = -\Delta G^c_i \tag{2.38}$$

$$W^a_{ikj} = -\Delta G^a_{ikj} \tag{2.39}$$

Therefore, the ER is expressed as follows:

$$ER = \frac{W^a_{ij} - W^c_i}{W^a_{ikj}} \tag{2.40}$$

According to the Equation 2.40, since W^a_{ij} defines work needed to break the bond between the asphalt binder and aggregate, the higher W^a_{ij} means better resistance to moisture-induced damage.

W^a_{ikj} is equal to the energy potential of water to separate the asphalt binder from the aggregate surface. Hence, a lower value of W^a_{ikj} indicates less susceptibility to moisture-induced damage (Howson et. al, 2007).

2.4.3 Wettability

Wetting is the ability of a liquid to maintain contact with a solid surface, which is resulting from intermolecular interactions when the two materials are brought together in contact. The degree of wetting (also known as wettability) is determined by a force balance between adhesive and cohesive forces.

As explained before, an interface interaction between a liquid and a solid causes the liquid drop to spread across the surface. Cohesive forces within the liquid cause the drop to form a spherical shape. The contact angle (θ), as seen in Figure 2.3, is the angle at which the liquid–vapor interface meets the solid–liquid interface. The contact angle is determined by the resultant between adhesive and cohesive forces at equilibrium. As the tendency of a drop to spread out over a flat, solid surface increases, the contact angle decreases. Thus, the contact angle provides an inverse measure of wettability (Sharfrin and Zisman, 1960).

A contact angle less than 90° (low contact angle) usually indicates that wetting of the surface is very favorable, and the fluid will spread over a large area of the surface. Contact angles greater than 90° (high contact angle) generally mean that wetting of the surface is unfavorable so the fluid will minimize the contact with the surface and form a compact liquid droplet (Sharfrin and Zisman, 1960).

When water is involved as the liquid, a wettable surface may also be termed hydrophilic and a non-wettable surface hydrophobic. Table 2.1 describes varying contact angles and their corresponding solid/liquid and liquid/liquid interactions (Eustathopoulos et al., 1999). For non-water liquids, the term lyophilic is used for low contact angle conditions and lyophobic is used when contact angles results are higher (Extrand, 2003).
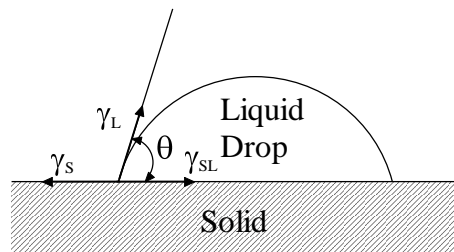
Figure 2.3 Schematic of Contact Angle between a Liquid and a Solid

Table 2.1 Varying Contact Angles and Their Corresponding Interactions (Eustathopoulos et al., 1999)

Contact Angle (Deg.)	Degree of wetting	Strength of Interaction	
		Solid/Liquid	Liquid/Liquid
$\theta = 0$	Perfectly wetting	Strong	Weak
$0 < \theta < 90°$	High wettability	Strong-weak	Strong-weak
$90° \leq \theta < 180°$	Low wettability	Weak	Strong
$\theta = 180°$	Perfectly non-wetting	Weak	Strong

2.4.4 Good-van Oss -Chaudhury (GVOC) Approach (The Acid-Base Theory)

Up to the middle 1980s, only van der Waals attractions and electrostatic repulsion forces were considered as acting forces between particle surfaces (Chaudhury, 1984). Van Oss et al. (1987) first applied Lifshitz theory to macroscopic scale interactions between material surfaces. The van Oss et al. (1987) study established for the first time a clear distinction between apolar, or Lifshitz – van der Waals (LW) and polar, or Lewis acid-base (AB) interactions. According to the van Oss et al. (1987) theory (or sometimes called the Good-van Oss-Chaudhury or acid-base theory), the total surface free energy of any material is divided into two components (assuming that the electrostatic component is negligible as compared to the LW and AB interactions) based on the type of the surface forces. These components are the non-polar component, also referred to as the LW or the dispersive component, and the Lewis acid-base component (AB) (van Oss et al., 1987):

$$\gamma = \gamma^{LW} + \gamma^{AB} \qquad (2.41)$$

where γ is the surface free energy of the solid material (i.e., aggregate or binder); γ^{LW} is the Lifshitz – van der Waals component; and γ^{AB} is the Lewis acid-base component. The

acid-base component can further be divided into two subcomponents as the Lewis acid component (γ^+) and the Lewis base component (γ^-) (van Oss et al., 1987).

Every material has a surface free energy from the fact that the molecules at the surface are subjected to unequal forces compared to their respective forces in the bulk material. It is not easy or rather not feasible to measure the surface components of the solid materials directly (van Oss, 2002). Therefore, the surface energy components of solid materials are usually determined indirectly using contact angle, vapor adsorption isotherm, or heat of immersion measurements. For the LW and AB interactions together, the method of choice is the determination of contact angles with drops of a small number of appropriate liquids deposited on a solid surface (Giese and van Oss, 2002). This method still remains the preferred approach, as it is the only method that allows the analysis of the surface properties of solid materials at their exact surfaces (not a few nanometers below the surface) (van Oss, 2002). This is particularly important because solid and liquid materials interact with one another through their exact surfaces (van Oss, 2002).

Thomas Young, in 1805, described the equilibrium (or the interaction energy) between a liquid drop and a solid material (as shown in Figure 2.3) in terms of their individual surface forces (or energy) and the interaction force between them as given in Equation 2.42 (van Oss, 1994). Contact angle (θ) measurement as described by Young remains at present the most accurate method for determining the interaction energy (or the work of adhesion) between a liquid (L) and a solid (S) (van Oss, 2002):

$$\gamma_L cos\theta = \gamma_S - \gamma_{SL} \tag{2.42}$$

where γ_S is the surface energy of the solid; γ_L is the surface energy (or surface tension) of the liquid; and γ_{SL} is the interfacial tension (or energy) between the liquid and the solid (Figure 2.3).

In Equation 2.42, γ_L and $cos\theta$ are known and γ_S and γ_{SL} are the unknown parameters. Using two different liquids gives rise to two equations with three unknowns.

31

Thus, Equation 2.42, in the form given above is not practically usable. However, Dupré equation along with Equation 2.42 can be used to determine contact angles. The Dupré equation below represents the free energy of interaction between a solid and a liquid (Fowkes, 1963):

$$\Delta G_{SL} = \gamma_{SL} - \gamma_S - \gamma_L \tag{2.43}$$

where, ΔG_{SL} represents the free energy of interaction between the solid and the liquid. Combining Equation 2.42 and Equation 2.43 results in the following form of Young-Dupré equation (Chaudhury, 1984):

$$1 + cos\theta \ \gamma_L = -\Delta G_{SL} \tag{2.44}$$

The total interaction energy consists of Lifshitz-van der Waals and Lewis acid-base interaction components and can be expressed as (van Oss et al., 1987):

$$\Delta G_{SL} = \Delta G_{SL}^{LW} + \Delta G_{SL}^{AB} \tag{2.45}$$

In terms of individual surface energy components, Equation 2.45 takes the following form (van Oss, 2002):

$$\Delta G_{SL} = -2 \ \ \sqrt{\gamma_S^{LW}\gamma_L^{LW}} + \ \sqrt{\gamma_S^{+}\gamma_L^{-}} + \ \sqrt{\gamma_S^{-}\gamma_L^{+}} \tag{2.46}$$

where γ_L^{LW} is the Lifshitz-van der Waals component of liquid; γ_S^{LW} is the Lifshitz-van der Waals component of solid; γ_L^{+} is the Lewis acid component of liquid; γ_S^{+} is the Lewis acid component of solid; γ_L^{-} is the Lewis base component of liquid; and γ_S^{-} is the Lewis

base component of solid. The combination of Equation 2.44 and Equation 2.46 gives the complete Young-Dupré equation that is widely used in determining the surface energy components of solid materials using contact angle measurements (van Oss, 2002):

$$1 + cos\theta \ \gamma_L = 2 \left(\sqrt{\gamma_S^{LW}\gamma_L^{LW}} + \sqrt{\gamma_S^+\gamma_L^-} + \sqrt{\gamma_S^-\gamma_L^+} \right) \quad (2.47)$$

To obtain the unknown surface energy values for the solid (i.e., aggregate or binder) it is necessary to measure contact angles with three different liquid probes. Surface energy components of five most used probe liquids are given in Table 2.2.

Table 2.2 Surface Energy Components of Three Liquid Probes Used in This Study (Van Oss, 2002)

Liquid Probe	γ^{Total}	γ^{LW}	γ^{AB}	γ^-	γ^+
	(ergs/cm^2 or mJ/m^2)				
Water	72.80	21.80	51.00	25.50	25.50
Diiodomethane	50.80	50.80	0.00	0.00	0.00
Ethylene Glycol	48.00	29.00	19.00	1.92	47.00
Glycerol	64.00	34.00	30.00	57.40	3.92
Formamide	56.00	39.00	19.00	39.60	2.28

The Universal Sorption Device (USD), Wilhelmy Plate (WP) and the Sessile Drop (SD) methods make use of GVOC theory (Equation 2.47). The SD method measures the contact angles *directly* and adopts Equation 2.47 in its present form. The WP is based on kinetic force equilibrium and uses Equation 2.47 as well, but the contact angles are determined indirectly.

2.4.5 Equilibrium Spreading Pressure

While WP and SD methods make use of GVOC approach by utilizing Equation 2.47, the USD method introduces a spreading pressure to the left side of Equation 3.47 and drops the contact angle from the equation:

$$\pi_e + 2\gamma_L = 2 \left[\overline{\gamma_S^{LW}\gamma_L^{LW}} + \overline{\gamma_S^+\gamma_L^-} + \overline{\gamma_S^-\gamma_L^+} \right] \tag{2.48}$$

where the π_e is the spreading pressure determined from adsorption isotherms.

First introduced by Bangham and Razouk in 1937, many researchers in the field of colloid and surface science assumed that condensation of the probe liquid causes the complete wetting on the solid surface. The terms γ_{LV} and γ_{SV} representing the liquid-vapor and solid-vapor interfaces, respectively have been used in Young's force balance.

$$\gamma_s = \gamma_{LV}\cos\theta + \gamma_{SV} + \pi_e \tag{2.49}$$

The equilibrium spreading pressure is represented as π_e, where $\pi_e = \gamma_S - \gamma_{SV}$. This assumption may work for materials with high energy surfaces. However, it may not be applicable for materials with low energy surfaces. For contact angles larger than 10°, π_e is negligible (Wu, 1982). Also, in the case of non-spreading liquids ($\gamma_L > \gamma_S$ and $\cos\theta < 1$), neither spreading nor pre-wetting occurs on low energy surfaces (van Oss, 1994). Van Oss (2002) states that the acid-base theory is applicable with the current form of Equation 2.47.

In this study, Young's equation was used with the spreading pressure term for analyzing the results of USD tests and without the spreading pressure term for analyzing the results of SD. The difference in SFE components obtained from USD and SD tests may be attributed to the spreading coefficient term in Young's equation applied for analyzing the test results using these two methods, as discussed above.

2.5 Contact Angle Measurements

Several methods are used and reported to be successfully applied for contact angle measurements. These methods are introduced in this section.

2.5.1 Sessile Drop Method

The Sessile Drop method is used to measure advancing contact angles of probe liquids with a solid surface and is suited for both asphalt binders and aggregates. Contact angles are measured directly by dispensing a drop of the probe liquid on the solid surface and capturing an image of the drop (van Oss, 1994). The captured image can be analyzed using a computer with image processing software to obtain the contact angle of the liquid at the edge of the drop (Figure 2.4).
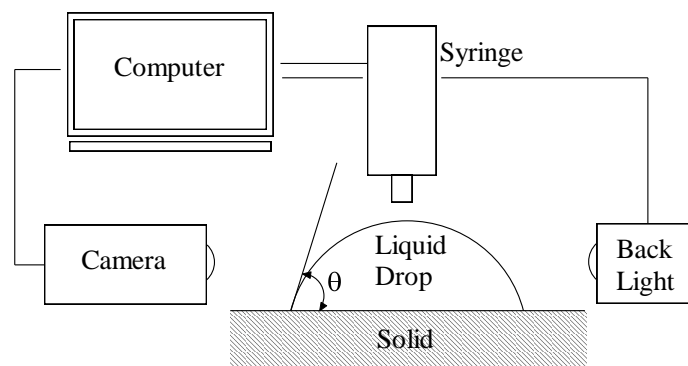
Figure 2.4 Schematic Drawing of the Sessile Drop Device

The Sessile Drop instrument (FTA 1000B Series from Firsttenangstroms) captures video images of liquid droplets and analyzes their shape and size to determine various surface chemistry quantities such as contact angles, interfacial tension, pendant and Sessile Drop volumes, and spreading. The instrument is fully automated and can be controlled with the provided software on a computer. The device is fitted with a precise stepper motor drive syringe pump that can both push out and pull in fluid. In this way, advancing and receding contact angles can be measured over the sample

surface. The fully automated single syringe dispenser can form drops of selected volume and automatically touch them off on samples for contact angle measurements. The advancing and receding contact angles can also be measured using the tilting plate mounted on the instrument. With the tilting plate frame, the instrument tilts up to a 90° angle. Figure 2.5 shows the instrument during testing a flat rock aggregate specimen.
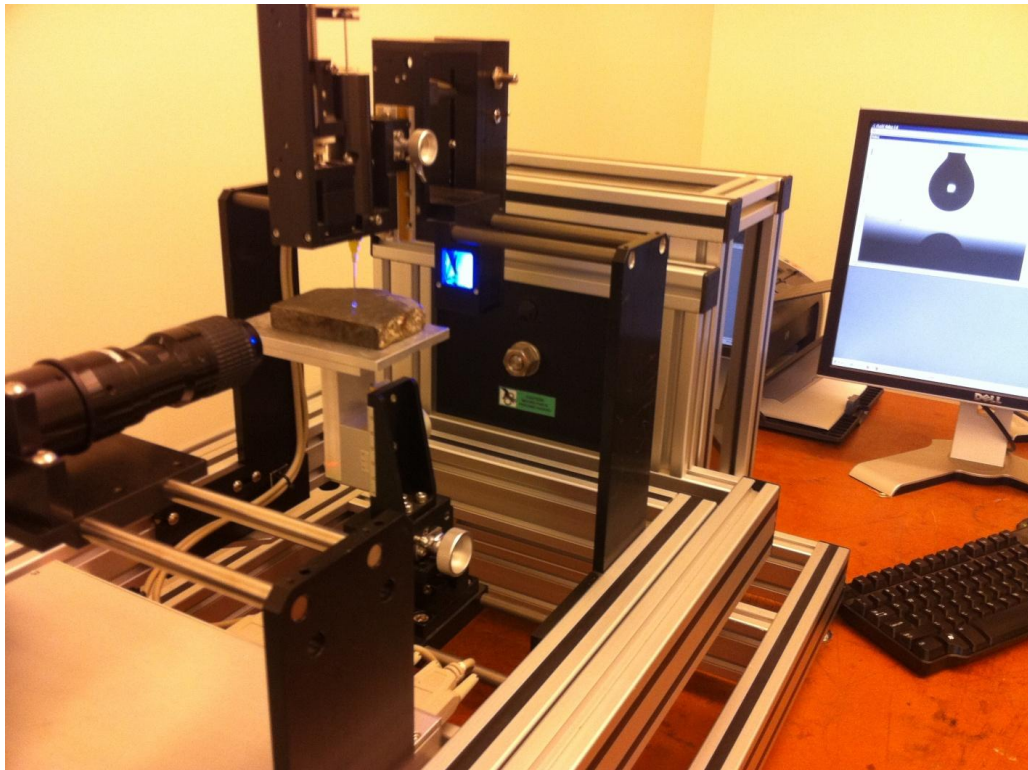
Figure 2.5 The Sessile Drop Device Testing a Flat Aggregate Specimen

2.5.2 Universal Sorption Device

The Universal Sorption Device (USD) is usually employed to measure the surface free energy components of the aggregates *indirectly*. The gas adsorption characteristics of the probe liquids, whose surface energy components are known, are used to calculate the Surface Free Energy (SFE) components of the aggregates in USD method (Cheng, 2002).

Both USD and SD methods can employ the same probe liquids in the analysis. However, while the SD uses the probe liquid in the form of liquid drops, the USD uses them in the gas form. The probe liquids in the USD method are used to measure the spreading pressure with the aggregate.

The USD consists of a magnetic suspension balance system to measure the mass of the sample, a computer (software), temperature control unit, vacuum system and regulator, pressure transducer, solvent container, and a vacuum desiccator (Cheng, 2002). A schematic illustration of USD is shown in Figure 2.6.
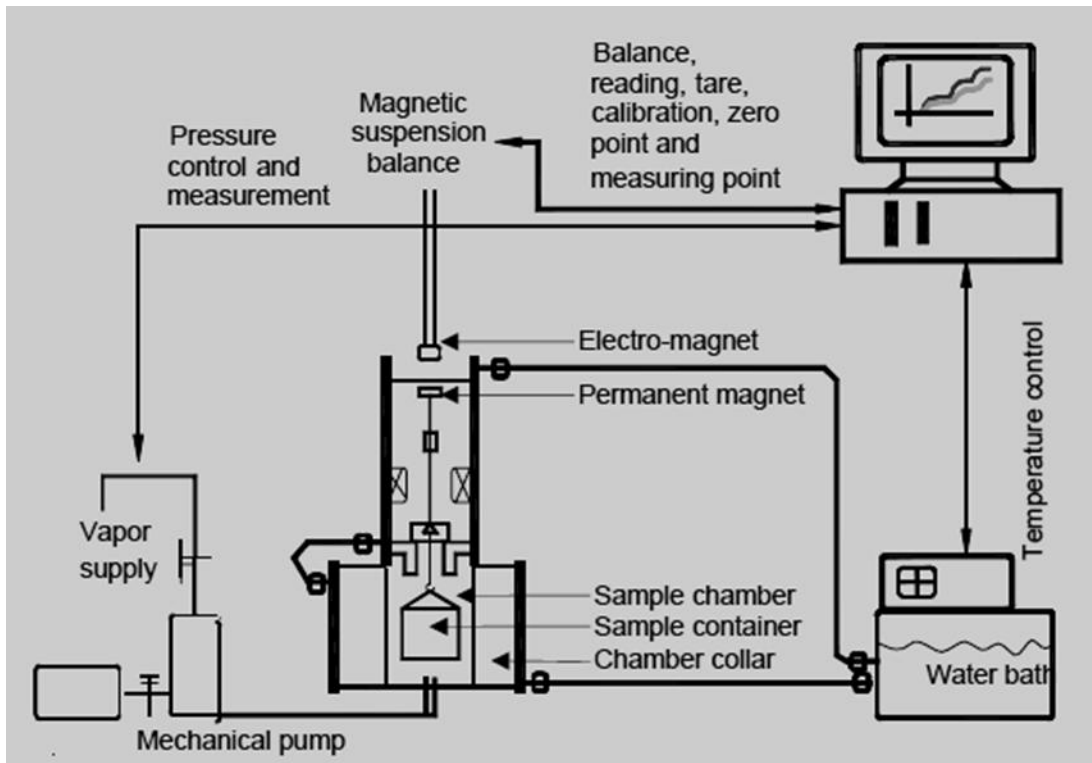
Figure 2.6 Schematic Illustration of the Universal Sorption Device (Cheng, 2002)

In order to use the USD on aggregates, the samples should be clean and degassed under high temperature. The samples are vacuumed in a sorption cell which is air-tight. Then the USD takes the probe vapor into the sorption cell with small quantities. The increments of the probe vapor are increased gradually to reach different relative pressure levels. Once the adsorption isotherm is obtained, the equilibrium spreading pressure (π_e) of that particular probe vapor on the aggregate sample can be calculated. This process is repeated with different probe vapors until the equilibrium spreading pressures on the aggregate are obtained. Then, using the Good-van Oss-Chaudhury (GVOC) approach for the work of adhesion (see Equation 2.8), the surface energy components of the aggregate are calculated (Howson et al., 2007; Bhasin, 2006; Cheng, 2002; van Oss, 1994;van Oss et al., 1988).

The testing protocol for the USD is rather complicated and time consuming. According the Cheng (2002), preparation and testing of one aggregate sample with one solvent can take about 64 hours after the sieve analysis and washing the aggregates. On top of 64 hours, more time is spent during the testing of the aggregates with different probe vapors. Furthermore, each and every unit of the USD must be calibrated for each test. The weight of the sample and the temperature in chamber unit must be precise. A high level of expertise is required to use the USD and conduct laboratory experiments.

2.5.3 Wilhelmy Plate Method

A Wilhelmy Plate is a thin plate that is used to measure equilibrium surface or interfacial tension at an air–liquid or liquid–liquid interface. In this method, the plate is oriented perpendicular to the interface, and the force exerted on it is measured. Based on the work of Ludwig Wilhelmy, this method finds wide use in the preparation and monitoring of Langmuir–Blodgett films which consist of the material deposited from the surface of a liquid onto a solid substrate by immersing the solid into the liquid (Holmberg, 2002). Figure 2.7 presents an illustration of Wilhelmy Plate test method.
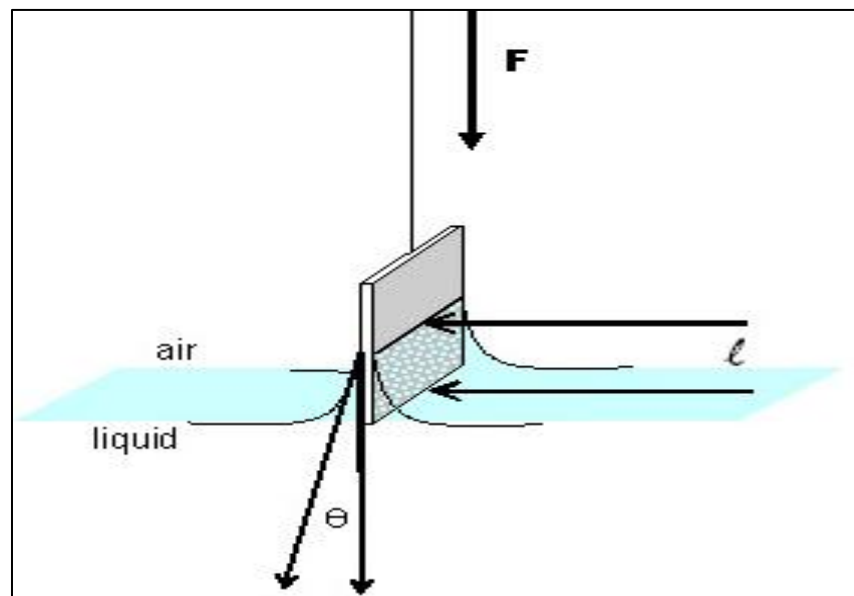
Figure 2.7 Illustration of Wilhelmy Plate Method (source: www.cscscientific.com)

Besides measuring the surface tensions, Wilhelmy Plate method is also an alternative method for measuring the contact angles indirectly (Shang et al., 2008). In this method, a sensitive force meter is employed in order to measure a force that can be

translated into a value of the contact angle. A small plate-shaped sample of the solid which is attached to the arm of a force meter is vertically dipped into the probe liquid, and the force exerted on the sample by the liquid is measured by the force meter.

In the Wilhelmy Plate testing, a specimen of an appropriate size must be produced with a uniform cross section in the submersion direction, and the wetted length must be measured with precision. In addition, this method is only appropriate if both sides of the specimen are identical; otherwise, the measured data will be a result of two completely different interactions (Rulison, 1996).

2.5.4 Column Wicking and Thin Layer Wicking Methods

The column wicking method is used to measure the contact angles on powdered or porous materials (van Oss, 1994). The contact angle is calculated after the speed of the capillary rise into the porous medium is measured. In order to obtain better results, the pore structure of the material must stay uniform during the capillary rise. On the other hand, the pore structure of the specimen changes for some colloids that are prone to shrink or swell (Shang et al., 2008).

This problem has been solved by the development of the thin-layer wicking method. In this method, a rigid thin layer is created by depositing the colloidal particles on a flat surface (van Oss et al., 1994). A large variety of minerals can be tested using these methods. According to Costanzo et al. (1995), thin-layer wicking method reveals almost identical contact angles compared to the Sessile Drop method on cubic hematite particles.

2.5.5 Heat of Immersion Method

The contact angles of powdered samples can also be measured by Heat of Immersion method (also known as Microcalorimetric method). In this technique, first the powder is degassed to remove the pre-adsorbed moisture. The sample is then immersed in the probe liquid (Groszek, 1962) for heat of immersion measurements. As the hydrophobicity of the sample increases, the heat of immersion in water decreases. The calculation of contact angles relies on rigorous thermodynamic relations (Yildirim, 2001). Once the contact angle values are determined from the heat of immersion of

three different probe liquids, the SFE components are calculated using the GVOC theory. Yildirim (2001) presented the SFE components of talc samples calculated by using the heat of immersion method.

3.1   General

Consistent with the scope of the present study, different types of materials including hot mix asphalt, warm mix asphalt, asphalt binders and aggregates are examined through different test methods. The materials and the testing methods are discussed in this chapter.

3.2   Collection of Warm Mix Asphalt

Foam is the most common WMA procedure used in Oklahoma. At the time of this study, plant produced asphalt mixes using WMA additives (e.g. Advera® and Evotherm®) were not readily available in Oklahoma. Therefore, the research team was actively seeking assistance from different agencies and individuals to collect loose WMA plant mixes from neighboring states (Texas, Kansas, Louisiana). Several active road construction projects were reviewed and contacted. Finally, two projects located in Texas, one using Advera® and the other using Evotherm® WMA technologies, were found suitable for material collection. The material collection activities from different construction sites are discussed in the next three sections.

3.2.1   Advera® Warm Mix Asphalt as Surface Course

The Advera® WMA mix (ADWM) was collected from an asphalt production plant located at Bridgeport, TX, on June 30, 2011. The produced WMA mix was being used by a local contractor for construction of an asphalt overlay project located at the southbound lane of US 287 located south of Rhome, TX. The research team was able to collect the bulk asphalt materials including 1600 lbs. of loose ADWM mix, 1400 lbs. of bulk aggregate, 300 lbs. of reclaimed asphalt pavement (RAP) and reclaimed asphalt shingles (RAS) each, 4 gallons of PG 64-22 Gary Williams asphalt binder, 2 lbs. of Advera® WMA additive, and 1 lb. of ArrMaz AD-here® (the antistripping agent generally used by the plant). Figure 3.1 through Figure 3.7 present photographic views of asphalt plant and material collection activities on June 30, 2011.

Figure 3.1 Photographic View of the Asphalt Plant in Bridgeport, TX

Figure 3.2 Aggregate Bins in Asphalt Plant in Bridgeport, TX

Figure 3.3 Manufactured Sand Stockpile in the Asphalt Plant in Bridgeport, TX

Figure 3.4 Collection of Natural Sand from the Asphalt Plant in Bridgeport, TX

Figure 3.5 RAP Collection from Asphalt Plant in Bridgeport, TX

Figure 3.6 Advera® WMA Mix Collection from Asphalt Plant in Bridgeport, TX

Figure 3.7 Loading the Collected Materials to the Truck

Also an ongoing asphalt overlay project on US 287 was visited during the the second trip to project location on July 7, 2011. 8 gallons of additional PG 64-22 Gary Williams asphalt binder were collected during the second trip. Figure 3.8 shows a photographic view of the overlay project located at US 287.

Figure 3.8 Overlay Project in US 287 using Advera® WMA

All of the collected materials were transported to the University of Oklahoma's Broce Asphalt Laboratory and stored appropriately for further testing.

Mix design details of the collected ADWM mix, according to the information received from the asphalt plant are shown in Table 3.1.

Table 3.1 Design Information of ADWM Mix Collected from Bridgeport, TX

Bin No.	Aggregate	Producer/Supplier			% Used
1	Type "D"	Bridgeport			48
2	Man. Sand	Bridgeport			29.6
3	Sand	Paradise			5
8	Fractionated RAP	Austin Br. & Rd.			15
9	RAS	Sustainable Pavement Tech-Schertz			2.4

Sieve Size		Percent Passing (%)					Comb.
AASHTO	(mm)	Bin No. 1	Bin No. 2	Bin No. 3	Bin No. 8	Bin No. 9	Agg.
3/4"	19	100	100	100	100	100	100
1/2"	12.5	100	100	100	100	100	100
3/8"	9.5	99.2	100	100	96.5	100	99.1
No. 4	4.75	40	99.3	100	66.3	100	65.9
No. 8	2.36	10.1	83.6	99	43.6	98.7	43.5
No. 30	0.6	6.2	39.1	96	27.7	62	25.0
No. 50	0.3	3.1	19.9	73	22.8	53.5	15.7
No. 200	0.075	1.5	3	3	7	21.7	3.3
AC		Valero (PG 64-22)					5.0%
Anti-Striping Agent		Arr Maz AD-Here® HP PLUS					1.0%

3.2.2 Evotherm® Type B Warm Mix Asphalt as Base Course

The Evotherm® Type B WMA mix (EVWM-B) was collected on October 25-27, 2011 from San Antonio, TX. The produced WMA mix by the asphalt plant was being used by a local contractor (Ramming Paving Co.) for construction of a city project, located at Foster Road, in San Antonio, TX (Figure 3.9). It was a base layer mix, produced at the Century Asphalt Co. plant, but collected from the field. The collected asphalt materials include 1800 lbs. of loose EVWM-B asphalt mix, about 1500 lbs. of bulk aggregates, 300 lbs. of RAP and RAS each, 10 gallons of PG 64-22 asphalt binder and 2 gallons of Evotherm® WMA additive. Figure 3.10 shows collection of loose mix from the field. Figure 3.11 and Figure 3.12 show photographic views of aggregate collection and loading loose materials on the truck in Century Co. Asphalt Plant in San Antonio, TX, respectively.

Figure 3.9 Placing the Evotherm® Type B Mix on Foster Rd. in San- Antonio, TX

Figure 3.10 Evotherm® Type B Mix Collection from Foster Road, San Antonio, TX

Figure 3.11 Aggregate Collection from Asphalt Plant, San Antonio, TX

Figure 3.12 Loading the Collected Materials on the Truck

In addition to loose mix, core samples from different stations and slab samples from three locations were collected. Figure 3.13 and Figure 3.14 show photographic views of 4.0 in.-diameter asphalt core collection and cutting of slab samples, respectively.

Figure 3.13 Evotherm® WMA Core Collection from Compacted Asphalt Layer

Figure 3.14 Cutting of Slab Samples

The mix design details for the EVWM-B mix, according to the information received from the asphalt plant, are shown in Table 3.2.

Table 3.2 Design Information of EVWM-B Collected from San Antonio, TX

Bin No.	Aggregate	Producer/Supplier	% Used
1	1.0" Rock	Balcones Quarry	25
2	D/F Blend	Balcones Quarry	27
3	Screening	Balcones Quarry	15.5
4	Fine Sand	Columbus	10
8	Fractionated RAP/Fine	Century Asphalt New Braunfels	20
9	RAS	Sustainable Pavement Tech-Schertz	2.5

Sieve Size		Percent Passing (%)					Comb.
AASHTO	(mm)	Bin No. 1	Bin No. 2	Bin No. 3	Bin No. 8	Bin No. 9	Agg.
1-1/2"	37.5	100	100	100	100	100	100
1"	25	96.4	100	100	100	100	99.1
3/4"	19	71.5	100	100	100	100	92.9
3/8"	9.5	16	97.5	100	92.9	100	76.9
No. 4	4.75	4	46.7	98.5	62.9	93.8	53.8
No. 8	2.36	1	13.7	88.8	48.3	81.5	38.6
No. 30	0.6	0.9	2.8	44.1	33.5	60.4	24.1
No. 50	0.3	0.8	2.3	24.9	28.3	34	17.4
No. 200	0.075	0.7	1.9	10.2	8.9	26.5	5.0
AC	PG 64-22						4.5%
WMA Technology	Evotherm®		Percent used (by weight of Asphalt)				0.4%

3.2.3 Evotherm® Type C Warm Mix Asphalt as Surface Course

Similarly, the Evotherm® Type C WMA mix (EVWM-C) was collected on January 3-7, 2012 from Foster Road, San Antonio, TX. A photographic view of placement of the Evotherm® Type C WMA mix is shown in Figure 3.15. It was a surface layer mix, produced at the Century Asphalt Co. plant, but collected from the field. Figure 3.16 shows a photographic view of collection of the loose EVWM-C mix from the field. Moreover, bulk aggregates, PG 70-22 asphalt binder and Evotherm® were collected for the production of 1800 lbs. of mix in the laboratory. The collected asphalt materials include 1800 lbs. of loose EVWM-C mix, about 1500 lbs. of bulk aggregates, 300 lbs. of RAP and RAS each, 12 gallons of PG 70-22 asphalt binder and 2 gallons of Evotherm® WMA additive. Figure 3.17 shows a photogaphic view of the temperature measurement of the asphalt mix in the field. Figure 3.18, Figure 3.19 and Figure 3.20 show

photographic views of aggregate stockpile, collection of the asphalt binder and loose asphalt materials loaded on the truck, in Century Co. Asphalt Plant in San Antonio, TX, respectively.

Figure 3.15 Placement of Evotherm® Type C Mix on Foster Road, San Antonio, TX

Figure 3.16 Collection of Evotherm® Type C Mix from Field

Figure 3.17 Temperature Measurement of Sampled Loose Mix in the Field

Figure 3.18 Aggregate Stockpile in Century Co. Asphalt Plant in San Antonio, TX

Figure 3.19 Collection of Asphalt Binder from Century Co. Asphalt Plant Located in San Antonio, TX

Figure 3.20 Collected Materials on Back of the Truck in Century Co. Asphalt Plant Located in San Antonio, TX

Mix design details of the collected EVWM-C mix, according to the information received from the asphalt plant are shown in Table 3.3.

Table 3.3 Design Information of EVWM-C Collected from San Antonio, TX

Bin No.	Aggregate	Producer/Supplier	% Used
1	C- Rock	Servtex	18
2	D/F Rock	Servtex	35
4	Screening	Servtex	28
5	Sand	Gem Materials	8
6	Lime	Chem Lime Century Co.	1
8	Fractionated RAP (<1/2")	Century Co.	10

Sieve Size		Percent Passing (%)						Comb.
AASHTO	(mm)	Bin No. 1	Bin No. 2	Bin No. 4	Bin No. 5	Bin No. 6	Bin No. 8	Agg.
1"	25	100	100	100	100	100	100	100
3/4"	19	100	100	100	100	100	100	100
3/8"	9.5	25.3	92.5	100	100	100	84.2	82.3
No. 4	4.75	2.5	43	98	100	100	65.8	58.5
No. 8	2.36	1.5	6	83.2	100	100	42.1	38.9
No. 30	0.6	1.1	1.3	35.3	95.3	100	25	21.7
No. 50	0.3	1.1	1.3	18.6	72.4	100	20	14.7
No. 200	0.075	0.9	0.9	4.6	4.6	100	7.4	3.9
AC	PG 70-22	Jebro Inc.						4.8%
WMA Technology	Evotherm®		Percent used (by weight of Asphalt)					0.5%
Anti-Striping Agent	Lime, Century Co.		Percent used (by weight of agg. from Bin No. 6)					1.0%

3.3   Laboratory Production of Baseline Control HMA

Control hot mix asphalt (HMA) mixes were produced in the laboratory and used for conducting different laboratory performance tests. The test results of control HMA mixes were compared with those obtained from testing the WMA mixes collected from the field. Aggregates, asphalt binder, anti-stripping agent, gradation and volumetric parameters used for production of the laboratory control HMA mixes were identical to those collected from the field. WMA additives (Advera® and Evotherm®) were not used for control HMA mix production in the laboratory. Hence, the mixing and compaction temperatures used for production of laboratory HMA mixes were selected based on the performance grade (PG) of the asphalt binder used in the mix production. For this purpose, recommended temperatures for mixing and compaction of HMA mixes

according to the 2009 ODOT Standard Specifications for Highway Construction (ODOT, 2009), were applied. Based on the above mentioned recommendations, all of the control HMA mixes were produced and compacted at 160° and 145 ºC, respectively. Also reheating and compaction temperatures of the field collected WMA mixes were set based on the mix design information received from the asphalt plant. Based on these information, ADWM mix was reheated and compacted at 130° and 115ºC, respectively. However, EVWM-B and EVWM-C mixes were reheated and compacted at 135° and 121°C, respectively. A summary of the mixing and compaction temperatures and other mix properties of the control HMA and WMA mixes, used in the present study are presented in Table 3.4. Since the air voids of 7.0 ± 0.5%, were targeted for compaction of the cylindrical test specimens, the Superpave Gyratory Compactor (SGC) was used for sample compaction in the "target height mode". The height value in SGC was set to the required height of the cylindrical specimens, according to the corresponding standard test method. In other words, the number of gyrations was not set for sample compaction. Three control HMA mixes were produced in laboratory: (i) control HMA mix of ADWM namely, Advera® control HMA (ADHM); (ii) control HMA mix of EVWM-B namely, Evotherm® control HMA Type B (EVHM-B); (iii) control HMA mix of EVWM-C namely, Evotherm® control HMA Type C (EVHM-C).

Table 3.4 Summary of the Asphalt Mix Properties used in the Study

Mix Type	NMAS* (mm)	Gradation Description	Mix Description	Temperature (ºC)		WMA Additive	Anti Stripping Agent
				Mixing	Compaction		
ADHM	9.5	Overly	Control HMA	160	145	-	ArrMaz AD-Here HP Plus®
ADWM	9.5	Overlay	Field WMA	130	115	Advera®	ArrMaz AD-Here HP Plus®
EVHM-B	19	Fine base	Control HMA	160	145	-	-
EVWM-B	19	Fine base	Field WMA	135	121	Evotherm®	-
EVHM-C	19	Coarse surface	Control HMA	160	145	-	Lime
EVWM-C	19	Coarse surface	Field WMA	135	121	Evotherm®	Lime

*Nominal maximum aggregate size.

3.4   Laboratory Tests on Asphalt Mix

3.4.1 Hamburg Wheel Tracking (HWT) Test

To determine rut and moisture-induced damage (stripping) potential, cylindrical WMA and HMA samples were prepared and compacted in the laboratory and were tested using a Hamburg Wheel Tracking (HWT) device in accordance with the OHD L-

55 test method (ODOT, 2010). A minimum of four specimens of each asphalt mix were compacted in the laboratory, using a Superpave Gyratory Compactor (SGC) with a 7.0 ± 0.5% target air voids. Cylindrical specimens were of 150 mm (6 in.) diameter and 60 mm (2.36 in.) height. Two gyratory specimens were cut from the side to match the HWT plastic mold dimensions, and were used as one set. Susceptibilities to rutting and moisture-induced damage are based on pass/fail criteria. The test procedure requires that the cylindrical samples be secured in the device, using plastic mounting molds. During testing, the 47 mm (1.85 in.) wide wheel is tracked across a sample submerged in a water bath at 50 ± 1°C temperature under 20,000 passes or until a rut depth of 20 mm occurs. The load on the wheel is 705 N (158 lbs.). The average speed of the wheel is approximately 1.1 km/h (0.68 mph); and travels approximately 230 mm (9.05 in.) before reversing the movement direction. The device operates at approximately 53±2 wheel passes/min. Rut depths were measured continuously with a LVDT. Figure 3.21 shows the HWT device used in this study.

Figure 3.21 Hamburg Wheel Tracking (HWT) Testing Device

The LVDT measures the depth of the rut with an accuracy of 0.01 mm (0.0004 in.). From a typical test curve, three characteristic regions are generally defined. The following features are noted: post-compaction consolidation, creep slope, stripping slope, and stripping inflection point (Lu and Harvey, 2008; Yildirim et al., 2007). Figure

3.22 shows the typical results of a HWT test, with post-compaction consolidation, creep slope, stripping slope, and stripping inflection point, noted on the figure.
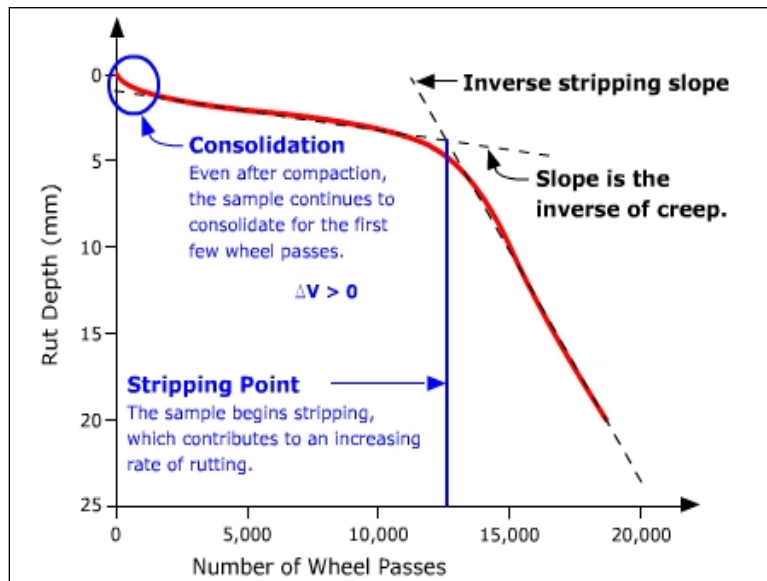
**Figure 3.22 A Typical Plot of HWT Rut Depths vs. Number of Wheel Passes
(source: www.pavemetinteractive.com)**

Texas Department of Transportation (TxDOT) has adopted this test and recommended a maximum allowable rut depth of 12.5 mm (0.5 in.) at 20,000 passes for PG 76 or higher, at 15,000 passes for PG 70 and at 10,000 passes for PG 64 or lower (Yildirim et al., 2007). It is worth mentioning that the Hamburg Wheel Tracking machine has been found to have excellent correlations with field performance (Yildirim et al., 2007).

3.4.2 Retained Indirect Tensile Strength Ratio (TSR) Test

Moisture-induced damage test based on retained indirect Tensile Strength Ratio (TSR) of WMA and HMA asphalt mixes were evaluated in accordance with the AASHTO T283 standard test method (AASHTO, 2010). In this method, moisture-induced damage potential is evaluated by measuring the change in diametric tensile strength resulting from the effects of water saturation and accelerated water and temperature conditioning, with a freeze-thaw cycle, on compacted asphalt mixes. A minimum of six cylindrical SGC specimens of 150 mm (6 in.) diameter and 95 mm (3.74 in.) height were compacted with 7.0 ± 0.5% target air voids. After compaction, each set

57

of specimens was divided into two subsets of three samples. One subset was tested under dry condition at a temperature of 25°C for indirect tensile strength. The other subset was vacuum-saturated under a 13 to 67 kPa absolute vacuum pressure. Saturation level was maintained between 70 to 80 percent. Each vacuum-saturated specimen was then tightly covered with a plastic film and placed in a plastic leak-proof bag containing 10 ml. water. Then the specimens was subjected to a freezing cycle of -18 °C for a minimum of 16 hours followed by a warm water soaking cycle of 60 °C for 24 hours. Then specimens were placed in a water tank of 25 °C temperature for another two hours, before being tested for indirect tensile strength. Numerical indices of retained indirect tensile strength are calculated from the test data obtained by the two tested dry and conditioned subsets. The results from this test are generally used for prediction of long term stripping susceptibility of the tested asphalt mixes and are widely used by DOTs as a pass/fail criterion at the mix design stage. Figure 3.23 shows a photographic view of the TSR test in progress.
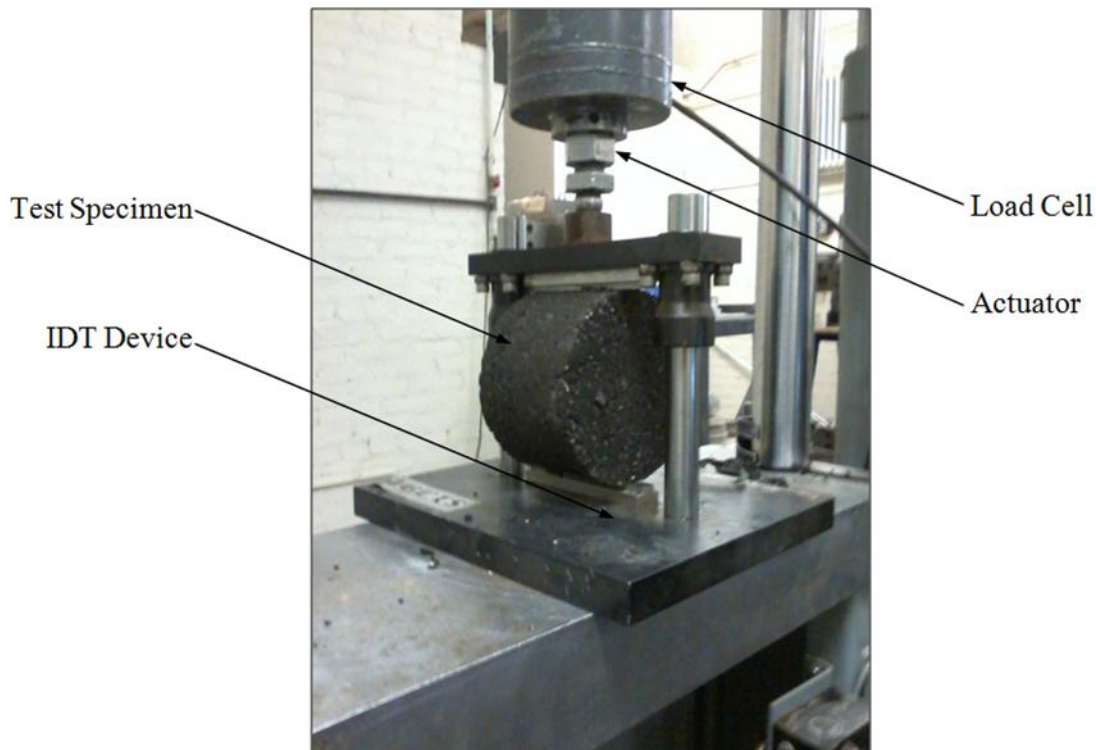
Figure 3.23 Indirect Tensile Strength Test in Progress

3.4.3 Four Point Bending Beam Fatigue Test (FTG)

In the present study, fatigue life of asphalt mixes was evaluated by testing beam specimens using a four-point bending beam fatigue (FTG) apparatus, according to AASHTO T321 standard test method (AASHTO, 2010). For this purpose, 406 mm (L) by 152 mm (W) by 76 mm (H) slab samples were compacted using a linear kneading compactor, shown in Figure 3.24. The weights of the asphalt mix used for compaction of slab samples were adjusted so as to attain air voids of 7.0 ± 0.5%. Thereafter, two beam specimens (380 mm (L) by 63 mm (W) by 50 mm (H)) were saw cut from each above mentioned slab, shown in Figure 3.25. Each beam specimen was then subjected to cyclic loading and unloading with a frequency of 10 Hz, inside a temperature chamber at 20°C, as recommended by AASHTO T321 (AASHTO, 2010). Figure 3.26 shows the beam specimen and fatigue fixture before starting the test. In this study, the beam fatigue tests were conducted at a deflection level of 400 micro-strain. A 5 kN (1100 lbf.) load cell was used to measure the loads applied to the beam specimen. A LVDT with a maximum stroke length of ±1mm (0.04 in.), mounted on a target glued at the center of the beam was used to measure the vertical deformation of the beam. The initial stiffness was determined at the 50th load cycle. The total number of load repetitions leading to a 50% reduction in the initial stiffness was considered as the test termination criterion, and was reported as the fatigue life (AASHTO, 2010). Figure 3.27 shows the GCTS ATM-100, used for conducting the FTG tests.

Figure 3.24 Linear Kneading Asphalt Compactor used for Compacting Slab Sample

Figure 3.25 Four-Point Bending Beam Fatigue Specimen with the Metalic Target Mounted

Figure 3.26 Beam Specimen in Fatigue Fixture Inside Temperature Chamber

Figure 3.27 GCTS ATM-100 used for Conducting Four Point Bending Beam Fatigue Tests

3.5   Surface Free Energy Method

The materials and methods used for measuring the surface free energy (SFE) parameters of the aggregates and asphalt binders in this study are discussed in this section. Three different methods were used to evaluate the SFE parameters of the materials, discussed herein: (i) Universal Sorption Device (USD) used for testing aggregates, (ii) Dynamic Wilhelmy Plate Test (WP) used for testing asphalt binder, and (iii) Sessile Drop (SD) test used for testing aggregates and asphalt binder.

3.5.1 Materials used for SFE Evaluation

A PG 64-22 asphalt binder and limestone aggregates were collected from the Valero refinery in Muskogee, OK and from the Dolese Hartshorne quarry in Pittsburg County, OK, respectively. In addition, the SFE components of commonly used aggregates for pavement construction, including granite and basalt, were adopted from the open literature (Buddhala et al., 2011; Bhasin et al., 2007) to evaluate the effect of aggregates' source and types on energy components and moisture-induced damage potential of asphalt binder-aggregates systems. Three different WMA-additives, namely Sasobit®, Advera®, and Evotherm®, were used in the present study. These additives are currently used in practice to produce WMA mixes. A brief description of each of the additives is provided in this section.

Advera® WMA is a product of PQ Corporation, Malvern, PA. It is a synthetic zeolite (Sodium Aluminum Silicate) containing 18 to 21 percent water by weight entrapped in its crystalline structure. This water releases at temperatures above 99°C (210°F), and creates a foaming of the asphalt binder in the mix. The released water and foaming effect improve the workability of the asphalt mix, with a minor increase in binder volume. This process enables lower production and placement temperatures by 28°C (50°F) to 39°C (70°F) compared to conventional HMA production and placement temperatures (Corrigan, 2011). PQ Corporation recommends use of 0.25% Advera® by weight of the mix, or 5 pounds of Advera® per ton of asphalt mix to gain desired workability at a lower temperature. According to the manufacturer, workability improvements can occur in many different types of mixes including those with higher

reclaimed asphalt pavement (RAP) contents. Due to its inorganic nature, Advera® does not alter the performance grade (PG) of the asphalt binder. The plants currently manufacturing Advera® are located in Jeffersonville, Indiana and Augusta, GA (Corrigan, 2011).

Sasobit® is a fine crystalline, long chain aliphatic hydrocarbon, known as an "asphalt flow improver" (Corrigan, 2011). Sasobit® is a type of paraffin wax, produced by conversion of carbon monoxide into higher hydrocarbons in catalytic hydrogenation followed by a distillation process, called Fischer-Tropsch (FT) synthesis. The final product consists of a long chain of 40 to 115 carbon atoms. Due to its very long molecular chain and fine crystalline structure, compared to those of naturally occurring bituminous waxes, Sasobit® has a melting point of around 99°C (210°F). This molecular structure results in complete solubility of Sasobit® in asphalt binder at temperatures in excess of 116°C (240°F). Sasobit® decreases the viscosity of the asphalt binder, which in turn makes it possible to drop the production temperatures by 10°C (18°F) to 30°C (54°F) (Corrigan, 2011). The manufacturer recommends use of 0.8 percent to 3.0 percent Sasobit® by the weight of the asphalt binder, to gain desired reduction in viscosity (Hurley and Prowell, 2005). Sasobit® for the current study was obtained from Sasol Wax plant, located in Richmond, CA.

Evotherm® is a product of MeadWestvaco Asphalt Innovations, Charleston, SC (Button et al., 2007). Evotherm® uses a non-proprietary technology that is based on a chemical package that includes cationic emulsification agents, such as the additives to improve aggregate coating, mix workability, and compactions as well as to promote adhesion (anti-stripping agents). Evotherm® utilizes a high-residue emulsion (approximately 70 percent binder) that improves adhesion between the asphalt binder and the aggregate. The product enhances mix workability at lower temperatures (Prowell and Hurley, 2007). A chemical additive technology and a dispersed asphalt technology delivery systems are used in the production of Evotherm® WMA. According to the manufacturer, a unique chemical compound customized for aggregate compatibility is delivered into an emulsion (dispersed) asphalt phase (Corrigan, 2011). Based on the MeadWestvaco reports, field testing of WMA with Evotherm® shows a 56°C (100°F) reduction in production temperature (Corrigan, 2011).

3.5.2 Universal Sorpltion Device (USD) Tests on Aggregates

The SFE components of selected limestone aggregate were measured using a SGA - 100 Universal Sorption Device (USD) and applying the methodology discussed by Bhasin and Little (2007), according to Table 3.5. The probe vapors of known SFE components, namely water, n-hexane, and methyl propyl ketone (MPK) were used to determine adsorption isotherms. A total of 9 aggregate samples were tested in the USD. Thereafter, Equations 2.33 and 2.36, discussed in Chapter 2, were used to determine the work of adhesion, and work of debonding in asphalt binder-aggregate systems, respectively.

Table 3.5 The materials Tested using USD and WPT Test Methods

Material	Types of Additives	Percentage of Additives*	Solvents	No. of Samples
PG 64-22	Sasobit®	0%, 1.0%, 1.5% and 2.0%	Water, Glycerin and Formamide	36
	Advera®	0%, 0.25%, 0.30 and 0.35%	Water, Glycerin and Formamide	36
	Evotherm®	0%, 0.25%, 0.50% and 0.75%	Water, Glycerin and Formamide	36
Limestone Aggregate		Set 1	Water	3
		Set 2	MPK	3
		Set 3	n-Hexane	3

The SGA -100 from VTI Corporation, used for conducting USD test, is a gravimetric sorption device designed for water and organic vapor sorption studies of materials. This technique works based on the development of a vapor sorption isotherm, i.e. the amount of vapor adsorbed, or desorbed, on the solid surface at a fixed temperature and partial pressure. The range of relative pressure (RP) can be designed from 0.02 to 0.98 and temperatures from 5° to 60°C. At each relative humidity (RH) or pressure step, the system monitors sample weight until equilibrium condition. Sample weight, temperature, and RH or RP are recorded in a data file. Identical conditions of temperature and humidity for a sample and a reference are achieved by using a symmetrical two-chamber aluminum block. Sample weight changes are recorded using a Cahn D-101 microbalance. Photographic views of the SGA -100 Water Vapor Sorption Analyzer is shown in Figure 3.28. To prepare aggregate samples for testing, aggregates were crushed from limestone rock. The portion passing No. 4 and retaining No. 8 sieves was selected and washed several times with distilled water to obtain a dust-free and clean surface of aggregates (Figure 3.29). Then the aggregate sample

was oven dried at 120°C for 12 hours and allowed to cool to room temperature in a desiccator sealed with silica gel. About 20 grams of aggregate was used to conduct one USD test. Test was repeated at least three times using each probe vapor to ensure consistency of the results.

Figure 3.28 Photographic View of SGA -100 USD Device

Figure 3.29 Aggregate Samples Prepared for USD Test

3.5.3 Dynamic Wilhelmy Plate (WP) Test on Asphalt Binder

The selected asphalt binder (i.e., PG 64-22) was modified with different amounts of Sasobit® (i.e., 1.0%, 1.5% and 2.0% by weight of asphalt binder), Advera® (i.e., 0.25%, 0.30% and 0.35% by weight of asphalt mix) and Evotherm® (i.e., 0.25%, 0.50% and 0.75% by weight of asphalt binder) (Table 3.5). The selection of the amounts of these additives was made based on their optimal dosages, as recommended in the literature or by the manufacturer. The SFE components of modified asphalt binders and neat asphalt binder were determined based on the measurement of the contact angles. Contact angles of asphalt binders were measured in the laboratory using the Wilhelmy Plate Test with using three different solvents of known SFE components, namely water, glycerin and formamide, according to the methodology used by Wasiuddin et al. (2007). A total of 108 asphalt binder samples were prepared in the laboratory and tested for contact angles. A brief description on Dynamic Contact Angle (DCA) measurements of asphalt binder is given below.

To prepare the asphalt binder samples, the bulk PG 64-22 asphalt binder was heated in the oven, according to the recommended temperatures for neat and modified asphalt binders for two hours. After two hours of heating, the asphalt binder was separated into small canisters. A photographic view of the separated asphalt binder specimens is shown in Figure 3.30. To measure DCA, a 24mm x 50mm glass plate was coated with asphalt binder. To maintain sufficient coating of asphalt binder, the glass plate was dipped in liquid asphalt binder and moved back and forward three times, in approximately five seconds. Thereafter, it was held out of the asphalt binder for another five seconds to let the excessive asphalt binder start to drop off the plate. Then the sample was placed in the oven upside down for two minutes to gain surface uniformity. Finally the sample was placed in the desiccator for 24 hours, prior to testing. The WP samples are shown in Figure 3.31. After the curing, each sample was visually inspected for any defects, specifically small air bubbles, on their surface or edges. In the case of any defects, the sample was discarded as it may cause significant variations in measurement of the contact angle. Then sample was attached to the microscale of the DCA device and WP procedure was initiated. The WP tests were conducted using asphalt binder in contact with Water, Glycerin and Formamide as solvents. The tests

with each of the above mentioned solvents were performed using a minimum of three replicates to ensure repeatability of the test and consistency of results. At least, twelve sets of DWP tests were conducted for each solvent and each percentage of WMA-additive, resulting in a total of thirty six DWP tests. Photographic views of the DCA device and DWP test in progress are shown in Figure 3.32 and Figure 3.33, respectively.
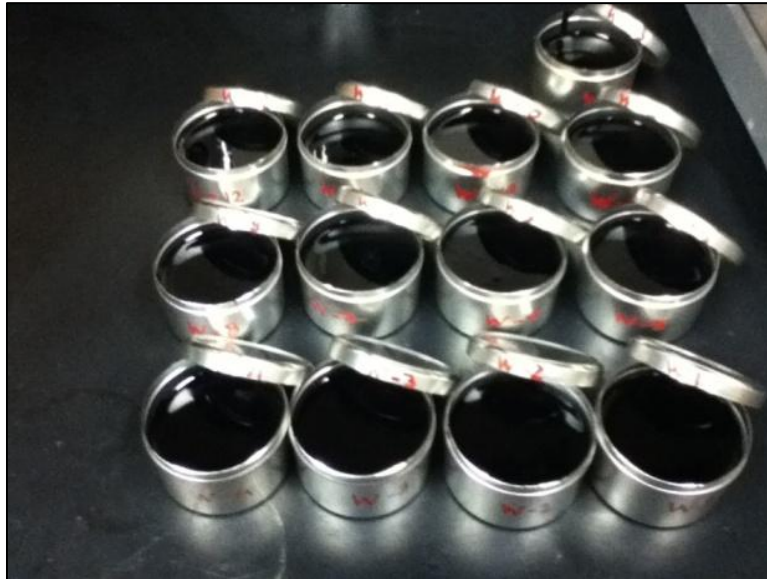
Figure 3.30 PG 64-22 Asphalt Binder Separated in Small Canisters
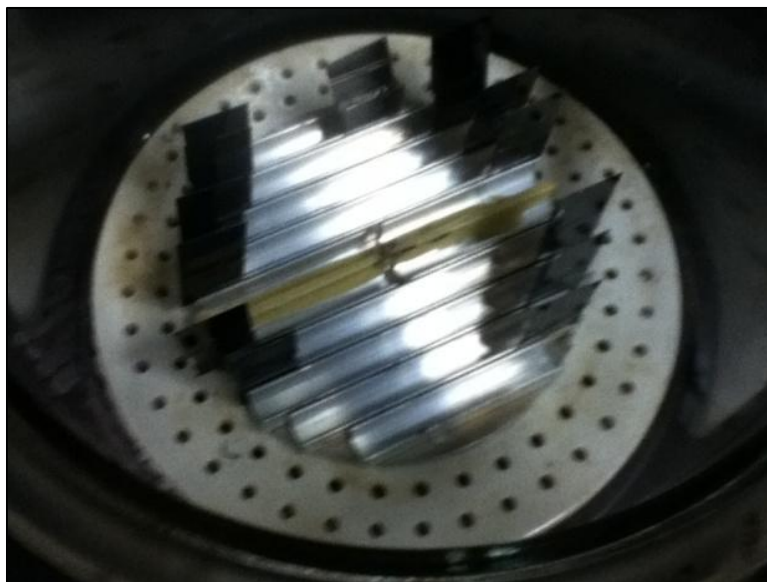
Figure 3.31 Curing WP Samples in Desiccator
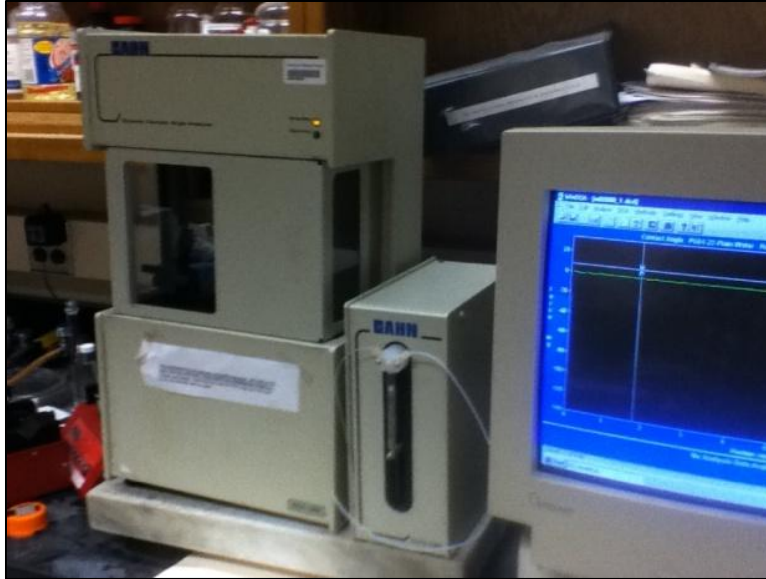
Figure 3.32 Photographic View of DCA Device

Figure 3.33 Photographic View of WP Test in Progress

3.5.4 Sessile Drop Test (SD) on Aggregates

In this section the sample preparation of aggregate specimens and contact angle measurements with Sessile Drop (SD) technique are discussed. The testing protocol introduced below includes cutting, polishing, cleaning, and drying protocols for aggregates. The sample preparation for asphalt binder is very similar to the sample preparation technique used for the Wilhelmy Plate method (Yildirim, 2001).

As part of this study, a testing protocol has been developed for the direct measurements of contact angles on aggregate specimens using the Sessile Drop device. Two different Oklahoma aggregates: Davis Limestone and Snyder Granite were tested in this research study. All measurements on the aggregates were done with high purity probe liquids, namely Water, Diiodomethane, and Ethylene Glycol.

The development of the testing protocol for aggregates for SD method is outlined in detail in this section. Large aggregate specimens (rocks) ranging in size from about 5 cm to about 20 cm in average diameter were obtained from different rock quarries in Oklahoma. Contact angle measurements can be conducted on small diameter (as small as 1 cm in diameter) specimens; however, it is more convenient to perform the tests on larger diameter specimens. The larger diameter specimens are easier to cut using a heavy duty saw. In order to measure contact angles on the aggregate surfaces using the Sessile Drop device, the aggregate surfaces must be relatively flat, smooth, and clean. It is, therefore, more practical to obtain flat surface aggregate specimens from relatively large size rocks.

- The rocks were cut with thicknesses varying from about 1 cm to about 2 cm using mechanical diamond saws. The Covington Engineering Heavy Duty Slab Saw at OSU was employed for cutting smaller size rocks and the Hillquist RF 20-24 Slab Saw at OSU (Figure 3.34) was employed for obtaining larger size, flat rock surfaces.
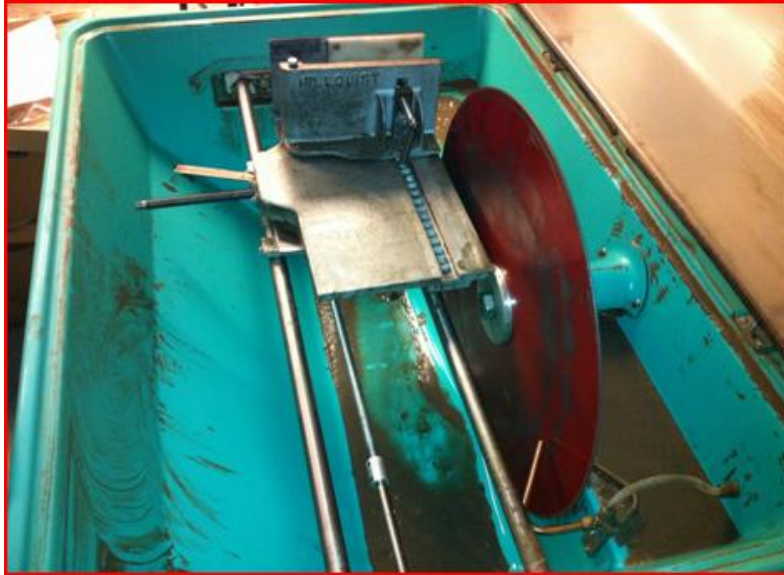
Figure 3.34 Hillquist RF 20-24 Slab Saw

Although the diamond saws have done a very good job in creating nice flat surfaces, there were still traces caused by the blades. To remove those traces and to reduce the amount of roughness on a sample, a polishing test was undertaken using different grades of specific silicon carbide grit powders. The polishing device has a circular plate which basically spins with the silicon carbide powder mixed with the water on the plate (Figure 3.35).

- The flat surfaces of the rock specimens are hold against the spinning plate for about 10 minutes.

- In order to achieve smoother surfaces, glass plates for specific silicon carbide grades were also used.

- In this stage of polishing process, the silicon carbide grits were saturated with water on the glass surface until the mixture achieved the form of a paste. Then the aggregates were put onto the paste and moved around the surface of the glass with a uniform pressure applied by hand.

- Davis limestone and Snyder granite samples were polished using number 200, 400, 600, and 1000 grade silicon carbide grits (Figure 3.36 and Figure 3.37).

The roughness of the sample surface plays a vital role in direct contact angle measurements. Polishing the aggregates with 1000 grade silicon carbide grits made a considerable difference in repeatability, reliability, and standard deviation of contact angle measurements. All the test results are given in the next chapter.

Figure 3.35 The Polishing Device
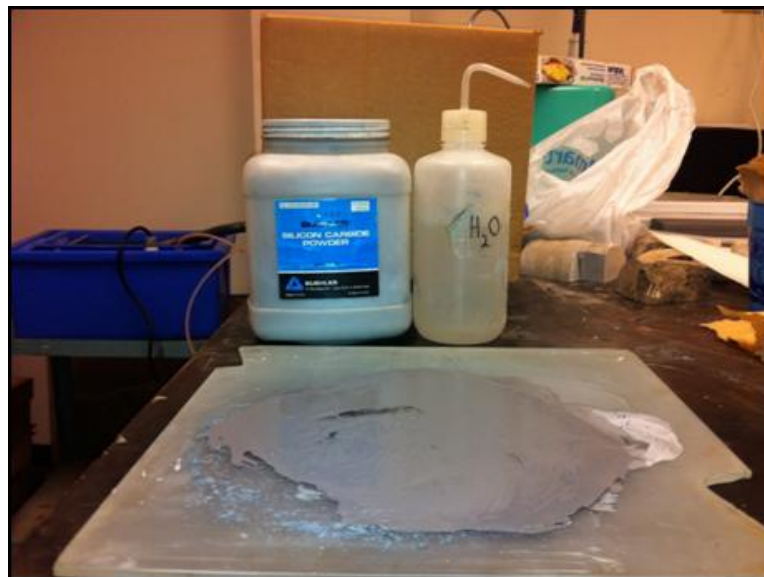
Figure 3.36 Silicon Carbide Grits
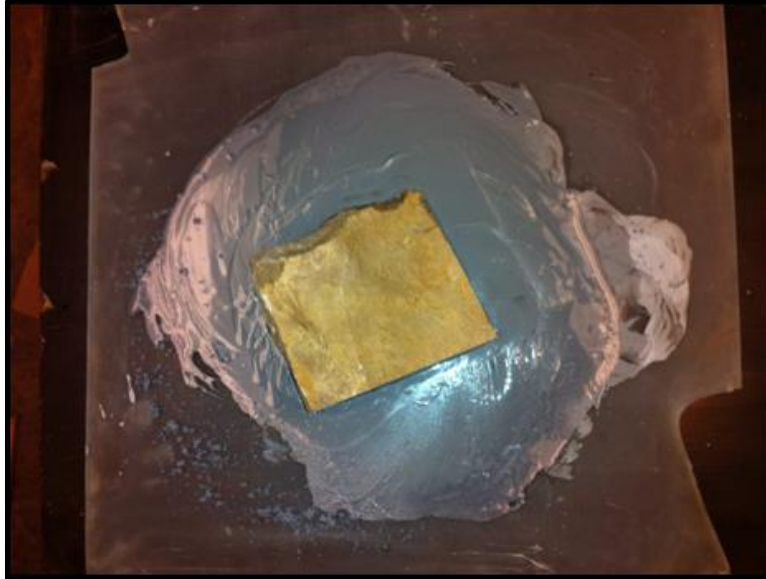
Figure 3.37 Application of Silicon Carbide Grits on a Specimen

During the cutting and polishing processes, the aggregates are usually contaminated with oil and grit powder material. Since oil and soap changes the cohesive and adhesive properties of solids (i.e., aggregates). Any change in the surface properties of the materials will change the surface tension and contact angles directly. For this reason, a cleaning protocol was applied as follows.

- In order to remove the oil and grit powder material from the surface of the aggregates, the samples were washed thoroughly with soap and warm distilled water.

- The flat rock specimens then were cleaned using Hexane. Paper towels were put in a pan and saturated with Hexane (Figure 3.38). Both surfaces of each flat rock specimens were rubbed by wet paper towels to remove the residues of the oil used in the diamond saw cutting process.

Figure 3.38 Cleaning the Sample with Hexane

Contact angle measurements must be performed on relatively dry specimens for representative measurements without the interferences of moisture on the results.

- After the cleaning process, the rock specimens were put inside an oven at $105\pm5^{o}C$ for 12 hours.

- The samples were then allowed to cool down to room temperature in a desiccator with anhydrous calcium sulfate crystals (Figure 3.39 and Figure 3.40).

Figure 3.39 The Desiccator with Anhydrous Calcium Sulfate Crystals
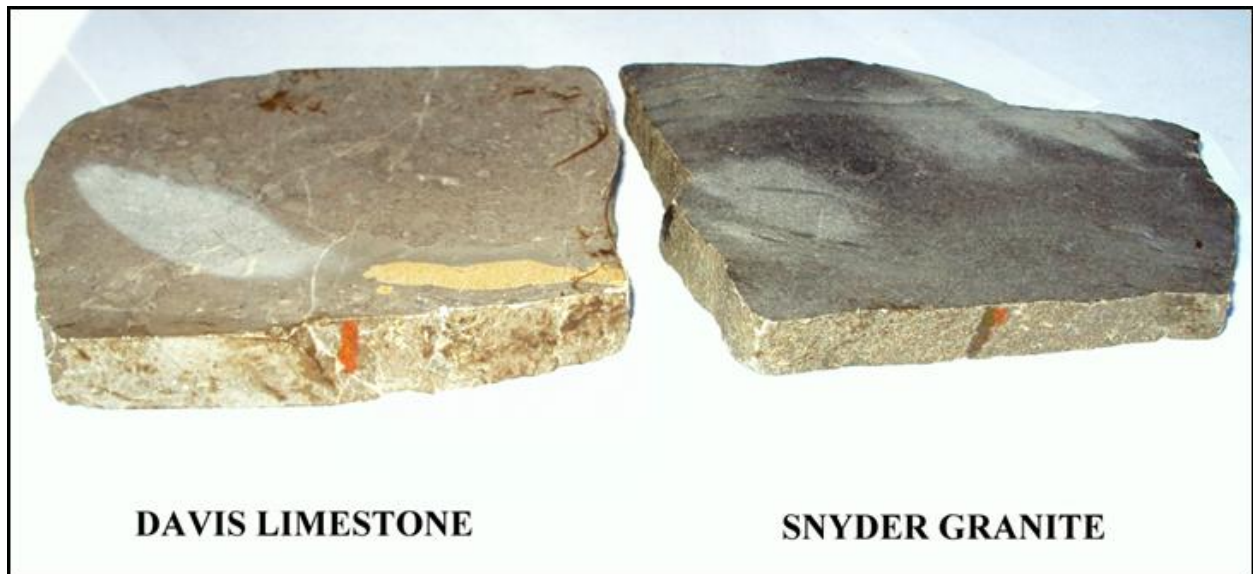
Figure 3.40 Davis Limestone and Snyder Granite Samples Before the Measurements

Once the sample preparation of aggregates is done as given in the preceding section, the contact angles of the samples with three different probe liquids (Water, Diiodomethane, Ethylene Glycol) are determined using the Sessile Drop device. The following process is followed in multiple sets for each sample with each probe liquid until the desired repeatability and standard deviation are achieved.

- The syringe that contains the probe liquid is refilled before the test. If a different probe liquid is going to be used, the syringe should also be replaced.

- The SD device is calibrated before each set (see Appendix A).

- Once the device is calibrated and the samples are at the testing temperature (i.e., at room temperature), the specimen is taken out of the desiccator and placed under the needle attached to the syringe in the automated pump system. Figure 3.41shows the exact location of the specimen in the Sessile Drop device.
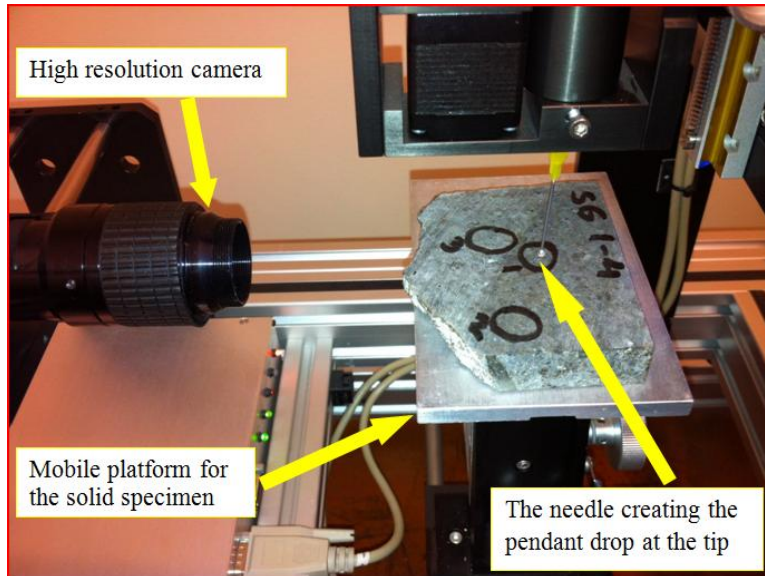
Figure 3.41 The placement of the solid specimen in the FTA 1000B

- About 10-15 μL of probe liquid is dispensed from the needle using the FTA software.

- While the liquid is still in the form of a pendant drop, the platform that holds the specimen is elevated slowly until the specimen touches the drop.

- The drop detaches from the needle and forms the Sessile Drop on the flat surface of the specimen.

- The high resolution camera constantly captures the images of the liquid-solid interface and sends it to the software to process. The number of the images per second and test duration can be adjusted from the software. In this study, three images per second are used. The time period for a single test was 45 seconds (Figure 3.42).

- Finally, the software processes each image and determines the average contact angles.
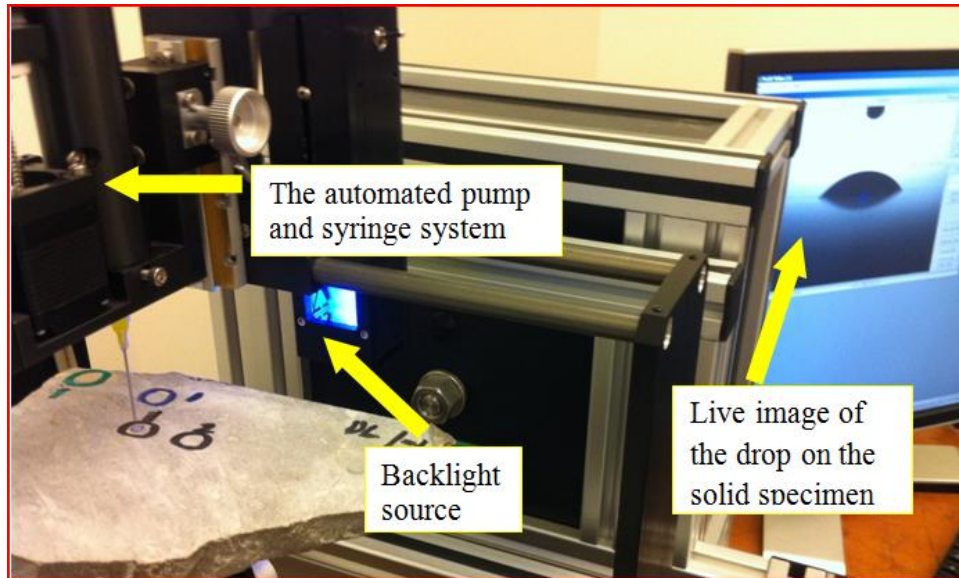
Figure 3.42 FTA 1000B Capturing the Images of a Solid Specimen to Determine the Contact Angles

3.5.5 Sessile Drop Test (SD) on Asphalt Binder

In this study, a PG 64-22 asphalt binder has been used (Figure 3.43). The sample preparation and testing protocols for the neat asphalt binder specimens with and without Warm Mix Asphalt (WMA) additives (Sasobit®, Permatac Plus®, and Evotherm®) are given in this section.

Sample preparation protocol for asphalt binder in Sessile Drop (SD) method is very similar to the sample preparation protocol for the Wilhelmy Plate (WP) method. However, SD method has two differences with WP. Firstly, larger surface area specimens can also be used in the SD method. Second and more significant benefit of SD is that it measures the contact angles *directly* while the WP measurements are based on the force equilibrium, and thus the contact angles are inferred *indirectly*. A detailed testing protocol for asphalt binders using the Wilhelmy Plate can be found in Lytton et al. (2005). The sample preparation process of asphalt binder for the SD device is given next.

Figure 3.43 PG 64-22 Binder Sample from Muskogee, Oklahoma

- For specimen preparation, the bulk asphalt binder sample (Figure 3.43) is heated in the oven at 105±5°C for one hour.

- After gaining some viscosity, the bulk material is divided into number of small canisters (Figure 3.44). The sample is divided into a number of canisters for maintaining the same level of aging for each consequent contact angle measurements using the Sessile Drop device.

Figure 3.44 PG 64-22 Binder Divided into a Number of Tin Canisters and Kept in the Oven

- Before each contact angle measurement, a canister with the binder inside is put into the oven at 105±5°C for a period of one hour.

- After heating the binder, a plain microscopic glass slide with 76 mm x 25 mm x 1 mm dimensions is dipped into the melted binder for a few seconds and then held out of the canister for another few seconds to let the excessive binder drop off the glass (Figure 3.45). This process is repeated a few times, if necessary, to obtain a flat and smooth surface area of the binder on the glass surface.

- The specimen is then allowed to cool down to room temperature in a desiccator with anhydrous calcium sulfate crystals overnight.

Figure 3.45 PG 64-22 Grade Asphalt Binder in Small Canisters and Glass Slide Specimen

Aside from the neat binder, the contact angle measurements can also be done on the binder samples mixed with the warm mix asphalt (WMA) additives using the Sessile Drop device. Three WMA additives (Sasobit®, Permatac Plus®, and Evotherm®) with different percentages (0.5%, 1.0%, and 1.5%) were used in this study. The sample preparation protocol for binder with WMA additives is almost same as the sample preparation for the neat binder.

- For specimen preparation, the bulk asphalt binder sample is heated in the oven at 105±5°C for one hour.

- After gaining some viscosity, the whole bulk material is divided into number of small canisters.

- The sample is divided into a number of canisters for maintaining the same level of aging process for each consequent contact angle measurements using the Sessile Drop device.

- Using an electronic scale, the binder samples are mixed with the corresponding percentages (by weight) of each additive.

- Each sample is kept in a different canister.

- Before each contact angle measurement, a canister with the binder inside is put into the oven at 105±5°C for one hour stirring occasionally for homogeneous distribution of the WMA additive in the mixture.

- After heating the binder, a plain microscopic glass slide with 76 mm x 25 mm x 1 mm dimensions is dipped into the melted binder for a few seconds and then held out of the canister for another a few seconds to let the excessive binder drop off the glass. This process is repeated a few times, if necessary, to obtain a flat and smooth surface area of the binder on the glass surface.

- The specimen is then allowed to cool down to room temperature in a desiccator with anhydrous calcium sulfate crystals overnight.

After the sample preparation, contact angle measurements on the PG 64-22 binder from Ergon, Muskogee, Oklahoma were conducted using the SD method. For each probe liquid, three glass slides were prepared. In total, six measurements were conducted for every probe liquid (two measurements on each slide). The glass slides were disposed after two measurements with the same probe liquid. This process was repeated for all three probe liquids. The contact angle measurements of the binder samples are done with three different probe liquids (Water, Diiodomethane, Ethylene Glycol) using the SD device. The following process is followed in multiple sets for each sample with each probe liquid.

- The syringe that contains the probe liquid is refilled before the test. If a different probe liquid is going to be used, the syringe should also be replaced.

- The SD device is calibrated before each set (see Appendix A).

- Once the device is calibrated and the samples are at the testing temperature (at room temperature), the specimen is taken out of the desiccator and placed under the needle attached to the syringe in the automated pump system.

- About 10-15 μL of probe liquid is dispensed from the needle using the FTA software.

- While the liquid is still in the form of a pendant drop, the platform that holds the specimen is elevated slowly until the specimen touches the drop.

- The drop detaches from the needle and forms the Sessile Drop on the flat surface of the specimen.

- The high resolution camera constantly captures the images of the liquid-solid interface and sends it to the software to process. The number of the images per second and test duration can be adjusted from the software. In this study, three images per second were used. The time period for a single test was 45 seconds

Finally, the software processes each image and determines the average contact angles. The testing protocol for asphalt binder with WMA additives is identical to testing protocol for the neat binder (Figure 3.46).
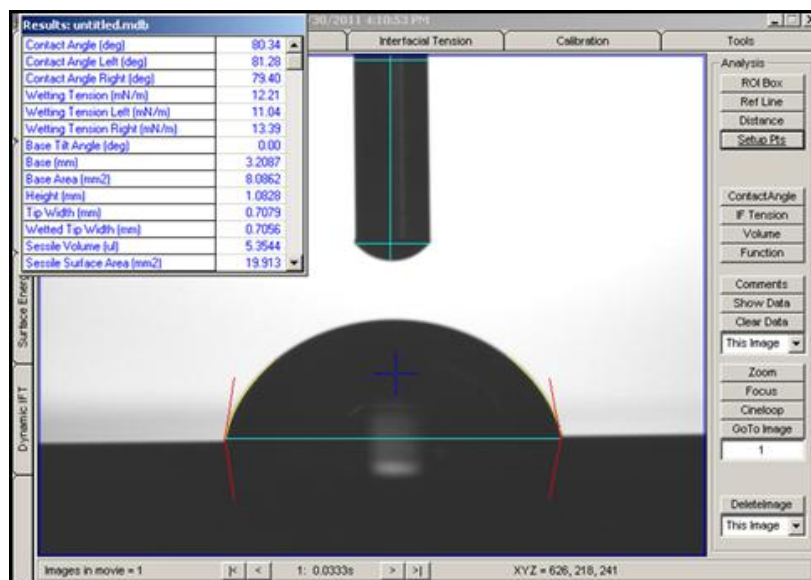
Figure 3.46 The FTA Software Processing a Snapshot of the Sessile Drop on a Solid Specimen

4.1   General

Results from testing of asphalt mixes, aggregates and asphalt binders used in this study are presented and discussed in this chapter. The test results are presented in two major sections: Section 4.1 focuses on the results obtained from the testing of WMA and control HMA, consisting of six asphalt mixes (ADHM, ADWM, EVHM-B, EVWM-B, EVHM-C and EVWM-C). Three different performance tests were conducted for each mix, including HWT, TSR and FTG. These tests were conducted in accordance with OHD L-55 (ODOT, 2009), AASHTO T283, and AASHTO T321 (AASHTO, 2010) standard test methods, respectively. Section 4.2 discusses the SFE test results . This test was conducted on the aggregates and WMA-modified asphalt binders. The results from three different test methods are reported in this section: USD tests conducted on aggregates, WP tests conducted on asphalt binders and SD tests conducted on both asphalt binders and aggregates.

4.2   Asphalt Mix Performance Test Results

4.2.1 Rut and Moisture-Induced Damage Potential Evaluation through HWT Test

The HWT test results for the tested asphalt mixes are presented in Table 4.1. Also for further evaluation of rut and moisture-induced damage potential of asphalt mixes, the average rut values for each mix were calculated and plotted. Graphical comparison of rut and resistance to moisture-induced damage of control HMA and WMA mixes including ADHM vs. ADWM, EVHM-B vs. EVWM-B and EVHM-C vs. EVWM-C are shown in Figure 4.1 through Figure 4.3, respectively.

From Table 4.1 and Figure 4.1, it is evident that ADHM showed an average rut depth of 1.4 mm after 20,000 cycles of wheel passes, which is very close to that of ADWM that exhibited a rut depth of 1.9 mm due to 20,000 wheel passes. None of the above mentioned mixes (ADHM and ADWM) showed any inflection points, which is an indicator of the moisture-induced damage. This may be a result of using anti-stripping agents (Arr Maz AD-Here® HP PLUS) in both asphalt mixes. Also, from Table 4.1, the

measured average inverse creep rate for ADHM was 47,627 cycles/mm, which is 60% higher than that of ADWM (29,683 cycles/mm). This is an indication of better long term rut performance of the ADHM compared to ADWM. This may be attributed to the lower mix production temperature of the ADWM (130 °C/ 266 °F) compared to control ADHM (160 °C/ 320 °F). Figure 4.4 and Figure 4.5 present photographic views of the ADHM and ADWM samples after 20,000 wheel passes in the HWT test, respectively.

Table 4.1 Summary of the Hamburg Wheel Tracking Tests on Asphalt Mixes

Mix Type	Set No.	Max Deformation		Rut Depth (mm)				Rutting Rate		Inflection Point	
		Cycles to Max. (cyc.)	Deformation (mm)	5,000 Passes	10,000 Passes	15,000 Passes	20,000 Passes	Creep (cyc./mm)	Stripping (cyc./mm)	Passes (cyc.)	Deflection (mm)
ADHM	Set-1	20,000	1.3	1.0	1.2	1.3	1.3	51,181	-	>20,000	-
	Set-2	20,000	1.5	1.1	1.2	1.3	1.4	44,535	-	>20,000	-
	Average	20,000	1.4	1.1	1.2	1.3	1.4	47,627	-	>20,000	-
ADWM	Set-1	20,000	1.8	1.3	1.5	1.6	1.6	33,333	-	>20,000	-
	Set-2	20,000	2.1	1.5	1.8	1.9	2.1	25,700	-	>20,000	-
	Average	20,000	1.9	1.4	1.6	1.8	1.9	29,683	-	>20,000	-
EVHM-B	Set-1	20,000	1.4	1.0	1.2	1.3	1.4	38,404	-	>20,000	-
	Set-2	20,000	1.5	0.9	1.1	1.3	1.5	25,857	-	>20,000	-
	Average	20,000	1.5	0.9	1.1	1.3	1.4	30,906	-	>20,000	-
EVWM-B	Set-1	20,000	1.7	1.1	1.3	1.6	1.7	27,344	-	>20,000	-
	Set-2	20,000	1.8	1.1	1.3	1.7	1.8	28,414	-	>20,000	-
	Average	20,000	1.7	1.1	1.3	1.6	1.7	27,879	-	>20,000	-
EVHM-C	Set-1	20,000	2.2	1.6	1.8	2.0	2.1	34,956	-	>20,000	-
	Set-2	20,000	2.2	1.3	1.6	1.9	2.2	16,172	-	>20,000	-
	Average	20,000	2.2	1.4	1.7	2.0	2.2	22,031	-	>20,000	-
EVWM-C	Set-1	20,000	3.6	1.8	2.3	2.7	3.6	11,332	5,422	16,159	2.8
	Set-2	20,000	9.3	2.3	3.2	5.8	9.3	5,254	1,440	12,064	3.9
	Average	20,000	6.4	2.1	2.8	4.3	6.4	7,127	2,314	12,593	3.4
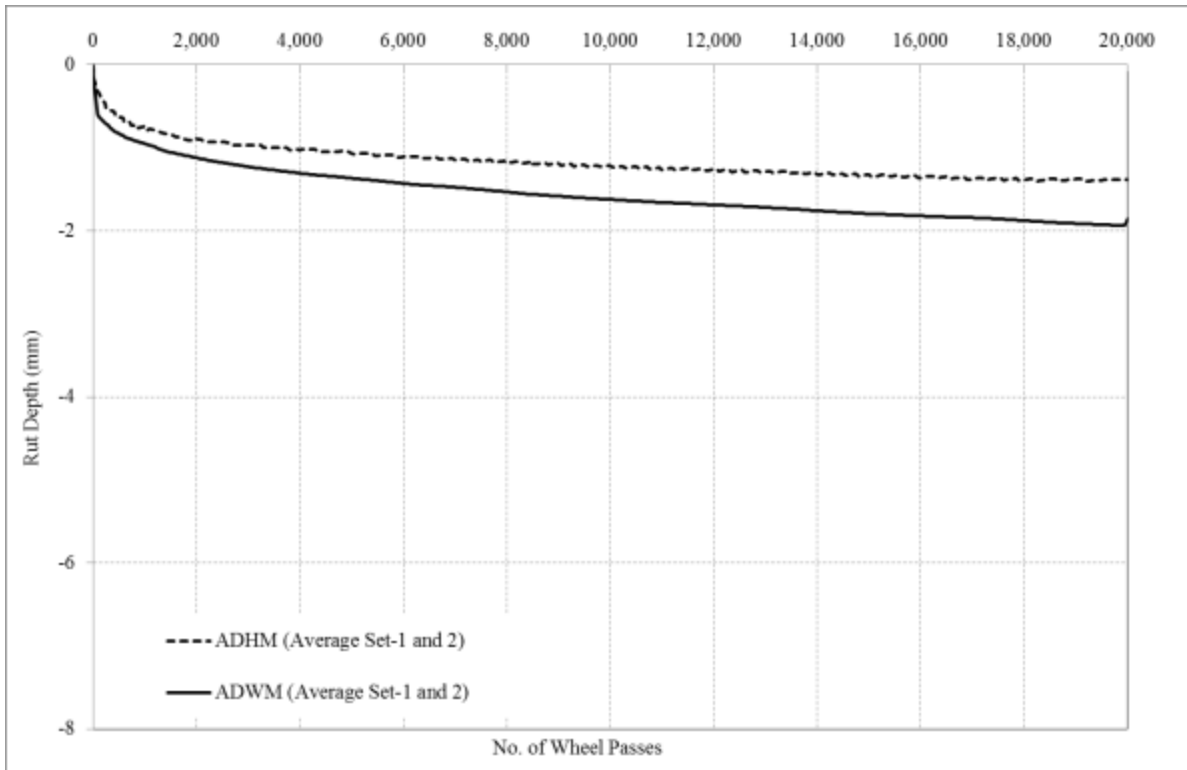
Figure 4.1 Hamburg Wheel Tracking Curves for ADHM and ADWM Mixes
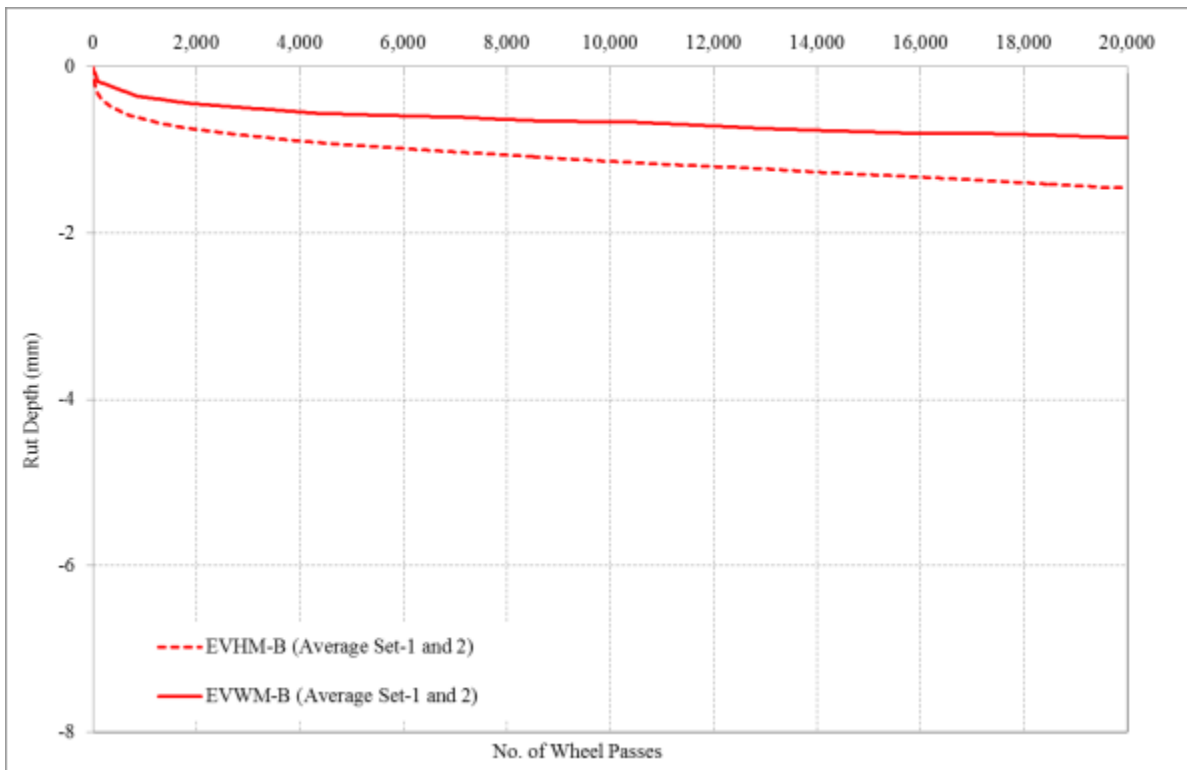
Figure 4.2 Hamburg Wheel Tracking Curves for EVHM-B and EVWM-B Mixes
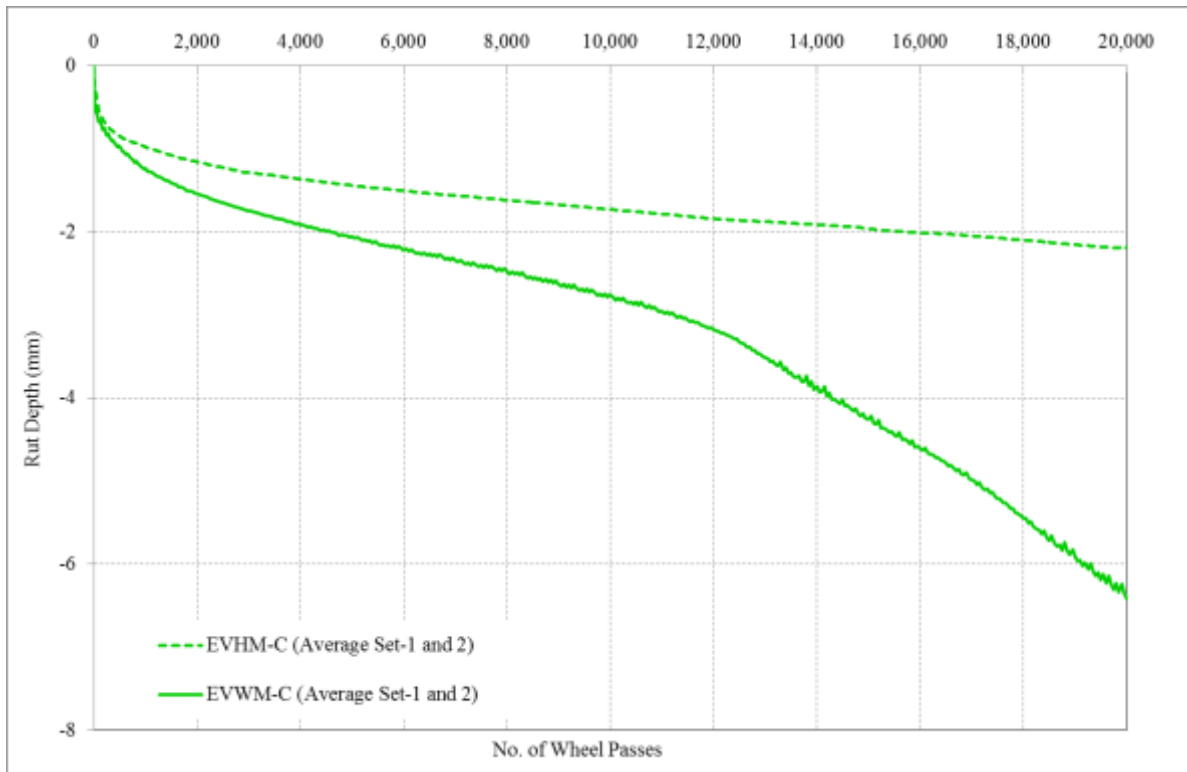
Figure 4.3 Hamburg Wheel Tracking Curves for EVHM-C and EVWM-C Mixes
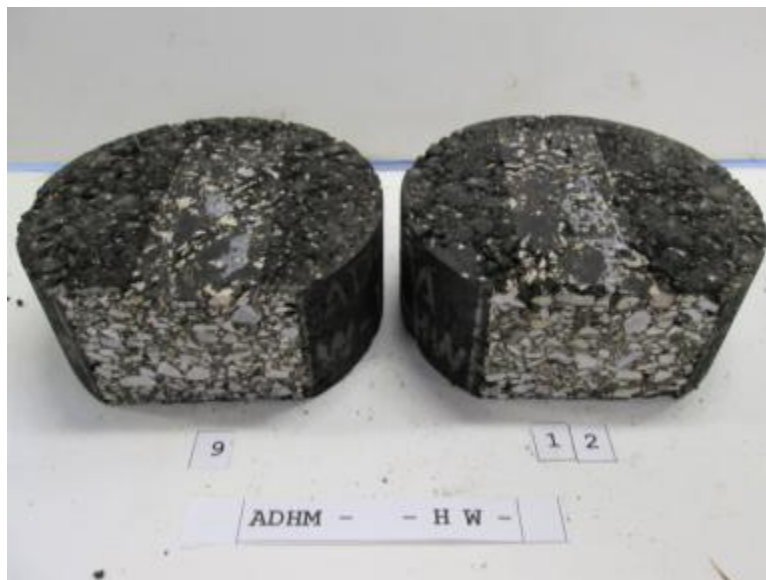
Figure 4.4 ADHM Samples after Hamburg Wheel Tracking Test

Figure 4.5 ADWM Samples after Hamburg Wheel Tracking Test

According to Table 4.1 and Figure 4.2, it was found that EVHM-B showed an average rut depth of 1.5 mm after 20,000 cycles of wheel passes, which is considered to be negligibly lower than that of EVWM-B, with an average rut depth of 1.7 mm, after 20,000 wheel passes. From Figure 4.2 one can say that none of the above mentioned mixes (EVHM-B and EVWM-B) showed any distinct inflection points, which is as an indicator of the resistance against stripping and moisture-induced damage. It should be noted that no anti-stripping agent is used in this case. Acceptable resistance to moisture-induced damage of the EVHM-B and EVWM-B may be attributed to their aggregate and asphalt binder compatibility, which will be further discussed in this report. Also, from Table 4.1 the measured average inverse creep rate for EVHM-B was 30,906 cycles/mm, which is slightly (11%) higher than that of EVWM-B (27,879 cycles/mm). This is an indication of better long term rut performance of the EVHM-B compared to EVWM-B. This may be attributed to the lower mix production temperature of the EVWM-B (135 °C/ 275 °F) compared to control EVHM-B (160 °C/ 320 °F). Figure 4.6 and Figure 4.7 present photographic views of the EVHM-B and EVWM-B samples after 20,000 wheel passes in HWT test, respectively.

86

Figure 4.6 EVHM-B Samples after Hamburg Wheel Tracking Test

Figure 4.7 EVWM-B Samples after Hamburg Wheel Tracking Test

From Table 4.1 and Figure 4.3, it was observed that EVHM-C showed an average rut depth of 2.2 mm after 20,000 cycles of wheel passes, which is significantly lower than that of EVWM-C, which showed an average rut depth of 6.4 mm, after 20,000 wheel passes. From Figure 4.3 it is observed that all three characteristic moisture-induced damage regions are evident in EVWM-C mix. EVWM-C becomes prone to moisture-induced damage and stripping aggregates from asphalt binder starts at an inflection point after 12,593 cycles of wheel passes with an inverse stripping rate of 2,314 cycles/mm. It is worth noting that since the number of the wheel passes

87

corresponding to the inflection point is greater than 10,000 cycles, EVWM-C passes the mix design requirements for resistance against moisture-induced damage. According to FHWA (2012), an inflection point below 10,000 wheel passes indicates significant moisture-induced damage potential of the mix. On the other hand, Figure 4.3 shows that there is no detectable inflection point associated with EVHM-C. Moisture-induced damage on EVWM-C was observed, while lime was used as an anti-stripping agent. It may be an indication of possible incompatibility between the aggregate-asphalt binder-lime and chemical WMA additive, used for production of EVWM-C. Also from Table 4.1 the measured average inverse creep rate for EVHM-C was 22,031 cycles/mm, which is 68% higher than that of EVWM-C (7,127 cycles/mm). This is an indication of better long term rut performance of the EVHM-C compared to EVWM-C. This may be attributed to the lower mix production temperature of the EVWM-C (135 °C/ 275 °F) compared to control EVHM-C (160 °C/ 320 °F). Figure 4.8 and Figure 4.9 present the photographic views of the EVHM-C and EVWM-C specimens after 20,000 wheel passes in HWT test, respectively.

Figure 4.8 EVHM-C Samples after Hamburg Wheel Tracking Test

Figure 4.9 EVWM-C Samples after Hamburg Wheel Tracking Test

4.2.2 Moisture-Induced Damage Evaluation through TSR Test

Retained indirect Tensile Strength Ratio (TSR) test in accordance to AASHTO T283 method was applied as an alternate method to HWT test to assess the resistance to moisture-induced damage of the WMA and control HMA mixes. In this test, the strength loss of different asphalt mixes due to moisture conditioning is measured with respect to the unconditioned samples. Table 4.2 presents the dry indirect tensile strength, moisture conditioned indirect tensile strength and TSR values corresponding to each asphalt mix tested in this study.

Table 4.2 TSR Values and Tensile Strengths for Dry and Moisture Conditioned Specimens

Mix Type	Dry Tensile Strength (psi)				Moisture Conditioned Tensile Strength (psi)				TSR
	No.1	No. 2	No. 3	Average	No.1	No. 2	No. 3	Average	
ADHM	288.9	275.0	283.0	282.3	264.9	263.1	258.8	262.3	0.93
ADWM	214.0	214.9	219.0	216.0	144.3	155.5	150.4	150.1	0.69
EVHM-B	252.6	260.2	278.5	263.8	129.5	155.3	147.1	144.0	0.55
EVWM-B	221.8	228.8	220.5	223.7	164.9	152.4	156.1	157.8	0.71
EVHM-C	148.9	184.3	216.8	183.4	141.7	143.5	160.1	148.4	0.81
EVWM-C	143.0	140.1	137.9	140.3	134.3	132.3	133.4	133.3	0.95

Furthermore, conditions of the fractured faces of each asphalt sample subjected to TSR test were examined for visual rating of the extent of stripping, according to

AASHTO T283. Photographic views of the fractured faces of the representative dry and moisture conditioned specimens under indirect tensile strength (IDT) test (as a part of TSR), are shown in Table 4.2.

The visual rating of the extent of moisture-induced damage was performed based on a scale of 1 to 4, ranging from no moisture damage (1) to severe moisture damage (4), defined as below.

- *Rating score 1*: Extent of moisture-induced damage: None – The specimen condition is solid with no evidence of asphalt binder withdrawing from aggregate. After the specimen has air-dried, the appearance is black.

- *Rating score 2:* Extent of moisture-induced damage: Slight – The specimen condition is solid to slightly soft with some evidence of the asphalt binder beginning to withdraw from edges and surfaces of the aggregates. After the specimen has air‑dried, the appearance remains black.

- *Rating score 3:* Extent of moisture-induced damage: Moderate – The specimen condition is soft, easily broken in half, with partial to completely exposed aggregates. After the specimen has air-dried, the appearance is slightly gray.

- *Rating score 4:* Extent of moisture-induced damage: Severe – The specimen condition is soft to falling apart with the majority of coarse aggregate completely exposed and asphalt binder almost nonexistent. After the specimen has air-dried, the appearance is gray.
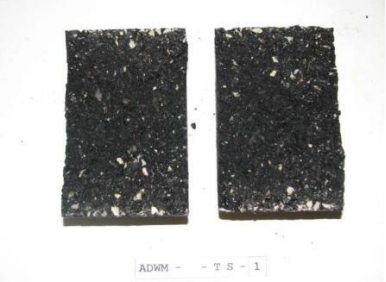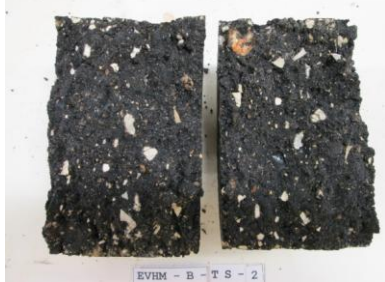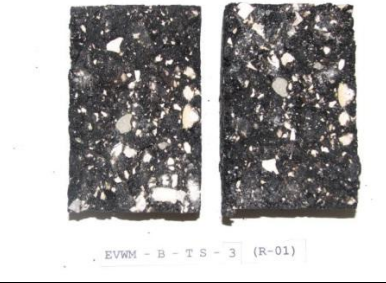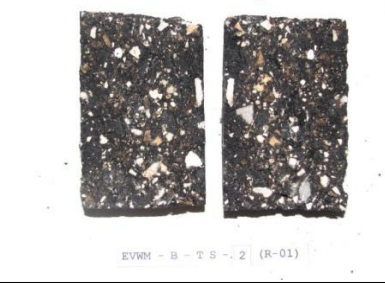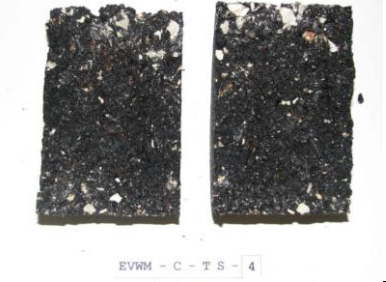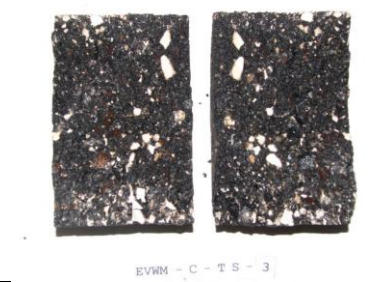
According to Table 4.2, based on the TSR values, only three mixes pass the specification's minimum TSR requirement (0.75 for field mixes). These three mixes are ADHM, EVHM-C and EVWM-C which had TSR values of 0.93, 0.81 and 0.95, respectively. In other words, based on the TSR results, the EVWM-C mix is expected to be the most resistant mix to moisture-induced damage. However, the HWT results, according to Table 4.1, suggest the EVWM-C mix to be the only tested asphalt mix prone to moisture-induced damage, with a detectable stripping inflection point (SIP).

Also, according to Table 4.2, based on the HWT test results, ADWM and EVWM-B mixes performed approximately equally well, against moisture-induced damage when compared to their HMA control mixes (ADHM and EVHM-B, respectively). To this end, a significant difference between the results from the TSR and the HWT tests in term of moisture-induced damage evaluation of the WMA and HMA mixes is observed.

Similar to the HWT test results, the visual fractured face rating as an extent of the moisture-induced damage shows that the EVWM-C is expected to have a high moisture-induced damage potential with a rating of 3 (see Table 4.3). The other five mixes do not show a high rating (ranging from 1 to 2), which is comparatively similar to the HWT test results.

In addition, according to Table 4.2, the EVWM-C mix has the lowest average conditioned indirect tensile strength (CIDT) value, compared to the other asphalt mixes tested for TSR. In the case of sufficient evidence as a result of future study on a larger number of mixes, the latter observation may suggest the use of (some form of) CIDT value instead of TSR, as an indicator of moisture-induced damage. Thus, a minimum CIDT value may also be considered as a pass/fail criterion of a mix. Further study of the data from the TSR and HWT tests was carried out to investigate the possible correlations between the rutting potential and IDT test results. Figure 4.10 shows the variations of rut depth at 20,000 wheel passes with dry IDT (DIDT) values of tested asphalt samples, resulting from HWT and TSR tests, respectively. As expected, from Figure 4.10 it was observed that the rut depths decrease as the DIDT of the tested asphalt samples increase.

Table 4.3 Fractured Faces of Asphalt Mixes, and Moisture-Induced Damage Visual Ratings of TSR Test

Mix Type	Fractured Section		Visual Inspection Rating of Stripping
	Tested in Dry Condition	Moisture Conditioned	
ADHM	Picture not Available	Picture not Available	2
ADWM			1
EVHM-B			2
EVWM-B			2
EVHM-C			2
EVWM-C			3
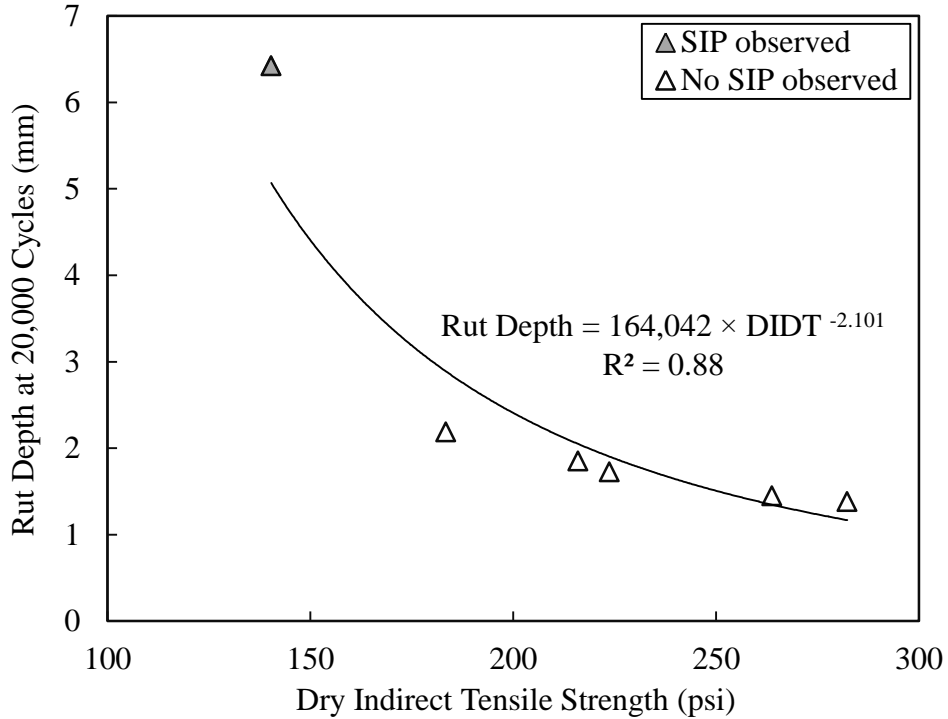
Figure 4.10 Variations of Average Rut Depth with Dry Indirect Tensile Strength of Asphalt Mixes

Also, a regression model in the form of a power equation was developed and displayed on the chart. The coefficient of determination calculated for this model (Rut Depth = 164,042 x DIDT$^{-2.101}$) is 0.88, which is an indication of good correlations between the measured rut depths (mm) and DIDT values (psi). The rut depths shown in Figure 4.10 are the deformations measured on the asphalt samples after 20,000 cycles of wheel passes in a HWT test. However, for the EVWM-C mix, in which the SIP was observed (shown with grey mark), the measured deformation at the end of a HWT test is the combined effects of rutting and the moisture-induced damage. For this reason, this asphalt mix appears to behave differently than those of other mixes, which did not exhibit a SIP. This introduces nonlinearity to the regression equation. In order to capture the correlation between rutting and the DIDT, while isolating the moisture-induced damage effects, selection of a characteristic factor representing the pure rutting due to the HWT test is necessary. For this purpose the variation of the inverse rutting rate (IRR) with respect to DIDT values was plotted, as shown in Figure 4.11.
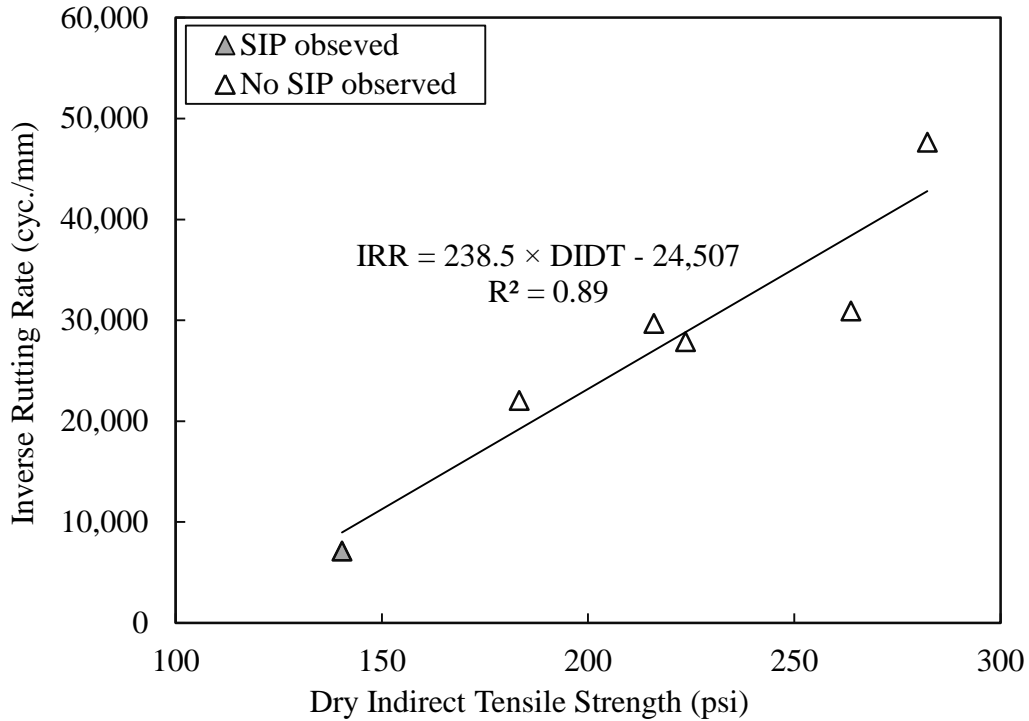
Figure 4.11 Variations of the Average Inverse Rutting Rates with Dry Indirect Tensile Strength

From Figure 4.11 it was observed that the IRR values of different asphalt samples increase with an increase in DIDT. In other words, resistance to rutting increases with increasing the tensile strength of the asphalt samples. Also, a linear regression model (IRR = 238.5 x DDIT - 24,507) was developed and is displayed on the chart. The coefficient of determination calculated for the above mentioned model is 0.89, which is an indication of good correlations between the measured rutting rate and the DIDT values. It was observed that use of the IRR value successfully eliminated the high values of the sample deformation as a result of SIP and moisture-induced damage effect. Hence, IRR is recommended to be used as the indication of rutting in asphalt mixes in which the SIP is observed.

In conclusion, it was observed that only the EVWM-C mix with lime showed significant moisture-induced damage, possibly due to incompatibility of its WMA additive with asphalt binder, aggregate and lime. Therefore, an in-depth study of the compatibility of the different chemicals used in the asphalt mixes is recommended. Also, it was observed that the TSR value by itself was not able to differentiate the mixes that were prone to moisture-induced damage, when the results were validated with the HWT

data. However, it was observed that useful information from the DIDT and CIDT tests data can be used in conjunction with the HWT test results to evaluate the moisture-induced damage potential.

4.2.3 Fatigue Life

Fatigue cracking as a result of repetitive stress and strain caused by traffic and environmental effects is considered a primary distress mechanism in asphalt pavements. Therefore, fatigue performance of asphalt pavements is an important design parameter. Although existing design standards aim to ensure the quality of the HMA, the fatigue performance of WMA mixes is not well understood. The mix design procedure currently used in Oklahoma is primarily intended to eliminate mixes that might be susceptible to rutting and moisture-induced damage, and fatigue performance is not directly evaluated in the mix design process. The fatigue life of an asphalt mix is its ability to withstand the repeated traffic loads without experiencing failure. Fatigue cracking becomes more important when a WMA technology is used in producing asphalt mixes. It is believed that the use of WMA which contains less aged binder compared HMA due to the lower mixing temperature, may result in a softer mix, and, therefore, it is expected to be less prone to fatigue cracking. Therefore, the primary purpose of conducting fatigue tests in this project was to evaluate the effects of using WMA technologies on the fatigue life of the asphalt mixes.

Four point beam fatigue tests (FTG) were conducted in OU Broce Asphalt Laboratory using a newly purchased universal asphalt material testing device, also called asphalt mix performance tester, from GCTS (ATM-100). This test was used as a valuable tool for accelerated laboratory testing of asphalt mixes for fatigue life under controlled-strain conditions. In this study, FTG tests were conducted according to the AASHTO T 321 test method, on WMA and control HMA mixes. The loose asphalt mixes were used for compaction of slab samples, using a linear kneading compactor. Figure 4.12 shows a photographic view of the compacted asphalt slab using the kneading compactor. Compacted slabs were then cut to the desired sizes to obtain beam samples. Beam samples were measured for dimensional accuracy, and a metallic LVDT stud was attached to the specimen. An asphalt beam sample ready for FTG test is

shown in Figure 4.13. FTG tests were conducted under a constant strain mode on the beam samples. Flexural stiffness was measured at the beginning of the test (average stiffness from the first 50 cycles) and the stiffness decay at 50% of initial stiffness was targeted as the test termination or fatigue failure criterion. Thus, the number of cycles giving 50% of the initial stiffness was reported as the fatigue failure cycle. Figure 4.14 shows the beam specimen in the fatigue fixture.

Table 4.4 presents a summary of the FTG test results. As indicated in Table 4.4, the tests were conducted at a temperature of 20°C and at a constant frequency of 10 Hz. All the tests were conducted under a constant strain level of 400 micro strains. From Table 4.4, it is evident that among all types of WMA and HMA mixes tested in this study, the HMA control mixes showed higher fatigue failure cycles compared to their WMA counterparts. For example, the ADHM mix showed an average fatigue failure cycles of 404,270, which is 108% more than that of the ADWM mix, which failed at 193,923 cycles.

Table 4.4 Four Point Bending Beam Fatigue Test Results Conducted on WMA and Control HMA Mixes

Mix Type	Strain Level (µe)	T (°C)	f (Hz)	Initial Stiffness (MPa)	AASHTO - Failure Cycles @50% Initial Stiffness
ADHM	400	20	10	7444.6	404,270
ADWM	400	20	10	6111.8	193,923
EVHM-B	400	20	10	7214.6	63,381
EVWM-B	400	20	10	8674.6	18,248
EVHM-C	400	20	10	7395.7	123,671
EVWM-C	400	20	10	5289.7	38,473

Similarly, the EVHM-B and EVHM-C mixes were found to have fatigue lives 247% and 221% higher than those of the EVWM-B and EVWM-C mixes, respectively. In other words, based on the asphalt mixes studied herein, HMA mixes showed a better performance when subjected to fatigue test.

Figure 4.12 Compacted Slab using a Kneading Compactor

Figure 4.13 Asphalt Beam Specimen with Installed Metallic LVDT Stud

Figure 4.14 Beam Sample in the Fatigue Fixture being Tested inside the Environmental Chamber

4.3   Surface Free Energy Test Results

The SFE test results conducted on the aggregates and WMA-modified asphalt binders are discussed in this section. The results from three different test methods are reported herein: (i) USD tests conducted on aggregates; (ii) WP tests conducted on asphalt binders; and (iii) SD tests conducted on both asphalt binders and aggregates. The SFE components of the tested materials were determined and combined in order to obtain the free energy of adhesion and free energy of deboning (also known as energy of adhesion in wet condition). These energy parameters were used to mechanistically evaluate the moisture-induced damage potential of different aggregate-asphalt binder systems.

4.3.1   Wilhelmy Plate Test Results on Asphalt Binders

Not many studies have examined the mechanics of the moisture-induced damage potential of the Evotherm® and Advera® WMA mixes in light of the SFE method. In addition, the capability of the current practice of moisture-induced damage assessment of asphalt mixes, like TSR testing according to AASHTO T283 (AASHTO, 2010) and its comparison with the SFE-based methods, has not been studied in detail. The present study was undertaken to evaluate the effect of three different WMA-additives (i.e., Sasobit®, Advera® and Evotherm®) on the wettability and moisture-

induced damage potential using the SFE method. For this purpose, the wettability, the work of adhesion and the work of debonding of six types of aggregates and a PG 64-22 asphalt binder modified with different percentages of WMA-additives are evaluated.

In order to determine the SFE components of the asphalt binder, a Wilhelmy Plate (WP) based DCA device was applied to measure the contact angles of the asphalt binder. Contact angles of asphalt binders were measured with three different solvents of known SFE components, namely water, glycerin and formamide. The selected asphalt binder (i.e., PG 64-22) was modified with different amounts of Sasobit® (i.e., 1.0%, 1.5% and 2.0% by the weight of asphalt binder), Advera® (i.e., 0.25%, 0.30% and 0.35% by the weight of asphalt mix) and Evotherm® (i.e., 0.25%, 0.50% and 0.75% by the weight of asphalt binder). A total of 108 asphalt binder samples were prepared in the laboratory and tested for contact angles. Figure 4.15 shows a typical output from the DCA device.
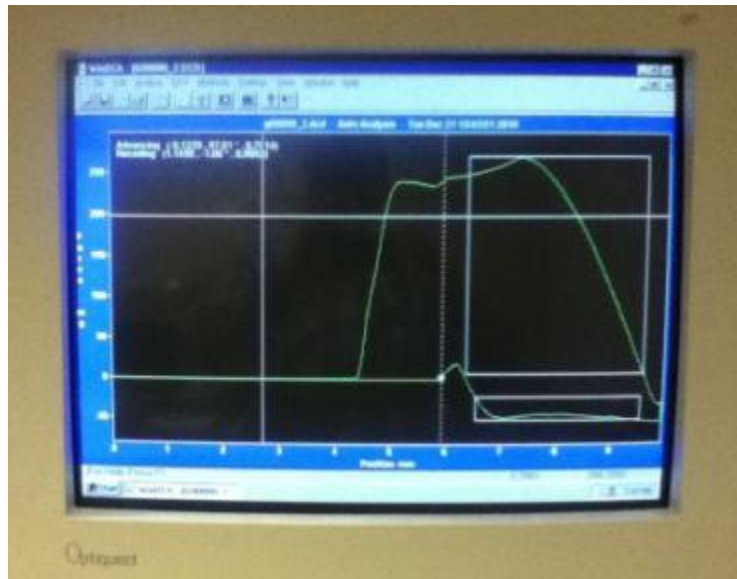
Figure 4.15 Example of Typical Output from WP Test

4.3.1.1   Contact Angles

The laboratory measured contact angles of modified asphalt binders and neat asphalt binder with water, glycerine, and formamide are presented in Table 4.5. In general, when the contact angle is more than 90°, the solvent is unable to wet the surface. When the contact angle is less than 90°, the solvent is able to wet the surface. When the contact angle is close to zero, spreading of the solvent on the surface can

happen. Overall, according to Table 4.5, addition of Sasobit[®] and Evotherm[®] resulted in reduced contact angles compared to those of the neat asphalt binder. A similar trend in contact angle variation with amounts of Sasobit[®] has also been reported by Buddhala et al. (2011). On the other hand, the addition of Advera[®] resulted in a mixed trend (i.e., increase or decrease) in contact angles depending upon the amount of Advera[®] added. It is expected that Advera[®] introduces free water to asphalt binder at mixing temperature (Goh and You, 2012), which in turn affects the contact angles. The implications of variations in contact angles on the properties of the asphalt binder are expected to influence the wettability, SFE components, and energy parameters such as work of adhesion and debonding and moisture-induced damage potential, which will be discussed later, in this chapter.

Table 4.5 Contact Angles of PG 64-22 Asphalt Binder Modified with WMA-Additives

Type and Amounts of Additives Mixed with PG 64-22 Binder		Advancing Contact Angle (Deg)					
		Water		Glycerine		Formamide	
		Mean	Std. Dev.	Mean	Std. Dev.	Mean	Std. Dev.
Neat		108.6	0.8	97.0	0.6	92.8	0.2
Sasobit[®]	1.00%	108.2	0.1	96.6	0.1	92.6	0.4
	1.50%	107.5	0.5	95.5	0.3	92.4	0.1
	2.00%	106.8	0.4	95.0	0.0	92.3	0.5
Advera[®]	0.25%	106.7	0.4	92.2	0.3	89.4	0.2
	0.30%	109.1	0.5	92.7	0.5	89.7	0.3
	0.35%	110.2	0.6	94.0	0.2	91.1	0.6
Evotherm[®]	0.25%	104.6	0.2	91.0	0.7	88.6	0.4
	0.50%	101.9	0.1	91.2	0.3	88.9	0.4
	0.75%	100.7	0.6	92.8	0.4	89.2	0.5

4.3.1.2   SFE Components of Asphalt Binders

The SFE components of the PG 64-22 asphalt binder modified with different percentages of Sasobit[®], Advera[®] and Evotherm[®] are presented in Table 4.6. Based on this table, it was found that the total SFE component (Γ^{Total}) and the non-polar Lifshitz-van der Waals component (Γ^{LW}) of asphalt binder decrease with an increase in the amount of Sasobit[®] and Advera[®]. For example, the addition of 2% of Sasobit[®] and 0.35% of Advera[®] decreased the total SFE to 10.39 mJ/m^2 and 8.91 mJ/m^2 compared to 11.57 mJ/m^2 for the neat asphalt binder, respectively. Similar observations on reduction

in total SFE with an increase in the amount of Sasobit® have been reported by Wasiuddin et al. (2008). The reduction in the total SFE may affect the adhesion of an asphalt binder with the aggregates (Wasiuddin, 2007; Arabani and Hamedi, 2011). Furthermore, Table 4.6 shows that an increase in the amounts of Sasobit® and Advera® increases the ratio of acid to base SFE component (Γ^+/Γ^-), indicating an increase in acidity of the asphalt binder (Wasiuddin et al., 2008; Buddhala et al., 2011). Highly acidic asphalt binders may not result in a good bond with acidic aggregates such as sandstone, gravel, and specifically granite, since the surface chemistry of Lewis acid and bases do not favor adhesion in this case (Arabani and Hamedi, 2011). On the other hand, no detectable trend of Γ^+/Γ^- was observed for Evotherm®-modified asphalt binder. Asphalt binder modified by 0.25% Evotherm® resulted in a reduction of the total SFE component by 0.58 mJ/m^2 compared to the neat binder. However, when the amount of Evotherm® was increased to 0.5% and 0.75%, the total SFE component increased to 12.24 and 13.69 mJ/m^2, respectively.

Table 4.6 SFE Components of PG 64-22 Asphalt Binder Modified with WMA Additives

		Surface Free Energy Components (mJ/m^2)					
		Γ^{LW} (Non-polar)	Γ^- (Base)	Γ^+ (Acid)	Γ^{AB}	Γ_{total}	Γ^+/Γ^-
PG64-22 Binder with Different Types and Amounts of Additives							
Neat	0%	9.44	0.93	1.22	2.13	11.57	1.30
Sasobit®	1.0%	9.09	1.00	1.36	2.34	11.43	1.35
	1.5%	7.44	1.14	2.11	3.10	10.54	1.86
	2.0%	6.78	1.33	2.44	3.61	10.39	1.83
Advera®	0.25%	7.36	0.76	3.08	3.07	10.43	4.03
	0.30%	7.58	0.28	3.14	1.88	9.46	11.14
	0.35%	7.16	0.25	3.04	1.75	8.91	12.12
Evotherm®	0.25%	6.84	1.24	3.45	4.14	10.99	2.77
	0.50%	6.74	2.50	3.03	5.50	12.24	1.21
	0.75%	9.17	3.03	5.50	4.52	13.69	1.82

4.3.2 USD Test Results on Aggregates

Similarly, the SFE components of selected limestone aggregates were determined using a Universal Sorption Device (USD) and applying the methodology discussed by Bhasin and Little (2007). The probe vapors of known SFE components, namely water, n-hexane, and methyl propyl ketone (MPK) were used to determine adsorption isotherms. SFE components of the selected limestone aggregate and other different types of aggregates (i.e., sandstone, gravel, granite and basalt) from literature (Bhasin et al., 2007; Buddhala et al., 2011) are presented in Table 4.7. The SFE components of the limestone aggregate used in the present study are comparable to the results reported for one other limestone aggregate by Buddhala et al. (2011). Γ^+/Γ^- ratio of different types of aggregates used in this study was found to be in the following order.

$$\Gamma^+/\Gamma^-_{Granite} > \Gamma^+/\Gamma^-_{Sandstone} > \Gamma^+/\Gamma^-_{Gravel} > \Gamma^+/\Gamma^-_{Limestone} > \Gamma^+/\Gamma^-_{Basalt}$$

From Table 4.7, it was observed that granite is the most acidic aggregate with an acid to base component ratio (Γ^+/Γ^-) of 0.251, and basalt is the most basic aggregate with a Γ^+/Γ^- ratio of 0.004. One should be careful using an acidic aggregate such as granite, with asphalt binder, which is acidic in nature that may result in a weak bond between asphalt binder and aggregate, and consequently high moisture-induced damage potential (Arabani and Hamedi, 2011).

Table 4.7 SFE Components of Aggregates

	Surface Free Energy Components (mJ/m^2)					
	Γ^{LW} (Non-polar)	Γ^- (Base)	Γ^+ (Acid)	Γ^{AB}	Γ_{total}	Γ^+/Γ^-
Aggregates from Testing and Literature						
Limestone (Tested)	51.4	741.4	17.5	227.8	279.2	0.024
Sandstone*	43.5	555.2	28.2	250.3	293.8	0.051
Gravel*	57.5	973	23	299.2	356.7	0.024
Granite*	133.2	96	24.1	96.2	229.4	0.251
Basalt*	52.3	164	0.6	19.8	72.1	0.004

* Adopted from literature.

4.3.3 Energy Parameters of Aggregate-Asphalt Binder Based on USD and WP

Important surface free energy parameters of the asphalt binder-aggregate combinations are discussed in this section. The energy parameters are determined based on the SFE results for the tested aggregates and asphalt binders with USD and WP methods, respectively. The parameters of particular interest include wettability, work of adhesion, work of debonding, and energy ratio (ER_1). Also the significance of each parameter is discussed.

4.3.3.1 Wettability

Asphalt binder and aggregates pose hydrophobic and hydrophilic characteristics, respectively (Tarrer and Wagh, 1991). For this reason, wetting and consequently coating aggregates' surface with the asphalt binder is not easy, by nature (Wasiuddin et al., 2008). Hence, it is important to understand the wettability of the liquid asphalt binder over the aggregate surface. The tendency of a liquid to wet a solid surface is expressed in terms of the spreading coefficient (Zettlemoyer, 1969). The spreading coefficient of the liquid asphalt binder over the aggregates ($S_{A/S}$) is the released energy as the liquid asphalt binder readily flows over the aggregates and coats it (Wasiuddin et al., 2008). Therefore, a higher spreading coefficient of an aggregate-asphalt binder system means a higher tendency of the aggregate to be coated by the liquid asphalt binder, which is in favor of better bonding and reduces the possibility of moisture-induced damage. In this study, the spreading coefficient of asphalt binder with and without WMA-additives over different types of aggregates, mentioned in Table 4.6 and Table 4.7, was determined and the results are presented in Table 4.8.

Table 4.8 shows that the spreading coefficient increases with an increase in the amount of Sasobit® for almost all types of the aggregates, compared to that of the neat asphalt binder. A significant improvement in the spreading coefficient (i.e., 25.4%) was found for gravel when 2% Sasobit® was added to asphalt binder (Table 4.8). However, only a 3.1% improvement in the spreading coefficient was observed in the granite case with the addition of 2% Sasobit®. This means that Sasobit®-modified asphalt binders may coat the sandstone, gravel, limestone, and basalt aggregates better than granite aggregates. Therefore, use of Sasobit®-modified asphalt binders with granite

aggregates may possibly increase the moisture-induced damage potential of the asphalt mixes.

Similarly, the addition of Advera$^®$ increased the spreading coefficients over almost all types of the aggregates. The maximum improvement in the spreading coefficient (i.e., 36.5%) was found for the limestone and gravel aggregates when 0.25% Advera$^®$ was added to the asphalt binder. Use of the same amount of Advera$^®$ improved the spreading coefficient up to 7.2% for granite aggregate. Consequently, Advera$^®$-modified asphalt binder when used with granite may possibly increase the moisture-induced damage potential of the mix due to a low spreading coefficient (i.e., insufficient coating of aggregates by asphalt binder), compared to the mixes produced with the other types of aggregates. Similar results have been reported by You and Goh (2011).

Furthermore, significant improvement in the spreading coefficient (i.e., 78.9% compared to neat asphalt binder) with the use of the Evotherm$^®$ was found for gravel when 0.75% Evotherm$^®$ was added to the asphalt binder (Table 4.8). In addition, a 33.9% improvement in the spreading coefficient was observed for granite aggregate with the addition of 0.75% Evotherm$^®$. The results indicate that a better granite aggregate coating is expected when Evotherm$^®$ is used with the asphalt binder. In other words Evotherm$^®$ -modified asphalt binder may be used over the different types of aggregate (discussed herein), with less concern over wettability, and therefore, a less moisture-induced damage potential, resulting from aggregate coating quality by binder.

4.3.3.2 Work of Adhesion

Work of adhesion (W_{AS}) is defined as the work required for separating the asphalt binder from aggregate interface (Bhasin et al., 2007). Higher W_{AS} indicates a stronger bond between asphalt mix components, leading to a more durable and a less moisture-induced damage susceptible mix. Hence, the study of the work of adhesion is very important to gain a better understanding of the moisture-induced damage mechanism (Wasiuddin et al., 2008). Table 4.8 shows the work of adhesion between the aggregates and the

PG 64-22 asphalt binder modified with different types and amounts of the WMA-additives.

According to Table 4.8, an increase in the amounts of Sasobit®, Advera®, and Evotherm® increased the work of adhesion between asphalt binder and aggregates. However, an increase in the work of adhesion is not significant when Sasobit® and Advera®-modified asphalt binders are used with granite aggregate. As mentioned before, addition of Sasobit® and Advera® increases the acidity of the asphalt binder. Granite aggregate is a highly acidic aggregate, with a Γ^+/Γ^- ratio of 0.25,which is significantly higher than that of other aggregates. Based on the work of adhesion, it can be concluded that the use of Sasobit® and Advera®-modified asphalt binders with sandstone, gravel, limestone and basalt aggregates may result in a better adhesion, compared to the mixes containing granite aggregates.

However, the addition of Evotherm® to the selected asphalt binder resulted in a significant improvement in the work of adhesion with all types of aggregates. For example, addition of 0.75% of Evotherm® results in an improvement in the work of adhesion. This improvement is more pronounced with a maximum increasing rate of 67.6% in the gravel case. The least improvement in the work of adhesion, with the use of same amount of Evotherm®, was observed in the case of granite. It is desirable for an asphalt mix to have a work of adhesion as high as possible to be durable and less prone to moisture-induced damage (Bhasin et al., 2007). Therefore, it is expected that the use of Evotherm®-modified asphalt binder may improve the durability and resistance against moisture-induced damage of the mixes produced with both acidic and basic aggregates.

4.3.3.3   Work of Debonding

Work of debonding (W_{ASW}^{wet}), also known as work of adhesion in wet condition, is another important energy parameter, defined as the reduction of the free energy of the asphalt binder and aggregate system when asphalt binder gets separated from its interface with aggregate in the presence of the water. Hence, a higher magnitude of the work of debonding implies a higher thermodynamic potential for stripping to occur in the

105

presence of water (Bhasin et al., 2007). Therefore, a lower work of debonding is more favorable to reduce the moisture-induced damage potential of the system.

Table 4.8 presents the work of debonding between the aggregates and the PG 64-22 asphalt binder modified with different types and amounts of WMA-additives.

According to Table 4.8, the addition of Sasobit® decreases the work of debonding, except in the granite case. The maximum desirable effect was observed when 2% Sasobit® was added to asphalt binder. Use of 2% Sasobit® with the selected asphalt binder and limestone aggregate resulted in the highest reduction (10.1%) in the work of debonding, compared to that of the neat asphalt binder. However, the use of 2% Sasobit®-modified asphalt binder with granite aggregate increased the work of debonding by 3.7%, which is not desirable when resistance to moisture-induced damage is of concern. Use of asphalt binder modified with Advera® resulted in a decrease in the work of debonding with all types of aggregates. A significant reduction in the work of debonding was obtained when 0.35% Advera® was added to the asphalt binder with basalt. This resulted in a 36.2% reduction in the work of debonding compared to the neat asphalt binder case. However, addition of 0.35% Advera® reduced the work of debonding by 3.6% for granite aggregate, indicating that use of Advera® -modified asphalt binder is not recommended for granite aggregates.

The reduction in work of debonding of the asphalt binder modified with Evotherm® with different aggregates are more significant compared to that of Sasobit® and Advera®. The maximum reduction in the work of debonding for basalt aggregates was observed when 0.75% of Evotherm® was added to the PG 64-22 asphalt binder. Similarly, a reduction of 18.9% was observed in the work of debonding for granite aggregate, which is significantly higher than those for Sasobit® and Advera®. Based on the work of debonding, it can be concluded that Evotherm® might be used with the aggregates discussed in this study, with possibly less concern over the moisture-induced damage potential of the mix compared to that of other types of additives discussed herein.

4.3.3.4   Moisture-Induced Damage Potential Based on SFE Parameters

Based on the definitions of the work of adhesion and work of debonding, it can be concluded that the moisture-induced damage potential of an asphalt binder-aggregate system decrease with an increase in the work of adhesion (W_{AS}), and increases with an increase in the magnitude of work of debonding ($\left|W_{ASW}^{wet}\right|$). Consequently, Bhasin et al. (2007) suggested combining W_{AS} and W_{ASW}^{wet} into a single parameter called energy ratio (ER_1), which is directly proportional to the resistance against moisture-induced damage, as shown in Equation 4.1.

$$ER_1 = \left|\frac{W_{AS}}{W_{ASW}^{wet}}\right|$$

(4.1)

A higher ER_1 value implies a better resistance against the moisture-induced damage, and therefore, a lower moisture-induced damage potential of the asphalt binder-aggregate system (Bhasin et al., 2007). This value is analogues to the TSR value obtained according to the AASHTO T283 (AASHTO, 2010) method. ER_1 values of different combinations of additives and aggregates are presented in Table 4.9.

Table 4.8 Energy Parameters of PG 64-22 Asphalt Binder with Additives and Aggregates

WMA Additive Type and Amount		Limestone	Sandstone	Gravel	Granite	Basalt
Spreading Coefficients (mJ/m^2)						
Neat PG64-22		89.0	79.6	101.5	78.9	51.0
Sasobit®	1.0%	92.3	82.5	105.3	79.4	52.2
	1.5%	106.0	94.7	121.1	80.8	57.2
	2.0%	111.3	99.5	127.3	81.3	58.7
Advera®	0.25%	120.9	106.9	138.2	84.7	64.7
	0.30%	121.5	106.6	138.5	84.6	67.1
	0.35%	119.7	105.0	136.4	83.0	66.3
Evotherm®	0.25%	126.0	111.9	144.3	85.8	65.2
	0.50%	120.8	108.6	138.7	85.1	60.1
	0.75%	158.3	141.6	181.6	105.6	79.2
Work of Adhesion (mJ/m^2)						
Neat PG64-22		112.2	102.7	124.6	102.0	74.2
Sasobit®	1.0%	115.2	105.4	128.1	102.3	75.0
	1.5%	127.1	115.7	142.2	101.9	78.3
	2.0%	132.1	120.2	148.0	102.1	79.5
Advera®	0.25%	141.8	127.8	159.0	105.6	85.5
	0.30%	140.5	125.5	157.4	103.5	86.0
	0.35%	137.5	122.8	154.2	100.9	84.2
Evotherm®	0.25%	148.0	133.9	166.3	107.7	87.1
	0.50%	145.2	133.1	163.1	109.6	84.6
	0.75%	185.7	169.0	208.9	133.0	106.6
Work of Debonding (mJ/m^2)						
Neat PG64-22		-176.0	-154.4	-213.6	-58.1	-34.5
Sasobit®	1.0%	-173.5	-152.2	-210.6	-58.2	-34.1
	1.5%	-162.4	-142.8	-197.3	-59.5	-31.7
	2.0%	-158.2	-139.1	-192.4	-60.2	-31.4
Advera®	0.25%	-148.7	-131.7	-181.5	-56.8	-25.4
	0.30%	-147.1	-131.1	-180.2	-56.0	-22.0
	0.35%	-148.7	-132.4	-182.1	-57.3	-22.6
Evotherm®	0.25%	-145.0	-128.2	-176.8	-57.2	-26.4
	0.50%	-151.1	-132.3	-183.3	-58.7	-32.3
	0.75%	-122.4	-108.2	-149.2	-47.1	-22.0

Table 4.9 SFE-Based Moisture-Induced Damage Potential Parameters, ER1

Type and Amount of Additive Mixed with PG 64-22 Binder		ER_1				
		Limestone	Sandstone	Gravel	Granite	Basalt
Neat	0%	0.6	0.7	0.6	1.8	2.2
Sasobit®	1.0%	0.7	0.7	0.6	1.8	2.2
	1.5%	0.8	0.8	0.7	1.7	2.5
	2.0%	0.8	0.9	0.8	1.7	2.5
	0.25%	1.0	1.0	0.9	1.9	3.4
Advera®	0.30%	1.0	1.0	0.9	1.8	3.9
	0.35%	0.9	0.9	0.8	1.8	3.7
	0.25%	1.0	1.0	0.9	1.9	3.3
Evotherm®	0.50%	1.0	1.0	0.9	1.9	2.6
	0.75%	1.5	1.6	1.4	2.8	4.8

The ER_1 values in Table 4.9 show that Sasobit® does not significantly increase or decrease the moisture-induced damage potential of the asphalt binder-aggregate systems. The same trend is observed for combinations of Advera® with different types of aggregates as well, except basalt. The use of the Advera® -modified asphalt binder with basalt aggregates increases resistance to moisture-induced damage by 68%. The addition of Evotherm® to the selected asphalt binder results in the highest resistance to moisture-induced damage, compared to that of other additives and neat asphalt binder used over different aggregates. Because of limited scope, the results from this study may not be generalized for other mixes. Additional research would be needed to correlate the SFE results with the moisture-induced damage potential of asphalt mixes through more traditional testing.

4.3.4 Sessile Drop Test Results on Asphalt Binders and Aggregates

In order to determine the SFE parameters of the asphalt materials with an alternative method, SD device was used. In this method, the contact angles of the aggregates and asphalt binders were measured with three different probe liquids (Water, Diiodomethane, and Ethylene Glycol). The contact angles were measured on the specimens of the following materials.

- Davis limestone,

- Snyder granite,

- PG 64-22 neat binder,

- PG 64-22 binder with the Warm Mix Asphalt (WMA) additives (Sasobit®, Permatac Plus®, and Evotherm®).

The average contact angle values of ten measurements for aggregate samples and six measurements for asphalt binder specimens can be found in this section. The average contact angles and standard deviations of aggregates and neat binder are given in Table 4.10, while Table 4.11 presents the contact angle data for PG 64-22 asphalt binder with WMA additives. For demonstration purposes, Ethylene Glycol was abbreviated as Eth. Gly., Diiodomethane as DIM and standard deviation as Std. Dev. All the raw data are provided in Appendix B.

4.3.4.1 Contact Angle

The contact angle measurements on Davis Limestone and Snyder Granite were conducted in three sets and each set involved 10 measurements. The average values of all these measurements were given in Table 4.10. Direct contact angle measurements on all samples using the Sessile Drop (SD) device were done using the sample preparation and testing protocols given in Chapter 3.

Table 4.10 Contact Angles of Aggregates and Neat Binder using the Sessile Drop Device

| Material Type | Contact Angles (Degrees) | | | | | |
| | Ethylene Glycol | | Water | | Diiodomethane | |
	Average	Std. Dev.	Average	Std. Dev.	Average	Std. Dev.
Davis Limestone	61.7	2.2	79.4	4.7	46.4	1.5
Snyder Granite	58.6	3.9	74.6	4.0	49.8	3.8
PG 64-22 Neat Binder	70.5	2.5	93.0	1.1	48.0	1.4

The contact angles with distilled water on aggregate and binder specimens produced the highest values compared to the other probe liquids. The reason for this behavior might be related to the interfacial tensions (IFT) of the probe liquids. The IFT of Diiodomethane and Ethylene Glycol are very close in magnitude and lower than the IFT

of Distilled Water. The exact relation was observed in the magnitude of their contact angles (Table 4.10) on different solid surfaces.

As far as the contact angle results on aggregates are concerned, it was observed that as the IFT decreased, the standard deviation of contact angles decreased as well. The contact angle is inversely related to the wettability. Higher wettability of solid surfaces results in decreased contact angle which means the liquid spreads over the solid surface. Wasiuddin et al. (2008) evaluated the SFE components of PG 64-22 and PG 70-28 with and without the addition of Sasobit®. According to Wasiuddin et al. (2008), wettability increases with higher amounts of Sasobit®. The manufacturer of Sasobit® (Sasol Wax, America) states that, it increases the wettability. The test results from the SD method (Table 4.11) indicate that, higher percentages of WMA additives has led to lower contact angles hence increased wettability.

Table 4.11 Contact Angles of Asphalt Binder with WMA Additives using Sessile Drop Device

WMA Additive and Percentage	Contact Angles (Degrees)		
	Water	Diiodomethane	Ethylene Glycol
Sasobit® 0.5%	92.5	48.0	71.0
Sasobit® 1.0%	90.0	46.5	69.5
Sasobit® 1.5%	89.0	44.0	67.0
Evotherm® 0.5%	90.0	48.0	70.0
Evotherm® 1.0%	88.5	46.5	68.0
Evotherm® 1.5%	85.0	45.5	68.5
Permatac Plus® 0.5%	91.0	45.0	69.0
Permatac Plus® 1.0%	89.5	42.5	68.5
Permatac Plus® 1.5%	88.0	42.0	67.0

4.3.4.2 Surface Free Energy Components of Aggregates and Asphalt Binder from SD Test

The surface energy components of aggregates and asphalt binder using SD test, are presented in Table 4.12 and Table 4.13, respectively.

Table 4.12 SFE Components of Aggregates using the Sessile Drop Method

Aggregate Type	γ^-	γ^+	γ^{AB}	γ^{LW}	γ^{Total}
	(ergs/cm^2 or mJ/m^2)				
Davis Limestone	10.12	0.05	1.35	36.26	37.61
Snyder Granite	13.97	0.01	0.28	34.39	34.66

Table 4.13 SFE Components of Asphalt Binder using the Sessile Drop Method

WMA Additive and Percentage	γ^-	γ^+	γ^{AB}	γ^{LW}	γ^{Total}
	(ergs/cm^2 or mJ/m^2)				
PG 64-22 Neat Binder	2.82	0.12	1.15	35.38	36.53
Sasobit® 0.5%	3.22	0.16	1.42	35.38	36.80
Sasobit® 1.0%	4.28	0.17	1.73	36.20	37.93
Sasobit® 1.5%	4.12	0.13	1.44	37.54	38.98
Evotherm® 0.5%	4.48	0.16	1.70	35.38	37.08
Evotherm® 1.0%	4.83	0.13	1.57	36.20	37.78
Evotherm® 1.5%	7.70	0.29	2.99	36.74	39.73
Permatac Plus® 0.5%	3.47	0.16	1.49	37.01	38.50
Permatac Plus® 1.0%	4.19	0.24	2.02	38.33	40.35
Permatac Plus® 1.5%	4.72	0.20	1.95	38.59	40.54

Because of the sample preparation protocols (oven drying and desiccation) given in the previous chapter, the contact angle measurements and the SFE calculations are done under dry condition. Table 4.12 and Table 4.13 show that Lewis-Acid (γ^+) components are almost negligible compared to the Lewis-Base (γ^-) components. Using the SD method Bargir et al. (2009) has measured the contact angles of various solid materials (stainless steel, gold, aluminum, etc.) and calculated the SFE components. The results showed that the values of γ^+ components of all materials were ranging from 0.01 ergs/cm^2 to 1.07 ergs/cm^2 (Bargir et al., 2009). They compared the results with the values available in the literature. As shown in Table 4.12 and Table 4.13, the γ^+ components of the aggregate and asphalt binder specimens used in this study are in the range of 0.01 ergs/cm^2 to 0.90 ergs/cm^2. The SFE components of different geological materials from the literature are presented in Table 4.14. The results presented in Table 4.14 are numbered based on the literature source as followings:

(1)Yildirim (2001) using Sessile Drop method, (2) Giese and van Oss (2002) using column wicking method), (3) Bhasin (2006) using Universal Sorption Device, (4) Wasiuddin et al. (2007) using Universal Sorption Device, (5) Yildirim (2001) using heat of immersion, and (6) Lytton et al. (2005) using Universal Sorption Device.

Table 4.14 SFE Components of Different Geological Materials from Literature

Material Type	γ^-	γ^+	γ^{AB}	γ^{LW}	γ^{Total}
	(ergs/cm^2 or mJ/m^2)				
Montana talc[1]	27.4	0.2	4.7	42.9	47.6
Vermont talc[1]	28.4	0.1	3.4	44.6	48.0
Montmorillonite[2]	33.4	2.3	17.3	42.4	59.8
Limestone[3]	259.0	2.4	49.5	44.1	93.6
Limestone[4]	540.7	13.0	168.0	51.9	219.9
Montana-ROM[5]	14.5	0.2	3.3	53.4	56.7
Granite[6]	782.7	43.6	368.9	56.3	425.2

[1]Yildirim (2001), [2]Giese and van Oss (2002), [3]Bhasin (2006), [4]Wasiuddin et al. (2007),

[5]Yildirim (2001), [6] Lytton et al. (2005)

The results from Table 4.12 show that, among all aggregates tested in this study, the lowest and the highest values of total SFE components are 34.66 ergs/cm^2 and 49.37 ergs/cm^2, respectively. These values are within typical range of the SFE components of the geological materials shown in Table 4.14. According to Table 4.14, the SFE components of the geological materials from the literature are in the same range, except for those tested using the USD method. The differences in the SFE components determined using the USD, especially in the SFE base components, is clearly observed in Table 4.14. The base components for the USD range from 259.0 to 782.7 ergs/cm^2, however, the range of base components' variation for all the other materials (including the results from the SD) is from 0.2 to 39.5 ergs/cm^2. In order to understand the difference between the results between USD and SD, the equilibrium spreading pressure (π_e) term should be investigated in detail. The USD introduces the π_e term into the Young's equation and drops the contact angle term, as discussed in Chapter 3. According to Bhasin (2006), for solids with low surface free energies (i.e., polymers), spreading pressures are negligible and can be assumed to be zero. This assumption works well for liquids that form finite contact angles on the solid surface. In

113

addition, aggregates (i.e., limestone and granite) are solids with high surface energies and the previous assumption does not apply anymore (spreading pressure should be greater than zero). Hence, contact angles are supposed to be zero on these high surface energy aggregates (Bhasin, 2006).

On the other hand, according to Table 4.10, all contact angles measured on aggregates using the SD device are actually finite contact angles and none of them are zero. Therefore, the Young-Dupré equation should be used in its present form without any modifications. Van Oss (2002) clearly states that, in all cases where finite contact angle occurs (where $\theta > 0^o$), there is no need to insert "equilibrium spreading pressures" into Young-Dupré equation. Wu (1982) claimed that if the contact angle is larger than 10°, the spreading pressure is negligible. According to Table 4.10 it was observed that all of the contact angles measured in this study were larger 10°.

In order to compare the SFE test results conducted on asphalt binder using SD test (Table 4.13) with those from the WP test, typical SFE components of the asphalt binders reported in the open literature (Lytton et al., 2005; Bhasin, 2006) are presented in Table 4.15.

Table 4.15 SFE Components of Neat Asphalt Binder from WP Test Reported in Literature

Asphalt Binder	γ^-	γ^+	γ^{AB}	γ^{LW}	γ^{Total}
	(ergs/cm^2 or mJ/m^2)				
PG 64-22[1]	1.02	0.01	0.05	29.95	30.07
AAF-1[2]	3.52	0.01	0.38	38.38	38.80

[1] Lytton et al. (2005), [2]Bhasin (2006), AAF-1 is equivalent to PG 64-22.

Comparing the SFE components of the neat PG 64-22 binder from Table 4.13 and Table 4.15 indicates that the surface free energy components obtained from the SD measurements are in close agreement with the results obtained from the WP method. Bhasin (2006) measured the total SFE of the PG 64-22 binder as 38.80 ergs/cm^2, while Lytton et al. (2005) reported a value of 30.07 ergs/cm^2. Using the test results from the SD method the total SFE of the PG 64-22 was 36.53 ergs/cm^2. Except for the Lewis-Acid component (γ^+), the values of all components of the SFE calculated using the SD method were in between the two results obtained from the literature. According to

Bhasin (2006) and Lytton et al. (2005), the Lewis-Acid component (γ^+) was 0.01 ergs/cm^2, which is smaller than the results from the SD method (0.12 ergs/cm^2). These similarities are resulted from the fact that, both SD and WP methods make use of the Young-Dupré equation without any modification and only using the contact angles. The difference between the SD and the WP method is that in the WP method the contact angles are measured indirectly while the contact angles in the SD method are measured directly.

4.3.5 Energy Parameters of Aggregate-Asphalt Binder Based on SD Test

Important surface free energy parameters of the asphalt binder-aggregate combinations are discussed in this section. The energy parameters are determined based on the SFE results for the tested aggregates and asphalt binders using the SD method. The above mentioned parameters presented herein consist of work of adhesion, work of debonding (also known as work of adhesion in wet condition) and energy ratio (*ER*). Also, the significance of each parameter is discussed in this section.

4.3.5.1 Works of Adhesion and Cohesion

The values of work of adhesion/cohesion were determined for Davis Limestone, Snyder Granite and PG 64-22 asphalt binder using the results of SFE calculations from direct contact angle measurements using the SD test. The results of work of adhesion and cohesion are presented in Table 4.16. The results from Table 4.16 shows that, among all aggregates and the asphalt binders, tested in this study, the highest and the lowest values of work of adhesion were 78.63 ergs/cm^2 and 72.35 ergs/cm^2, for DL aggregate in contact with PG 64-22 asphalt binder with 1.5% Perma-tac Plus$^®$, and SG aggregate in contact with neat PG 64-22 asphalt binder, respectively.

4.4 Energy Ratio

First introduced by Little and Bhasin (2006), the Energy Ratio (ER) can be used as a parameter to evaluate the moisture-induced damage potential of an aggregate-binder pair. The ER values of the aggregates and asphalt binder (neat and modified) were calculated using this approach and are given in Table 4.16. The ER was

calculated using the formula given by Little and Bhasin (2006), as shown in Equation 4.2.

$$ER = \frac{W_{ij}^a - W_i^c}{W_{ikj}^a} \tag{4.2}$$

In order to calculate the ER of a mix, the SFE components of the aggregate and asphalt binder must be known. The SFE components of the specimens were calculated and given in Table 4.12 and Table 4.13. In order to compare aggregate-binder pair according to the resistance to moisture-induced damage, the Energy Ratio (ER) approach was used. The ER values of Davis Limestone (DL) and Snyder Granite (SG) with different binder specimens (neat and modified with WMA additives) were calculated and are given in Table 4.16. For example, DL-1.0% Evotherm® represents a mix of Davis Limestone and PG 64-22 asphalt binder with 1.0% Evotherm ® (by the weight of binder). According to this approach, a higher adhesive energy between the aggregate and binder, and a lower energy potential of water to separate the asphalt binder from the aggregate surface result in increased ER (Little and Bhasin, 2006). Therefore, the higher ER can represent better resistance to moisture-induced damage. According to Table 4.16 the ER value of Davis Limestone and Snyder Granite with neat PG 64-22 asphalt binder were calculated as 0.029 and 0.014, respectively. From these results, one can conclude that the former pair will perform better against moisture-induced damage. The effect of Warm Mix Asphalt (WMA) additives can also be investigated using the ER approach. Table 4.16 provides enough data to state that, addition of WMA additives, such as Sasobit®, Evotherm® and Perma-tac® Plus increased the resistance to moisture-induced damage. However, in order to get maximum resistance to moisture-induced damage from a WMA additive, the amount of additive in the binder should be selected carefully. The WMA additives used in this study were mixed with the PG 64-22 binder at different percentages (0.5%, 1.0%, and 1.5%).

According to Table 4.16 it was found that use of Sasobit®-modified asphalt binder with limestone aggregate leads to reduced amounts of ER value. For example use of

PG 64-22 asphalt binder modified with 0.5% Sasobit® with limestone aggregate reduces the ER value from 0.029, for neat asphalt binder to 0.026. The decrease in ER value is more significant when 0.1% and 0.15% Sasobit® are used, resulting in ER values of 0.003 and 0.019, respectively.

Table 4.16 Work of adhesion/cohesion and ER of Davis Limestone (DL) and Snyder Granite (SG) with Asphalt Binders

Aggregate-Asphalt Mix	Work of cohesion	Work of adhesion (Dry)	Work of adhesion (Wet)	Energy Ratio (*ER*)
	(ergs/cm^2 or mJ/m^2)			
Neat PG 62-22	73.06	N/A	N/A	N/A
DL-Neat Binder	73.06	74.59	-53.57	0.029
DL-0.5% Sasobit®	73.60	74.98	-52.26	0.026
DL-1.0% Sasobit®	75.86	76.01	-49.75	0.003
DL-1.5% Sasobit®	77.96	76.99	-50.62	0.019
DL-0.5% Evotherm®	74.16	75.13	-49.15	0.020
DL-1.0% Evotherm®	75.56	75.74	-48.70	0.004
DL-1.5% Evotherm®	79.46	77.67	-42.58	0.042
DL-0.5% Perma-tac®Plus	77.00	76.64	-51.96	0.007
DL-1.0% Perma-tac® Plus	80.70	78.59	-50.14	0.042
DL-1.5% Perma-tac®Plus	81.08	78.63	-49.15	0.050
SG-Neat Binder	73.06	72.35	-49.44	0.014
SG-0.5% Sasobit®	73.60	72.75	-48.14	0.016
SG -1.0% Sasobit®	75.86	73.65	-45.50	0.049
SG -1.5% Sasobit®	77.96	74.56	-46.29	0.074
SG -0.5% Evotherm®	74.16	72.75	-44.88	0.031
SG -1.0% Evotherm®	75.56	73.26	-44.33	0.052
SG -1.5% Evotherm®	79.46	75.12	-38.14	0.114
SG -0.5% Perma-tac® Plus	77.00	74.34	-47.77	0.056
SG -1.0% Perma-tac® Plus	80.70	76.28	-45.93	0.096
SG -1.5% Perma-tac® Plus	81.08	76.20	-44.82	0.109

This may result in increased moisture-induced damage potential. Unlike Sasobit®, use of certain amounts of Evotherm® and Perma-tac®Plus-modified PG 64-22

asphalt binder with limestone aggregate result in an increase in ER values. For example, the use of 1.5% Evotherm[®] and Perma-tac[®]Plus-modified PG 64-22 asphalt binder with limestone aggregate results in ER values of 0.042 and 0.05 which are significantly larger than that of neat PG 64-22 asphalt binder with limestone aggregate (0.029). Also from Table 4.16 it was found that, use of granite with Sasobit[®], Evotherm[®] and Perma-tac[®]Plus-modified PG 64-22 asphalt binders result in increased ER value, compared to the neat asphalt binder case. For example use of 1.5% a Sasobit[®], Evotherm[®] and Perma-tac[®]Plus-modified PG 64-22 asphalt binder with granite aggregate results in ER values of 0.074, 0.114 and 0.109, respectively. This show an increasing ER trend in all cases compared to granite used with neat PG 64-22 asphalt binder with an ER value of 0.014.

Chapter

5

CONCLUSIONS AND RECOMMENDATIONS

Currently, there is no reliable test data available on Warm Mix Asphalt (WMA), in Oklahoma. This study was undertaken to generate laboratory test data, to help to promote the use of WMA technology in Oklahoma. Furthermore, relative performance of different WMA additives was evaluated through laboratory performance tests on asphalt mixes and mechanistic approach. This research was limited to laboratory evaluation of six types of WMA and control HMA mixes and mechanistic moisture-induced damage investigation of aggregates and asphalt binders with WMA additives. To this end, asphalt mixes consisting of three WMA mixes (one Advera$^®$ mix and two Evotherm$^®$ mixes) were collected and three HMA control mixes were produced for laboratory moisture-induced damage evaluation using Hamburg Wheel Tracking (HWT) and retained indirect Tensile Strength Ratio (TSR) tests. Also, the surface free energy (SFE) approach using a Universal Sorption Device (USD), a Wilhelmy Plate (WP) and a Sessile Drop (SD) device was applied to mechanistically evaluate the moisture-induced damage potential of combined aggregates and asphalt binders with different percentages of WMA additives. For this purpose, PG 64-22 OK asphalt binders, modified with different percentages of four selected WMA additives, namely Sasobit$^®$ Advera$^®$, Evotherm$^®$ and Perma-tac$^®$ Plus, were tested for SFE components. The SFE testing of asphalt binder was conducted using the Wilhelmy Plate and the Sessile Drop methods. Furthermore, different local aggregates including Snyder granite and Davis limestone from Oklahoma were tested for SFE evaluation using the Universal Sorption Device and the Sessile Drop test methods. The SFE components of other aggregates adopted from the literature were also incorporated in energy parameter evaluations with the tested local binders. It was found that there is a need for using mechanistic-based methods such as SFE (WP, USD, and SD) for characterization of moisture-induced damage, in addition to the existing empirical test methods (HWT and TSR). Findings of this study are expected to be useful to pavement professionals in understanding the moisture-induced damage mechanisms and designing WMA mixes.

Based on the test results obtained from different laboratory tests conducted on asphalt mixes, aggregates and binders and their analyses, the following conclusions were made:

- Based on the Hamburg Wheel Tracking test results, obtained from the tested WMA and control HMA mixes[1], ADHM, ADWM, EVHM-B, EVWM-B and EVHM-C mixes performed almost equally well against rutting. Also, none of the above mentioned mixes exhibited moisture-induced damage in the form of a stripping inflection point.

- Based on the Hamburg Wheel Tracking test results, among the tested WMA and control HMA mixes only the EVWM-C mix exhibited the stripping inflection point (SIP) with considerable rutting. Observed moisture-induced damage was attributed to possible incompatibility of the Evotherm® WMA additive and lime with the type of aggregates used in this mix.

- According to the retained indirect Tensile Strength Ratio (TSR) test results, only ADHM, EVHM-C and EVWM-C passed the minimum TSR requirement (0.75), and other mixes showed a lower TSR values, meaning they did not pass the TSR requirement.

- From the TSR and the Hamburg Wheel Tracking test results, it was concluded that these two tests can give contradictory results, as seen in the present study.

- From the TSR test results, it was observed that conditioned samples' fractured face rating parameter (which is more of a qualitative type measure) shows consistency with the Hamburg Wheel Tracking test results but is not in agreement with TSR values.

---

[1] ADHM = Control HMA mix corresponding to Advera® WMA mix; ADWM = Advera® WMA mix; EVHM-B = Control HMA mix corresponding to Evotherm® WMA Type-B mix; EVWM-B = Evotherm® WMA Type-B mix; EVHM-C = Control HMA mix corresponding to Evotherm® WMA Type-C mix; EVWM-C = Evotherm® WMA Type-C mix.

- It was observed that significant correlations exist between rut depths and inverse rutting ratios obtained from the Hamburg Wheel Tracking test and the indirect tensile strength test under dry condition.

- According to four-point bending beam fatigue test results, all of the HMA mixes showed a higher number of cycles to fatigue failure than their WMA counterparts.

Based on the SFE test results obtained from the Wilhelmy Plate apparatus and the Universal Sorption Device and conducted on asphalt binders and aggregates, respectively, the following conclusions were made:

- Sasobit® and Advera® additives were found to reduce the total SFE component of the asphalt binder. Evotherm®, on the other hand, increased the total SFE of the asphalt binder.

- Sasobit®, Advera® and Evotherm® increased the wettability of the asphalt binder over the aggregates, observed as an increase in the spreading coefficient. However, Evotherm® was found to cause a more signifincant increase in the spreading coefficient for all aggregates, specifically with gravel. This implies a better aggregate coating by asphalt binder.

- Sasobit®, Advera® and Evotherm® increased the work of adhesion of asphalt binder over the aggregates. Evotherm® was found to cause a more significant improvement in the work of adhesion for all aggregates, specifically for gravel. This may result in a more durable asphalt mix relative to moisture-induced damage potential.

- Sasobit®, Advera® and Evotherm® reduced the magnitude of work of debonding of the asphalt binders over the aggregates. Based on SFE test results, addition of Evotherm® was found to result in a more significant reduction in the magnitude of the work of debonding, and is expected to lower the moisture-induced damage potential of the mix.

- Works of adhesion to debonding ratios were used as indicators of the moisture-induced damage potential of the asphalt binder-aggregate

121

systems. Based on these indicators, Sasobit® and Advera® do not significantly increase or decrease the moisture-induced damage potential of the asphalt binder, over different aggregates. However, use of Advera®-modified asphalt binder with basalt results in a measurable decrease in moisture-induced damage potential of the mix. Based on the SFE test results, Evotherm® was observed to more effectively increase the resistance to moisture-induced damage, when compared to the other types of WMA additives, tested in this study.

Based on the SFE test results obtained from the Sessile Drop device, and conducted on asphalt binders and aggregates, the following conclusions were made:

- Since the use of Sessile Drop for SFE measurements of asphalt binder and aggregates is a new technique, the results from this method were compared with the literature. It was found that the measured contact angle results have acceptable standard deviations and the calculated SFE components were in agreement with those reported in the literature.

- The sample preparation and testing protocols for aggregates, neat asphalt binder and asphalt binder mixed with WMA additives were introduced. The sample preparation and testing processes were simple and did not need extensive training.

- As a result of polishing the aggregates with a finer grade polishing material (up to 1000 grade silicon carbide grits) before conducting Sessile Drop tests, the standard deviations of the measured contact angles decreased. Hence, an increase in the accuracy of the contact angles was observed.

- It was observed that, based on SD test results, the acidic components of tested aggregates and asphalt binders were almost negligible as opposed to their basic SFE components. However, from the USD test results, it was observed that acidic SFE components of aggregates and asphalt binders cannot be considered negligible, when compared with their basic SFE component.

- Using the energy ratio parameter, it was observed that the addition of WMA additives used in this study, namely Sasobit®, Evotherm®, and Perma-tac® Plus increased the resistance to the moisture-induced damage in almost all cases.

Based on a comparison of the SFE test results using Universal Sorption Device, Wilhelmy Plate test and Sessile Drop device conducted on asphalt binders and aggregates, the following conclusions are made:

- It was observed that the SFE components measured on aggregates with the Universal Sorption Device (USD) were significantly higher than those measured by the Sessile Drop (SD) device. This difference was attributed to different approaches used for calculation of SFE components for each test method. For example, spreading pressure (π_e) was introduced in calculation of SFE components, using USD test results (van Oss, 2002). However, π_e is not used in calculation of SFE components, when the contact angle is directly measured, using SD test.

- The comparison of the test results on asphalt binder, obtained from the Sessile Drop (SD) and the Wilhelmy Plate (WP) methods, revealed that the total SFE components calculated for the tested asphalt binder, using SD method are (approximately 3 times) higher than those, calculated using the results obtained from WP method. Furthermore, it was observed that the acidic SFE components of the asphalt binders, obtained from SD method, are (approximately 25 times) lower than their basic SFE components. However, it was found that the acidic SFE components of the asphalt binders, obtained from WP method, are (approximately 1.3 to 11 times) higher than their basic SFE components. The WP test results obtained from this study is confirmed by the pertinent literature (e.g. Buddhala et al., 2012; Wasiuddin et al., 2008; Bhasin et al., 2007).

Based on the test results and findings of this study, the following recommendations were made, for future study:

- o The aggregates and asphalt binders from different sources may have different chemical and SFE properties. Due to limited scope of this study one type of asphalt binder, limestone and granite aggregates were studied. Therefore, it is recommended that a study be conducted to investigate the influence of source of aggregates and asphalt binder on SFE-based moisture-induced damage potential of asphalt mixes.

- o It is recommended to investigate the compatibility of different additives (i.e., WMA additives, anti-stripping agents, lime, etc.) and asphalt binders with the type of the aggregates used in WMA mixes, against moisture-induced damage.

- o Long-term field measurements and observations of the rutting, moisture-induced damage potential and fatigue cracking of the pavement sections constructed with WMA is required for validation of the laboratory observations based on mix performance and SFE test results.

- o The existing minimum TSR requirement is recommended to be used in conjunction with a minimum dry indirect tensile strength requirement, as pass/fail criterion, in asphalt mix design. More field and laboratory test data are required for this task.

6.1 Technology Transfer

Technology transfer has occurred continuously during this project at a number of levels. First, a close collaboration for identification and collection of the WMA mixes was established between the OU research team and three paving companies, namely Austin Bridge and Road Inc., Ramming Pavement Co. and Century Asphalt Co., all based in Texas. Dr. Dar Hao Chen, from the Texas Department of Transportation assisted in arranging these site visits and material collection. The collection of the WMA mixes Texas was due to the fact that, the research team was not able to locate any Oklahoma-based company which produces WMA mixes. This means that, Oklahoma is behind in terms of using various WMA technologies. This has to change and this study is an effort in this direction. Secondly, a presentation titled "*Warm Mix Asphalt in Oklahoma Moisture Damage and Performance Issues,*" was made during the visit of ODOT Personnel to the University of Oklahoma on June 22, 2011. Furthermore, an invited lecture on "*Green Paving Technology,*" was made to a group of about 35 individuals representing K-12 Middle School Teachers in Oklahoma on June 16, 2011. This project was also helpful in terms of receiving additional external founds from Oklahoma Department of Transportation (ODOT)/ Federal Highway Administration (FHWA) through two research projects: (i) Fatigue Performance of Asphalt Pavements Containing RAS and RAP (SP&R Item Number: 2245), which focuses on recycling and implementation of green pavements, and (ii) Recommended Fatigue Test for Oklahoma Department of Transportation (SP&R Item Number: 2243).

6.2 Journal and Proceeding Papers

The scale and breadth of this project have drawn national and international attention. The research team has published/submitted 3 journal articles, 3 proceedings papers, and made 5 platform and 5 poster presentations. Furthermore, the test data from this project are integral part of a Master's thesis and a Ph.D. dissertation. The publication records of the research team related to the project are listed below:

6.2.1 Referred Journal Papers

- Ghabchi, R., Singh, D., Zaman, M. and Tian, Q. (2013). "Mechanistic Evaluation of Effect of WMA-Additives on Wettability and Moisture Susceptibility Properties of Asphalt Mixes," Journal of Testing and Evaluation, Vol. 41, No. 6, pp. 1-10.

- Koc, M. and Bulut, R. (2013). Assessment of a New Device and Testing Approach for Measuring Contact Angles on Aggregates and Asphalt Binders. ASCE Journal of Materials in Civil Engineering (In Press).

- Koc, M. and Bulut, R. (2012). Surface Free Energy Components of Aggregates from Contact Angle Measurements Using Sessile Drop Method, Advances in Transportation Geotechnics II, Miura et al. (eds), Taylor & Francis Group, Digital Media (6 pages).

6.2.2 Referred Conference Papers

- Ghabchi, R., Singh, D., Zaman, M., and Tian, Q. (2013). "A Laboratory Study of Warm Mix Asphalt for Moisture Damage Potential Using Surface Free Energy Method," ASCE Airfield and Highway Pavement 2013 Conference, June 9-12, 2013, Los Angles, CA. Compendium of Papers CD-ROM, pp. 54-63.

- Ghabchi, R., Singh, D., Zaman, M., and Tian, Q. (2013). "Application of Surface Free Energy Method for Moisture Susceptibility Evaluation of Asphalt Mixes" 2nd Conference of Transportation Research Group of India (CTRG), 12-15 December, 2013, Agra, India (under review).

- Koc, M. and Bulut, R. (2012). "Initial Assessment of a New Device & Testing Method for Measuring Contact Angles on Aggregates," Transportation Research Board, TRB 91st. Annual Meeting Compendium of Papers CD-ROM, National Research Council, Washington, D.C.

6.2.3 Posters

- Ghabchi, R., Singh, D., Tian, Q., Koc, M., Bulut, R., Zaman, M., and Cross, S. (2012). "Moisture Susceptibility Evaluation of Warm Mix Asphalt", ODOT-OkTC Transportation Research Day 2012, Oklahoma city, OK, October 4, 2012.

- Koc, M. and Bulut, R. (2012). "Initial Assessment of a New Device & Testing Method for Measuring Contact Angles on Aggregates," Transportation Research Board, TRB 91ST Annual Meeting Compendium of Papers CD-ROM, National Research Council, Washington, D.C.

- Ghabchi R., Singh D., Tian Q., Zaman M. (2012). "Mechanistic Approach for Evaluation of Moisture Damage Potential of Green Pavement Technologies," ASCE GeoCongress 2012, Oakland, CA, March 25-29, 2012.

- Ghabchi R., Tian Q., Singh D., Zaman M. (2012). "Environmentally Friendly Asphalt Technologies for Pavement Applications: Advantages and Technical Challenges," Student Research and Performance Day, Graduate College, National Weather Center, University of Oklahoma, Norman, OK, March 2, 2012.

- Ghabchi R., Tian Q., Singh D., Zaman M., Bulut R., Cross S. (2011). "Green Pavement Technology: Warm Mix Asphalt Moisture Susceptibility Evaluation Using Surface Free Energy Approach," ODOT-OkTC Research Day 2011, Oklahoma Department of Transportation, Oklahoma City, OK, October 11, 2011.

6.2.4 Presentations

- Ghabchi, R., Singh, D., Zaman, M., and Tian, Q. (2013). "A Laboratory Study of Warm Mix Asphalt for Moisture Damage Potential Using Surface Free Energy Method," ASCE Airfield and Highway Pavement 2013 Conference, Los Angeles, CA, June 9-12, 2013,

- Ghabchi, R., Singh, D., Zaman, M., and Tian, Q. (2013). "Application of Surface Free Energy Method for Evaluation of Moisture Susceptibility of Warm Mix Asphalt," OkTC First Annual Hearthand Transportation Consortium, Oklahoma city, OK, April 2-4, 2013,

- Koc, M. and Bulut, R.(2012). "Surface Free Energy Components of Aggregates from Contact Angle Measurements Using Sessile Drop Method," 2nd International Conference on Transportation Geotechnics (IS-Hokkaido 2012), Sapporo, Japan, September 10-12, 2012.

- Koc, M. and Bulut, R. (2012). "Initial Assessment of a New Device & Testing Method for Measuring Contact Angles on Aggregates," Transportation Research Board, TRB 91ST Annual Meeting, National Research Council, Washington, D.C., January 22-26, 2012.

- Ghabchi R., Tian Q., Zaman M. (2011). "Warm Mix Asphalt in Oklahoma Moisture Damage and Performance Issues," Oklahoma Department of Transportation Planning and Research Division Visit, The University of Oklahoma, School of Civil Engineering and Environmental Science, Norman, OK, June 22, 2011.

6.2.5 Thesis/Dissertation

Koc, M. (2013). "Development of Testing Protocols for Direct Measurements of Contact Angles on Aggregate and Asphalt Binder Surfaces Using a Sessile Drop Device." M.Sc. Thesis, Oklahoma State University, Stillwater, Oklahoma.

Ghabchi, R., "Laboratory Characterization of Recycled and Warm Mix Asphalt for Enhanced Pavement Applications," Ph. D. Dissertation, Department of Civil Engineering and Environmental Science, the University of Oklahoma, Norman, Oklahoma, 2014 (Expected), in Preparation.

1. AASHTO (2010). "Standard Specifications for Transportation Materials and Methods of Sampling and Testing," Part 2A and Part 2B: Test, 27th Edition.

2. AASHTO T283, (2010). "Standard Method of Test for Resistance of Compacted Hot Mix Asphalt (HMA) to Moisture-Induced Damage."

3. AASHTO T321, (2010). "Standard Method of Test for Determining the Fatigue Life of Compacted Hot-Mix Asphalt (HMA) Subjected to Repeated Flexural Bending."

4. Adamson, A.W., and Gast, A.P. (1997). "Physical Chemistry of Surfaces", 6th ed., John Wiley and Sons, New York.

5. American Road & Transportation Builders Association (2012). "Transportation and General Public F.A.Q.". Retrieved October 14, 2012, from http://www.artba.org.

6. Arabani, M., and Hamedi, Gh. H. (2011). "Using the Surface Free Energy Method to Evaluate the Effects of Polymeric Aggregate Treatment on Moisture Damage in Hot Mix Asphalt," Journal of Materials in Civil Engineering, Vol. 23, No. 6, pp. 802–818.

7. Arabani, M., Roshani, H., and Hamedi, Gh. H. (2012). "Estimating Moisture Sensitivity of Warm Mix Asphalt Modified with Zycosoil as an Antistrip Agent Using Surface Free Energy Method," Journal of Materials in Civil Engineering, Vol. 24, No. 7, pp. 889–897.

8. Bargir, S., Dunn, S., Jefferson, B., Macadam, J., Parsons, S. (2009). "The Use of Contact Angle Measurements to Estimate the Adhesion Propensity of Calcium Carbonate to Solid Substrates in Water," Applied Surface Science, Vol. 255, No. 9, pp. 4873-4879.

9. Bhasin, A., (2006). "Development of Methods to Quantify Bitumen-Aggregate Adhesion and Loss of Adhesion Due to Water," Ph.D. Dissertation, Texas A&M University, College Station, Texas.

10. Bhasin, A., and Little, D. N. (2007). "Characterization of Aggregate Surface Energy Using the Universal Sorption Device," Journal of Materials in Civil Engineering, Vol. 19, No. 8, pp. 634-641.

11. Bhasin, A., Masad, E., Little, D., and Lytton, R. (2006). "Limits on Adhesive Bond Energy for Improved Resistance of Hot Mix Asphalt to Moisture Damage," Transportation Research Record, No. 1970, pp. 3-13.

12. Bhasin, A., Little, D. N., Vasconcelos, K. L., and Masad, E. (2007). "Surface Free Energy to Identify Moisture Sensitivity of Materials for Asphalt Mixes," Transportation Research Record, Vol. 2001, pp. 37-45.

13. Bistor, B. (2009). "A Tale of Two Mixes," Presentation at WMA Technical Working Group Meeting, December 15-16, 2009, 17620 International Blvd, Seattle, WA, 98188.

14. Buddhala, A., Hossain, Z., Wasiuddin, N. M., and Zaman, M. (2011). "Effects of an Amine Anti-Stripping Agent on Moisture Susceptibility of Sasobit and Aspha-Min Mixes by Surface Free Energy Analysis," Journal of Testing and Evaluation, Vol. 40, No. 1, pp. 1-9.

15. Button, J. W., Estakhri, C., and Wimsatt, A. (2007). "A Synthesis of Warm Mix Asphalt," Report FHWA/TX-07/0-5597-1, Texas Transportation Institute, College Station, TX.

16. Chaudhury, M.K. (1984). "Short Range and Long Range Forces in Colloid and Macroscopic Systems," Ph.D. Dissertation, SUNY, Buffalo.

17. Cheng, D. (2002). "Surface Free Energy of Asphalt-Aggregate Systems and Performance Analysis of Asphalt Concrete Base on Surface Free Energy," Ph.D. Dissertation, Texas A&M University, College Station, Texas.

18. Cheng, D., Little, D.N., Lytton, R.L. and Holste, J. (2002). "Use of Surface Free Energy Properties of the Asphalt- Aggregate System to Predict Moisture Damage

Potential." Journal of the Association of Asphalt Paving Technologists, AAPT, Vol.71, pp. 59-88.

19. Corrigan, M. (2011)."Warm Mix Asphalt Technologies and Research," Federal Highway Administration, http://www.fhwa.dot.gov/pavement/asphalt/wma.cfm. (Last accessed July 2012).

20. Costanzo, P. M., Wu, W., Giese, R. F., & van Oss, C. J. (1995). "Comparison between Direct Contact Angle Measurements and Thin Layer Wicking on Synthetic Monosized Cuboid Hematite Particles." Langmuir, Vol. 11, No. 5, pp. 1827-1830.

21. Curtis, C.W., Perry, L.M. and Brannan C.J. (1991). "Investigation of Asphalt-Aggregate Interactions and Their Sensitivity to Water." VTI Report 372A, Part 4. Swedish National Road and Transport Research Institute.

22. D'Angelo, J., Harm, E., Bartoszek, J., Baumgardner, G., Corrigan, M., Cowsert, J., Harman, T., Jamshidi, M., Jones, W., Newcomb, D., Prowell, B., Sines, R., and Yeaton, B. (2008). "Warm-Mix Asphalt: European Practice," Report FHWA-PL-08-007, American Trade Initiatives, Alexandria, VA.

23. Eustathopoulos, N.; Nicholas, M.G. and Drevet B. (1999). "Wettability at High Temperatures." Oxford, UK: Pergamon. ISBN 0-08-042146-6.

24. Extrand, C. W. (2003). "Contact Angles and Hysteresis on Surfaces with Chemically Heterogeneous Islands". Langmuir, Vol.19, No. 9, pp. 3793-3796.

25. Fowkes, F. M. (1964). "Attractive forces at interface," Ind. Eng. Chem., Vol. 56, No. 12, pp. 40-52.

26. Fowkes, F.M. (1963). "Additivity of intermolecular forces at interfaces. I. Determination of the contribution to surface and interfacial tensions of dispersion forces in various liquids," Journal of Physical Chemistry, Vol. 67, pp. 2538-2541.

27. Fowkes, F.M. (1987). "Role of Acid-Base Interfacial Bonding in Adhesion." Journal of Adhesion Science and Technology, Vol. 1, No. 1, pp. 7-27.

28. Ghabchi, R., Singh, D., Zaman, M. and Tian, Q. (2013). "Mechanistic Evaluation of Effect of WMA-Additives on Wettability and Moisture Susceptibility Properties of Asphalt Mixes," Journal of Testing and Evaluation, Vol. 41, No. 6, pp. 1-10.

29. Ghabchi, R., Singh, D., Zaman, M., and Tian, Q. (2013). "A Laboratory Study of Warm Mix Asphalt for Moisture Damage Potential Using Surface Free Energy Method," ASCE Airfield and Highway Pavement 2013 Conference Compendium of Papers CD-ROM, pp. 54-63.

30. Giese Jr., R. F., Wu, W., and Oss, C. V. (1996). "Surface and Electrokinetic Properties of Clays and Other Mineral Particles, Untreated and Treated with Organic or Inorganic Cations." Journal of Dispersion Science and Technology, Vol. 17, No. 5, pp. 527-547.

31. Giese, R.F. and van Oss, C.J. (2002). "Colloid and Surface Properties of Clays and Related Materials," Marcel Dekker, Inc., New York.

32. Girifalco, L.A. and R.J. Good. (1957). "A Theory for Estimation of Surface and Interfacial Energies. I. Derivation and Application to Interfacial Tension," Journal of Physical Chemistry, Vol. 61, pp. 904-909.

33. Goh., S. W., and You, Z. (2012). "Mechanical Properties of Porous Asphalt Pavement Materials with Warm Mix asphalt and RAP," Journal of Transportation Engineering, Vol. 138, No.1, pp. 90-97.

34. Good, R. J., and van Oss, C. J. (1991). "The Modern Theory of Contact Angles and the Hydrogen Bond Components of Surface Energies," Plenum Press, New York, NY.

35. Good, R. J. (1992) "Contact Angle, Wetting and Adhesion: A Critical Review," Journal of Adhesion Science and Technology, Vol. 6, No.12, pp. 1269-1302.

36. Good, R.J. (1966). "Physical Significance of Parameters γc, γs, and Φ that Govern Spreading on Adsorbed Films," S. C. I. Monograph, Vol. 25, No. 25, pp. 328-350.

37. Groszek, A. J. (1962). "Preferential Adsorption of Normal Hydrocarbons on Cast Iron," Nature, Vol. 196, pp. 531-533.

38. Gugliotti, M. (2004). "Tears of Wine," Journal of Chemical Education, Vol. 81, No. 1, pp. 67-68.

39. Hefer, A.W., Bhasin, A., and Little, D.N. (2006). "Bitumen Surface Energy Characterization Using Contact Angle Approach." ASCE Journal of Materials in Civil Engineering, Vol. 18, No.6, pp. 759-767.

40. Holmberg, K. (2002). "Handbook of Applied Surface and Colloid Chemistry," Wiley and Sons, New York.

41. Hossain, Z., Bhudhala, A., Zaman, M., O'Rear, E., Cross, S., and Lewis, S. (2009). "Evaluation of the Use of Warm Mix Asphalt as a Viable Paving Material in the United States," Research Report, Federal Highway Administration, Turner-Fairbank Highway Research Center, Virginia.

42. Hossain Z., Zaman, M., O'Rear, E. A., and Chen. D.H. (2011). "Effectiveness of Advera in Warm Mix Asphalt," ASCE GeoHunan 2011 GSP 218, Hunan, China, June 9-11, 2011.

43. Howson, J., Masad, E.A, Bhasin, A., Branco, V.C., Arambula, E., Lytton, R., and Little, D. (2007). "System for the Evaluation of Moisture Damage Using Fundamental Material Properties," TxDOT Report Number 0-4524-2. FHWA, Texas Transportation Institute, Texas A&M University, College Station, Texas.

44. Hurley, G. C., and Prowell, B. D. (2006). "Evaluation of Evotherm® for Use in Warm Mix Asphalt," NCAT Report 06-02, National Center for Asphalt Technology, Auburn, Ala., June 2006.

45. Hurley, G. C., and Prowell, B. D. (2005). "Evaluation of Sasobit for use in warm mix asphalt," NCAT Report 05-06, National Center for Asphalt Technology, Auburn, AL.

46. Hurley, G., Prowell, B., and Kvasnak, A. (2010). "Wisconsin Field Trial of Warm Mix Asphalt Technologies: Construction Summary," NCAT Report 10-04, National Center for Asphalt Technology, Auburn, AL.

47. Kanitpong, K. and Bahia, H.U. (2005). "Relating Adhesion and Cohesion of Asphalts to the Effects of Moisture on Laboratory Performance of Asphalt

Mixtures," Transportation Research Record No. 1901, Transportation Research Board, Washington, D.C., pp. 33-43.

48. Kanitpong, K., Nuttaporn, C., and Suched, L. (2012). "Investigation on the effects of gradation and aggregate type to moisture damage of warm mix asphalt modified with Sasobit." International Journal of Pavement Engineering, Vol. 13, No. 5, pp. 451-458.

49. Kim, Y. R., Little, D. N., and Lytton, R. L. (2004). "Effect of Moisture Damage on Material Properties and Fatigue Resistance of Asphalt Mixtures," Transportation Research Record, Vol. 1891, pp. 48-54.

50. Kvasnak, A. N., and West, R. C. (2009) "Case Study of Warm-Mix Asphalt Moisture Susceptibility in Birmingham, Alabama," Transportation Research Board 88th Annual Meeting. No. 09-3703.

51. Little, D. N. , and Bhasin, A. (2006). "Using Surface Energy Measurements to Select Materials for Asphalt Pavements," NCHRP Project No. 9-37, Draft Final Report (submitted to NCHRP), Texas Transportation Institute, College Station, Texas.

52. Lobato, E.M.C. (2004)"Determination of Surface Free Energies and Aspect Ratio of Talc," Ms. Thesis, Virginia Polytechnic Instute and State University, Blacksburg, Virginia.

53. Lu, Q. and Harvey, J.T. (2008). "Investigation of Conditions for Moisture Damage in Asphalt Concrete and Appropriate Laboratory Test Methods," Research Report No.: UCPRC-RR-2005-15, California Department of Transportation.

54. Lytton, R.L., Masad, E., Zollinger, C., Bulut, R., and Little, D.N. (2005). "Measurement of Surface Energy and Its Relationship to Moisture Damage," TxDOT Report Number 0-4524-2. FHWA, Texas Transportation Institute, Texas A&M University, College Station, Texas.

55. Masad, E., Zollinger, C., Bulut, R., Little, D.N., and Lytton, R.L. (2006). "Characterization of Moisture Damage Using Surface Energy and Fracture

Material Properties," Journal of the Association of Asphalt Paving Technologists, AAPT, Vol. 75, pp. 713-732.

56. NAPA (2007). "Warm Mix Asphalt the Wave of the Future," Online, National Asphalt Pavement Association, Landham, MD. http://www.warmmixasphalt.org, Last Accessed Feb. 2012.

57. NAPA (2011). "Mix Production Survey Reclaimed Asphalt Pavement, Reclaimed Asphalt Shingles, Warm-mix Asphalt Usage: 2009-2010," Technical Report, National Asphalt Pavement Association, Washington, DC.

58. ODOT (2009). "Standard Specification for Highway Construction," Online, Oklahoma Department of Transportation, http://www.okladot.state.ok.us/officeeng/specbook/2009specbook.pdf, Last Accessed: Feb. 2012.

59. ODOT (2010). "OHD L-55, Method of Test for Hamburg Rut Testing of Compacted Hot-Mix Asphalt (HMA)." Material and Testing e-Guide, Department Test Methods (OHDL), http://www.okladot.state.ok.us/materials/pdfs-ohdl/ohdl55.pdf. Accessed January 20, 2013.

60. Petrucci, R.H., Harwood, W.S., Herring, G.E., and Madura, J. (2007). "General Chemistry: Principles & Modern Applications." Prentice Hall, Upper Saddle River, New Jersey.

61. Pinto, I., Kim, Y.K., and Ban, H. (2009). "Moisture Sensitivity of Hot-Mix Asphalt (HMA) Mixtures in Nebraska – Phase II." NDOR Research Project Number: MPM-04, Nebraska Department of Roads.

62. Prowell, B. D., and Hurley, G. C. (2007). "Warm- Mix Asphalt: Best Practices," Quality Improvement Series 125, National Asphalt Pavement Association, Lanham, MD.

63. Prowell, B. D., Hurley, G. C. and Crews, E. (2007). "Field Performance of Warm Mix Asphalt at the NCAT Test Track," Transportation Research Record, Vol. 1998, pp. 96-102.

64. Rulison, C. (1996). "So you Want to Measure Surface Energy?" KRÜSS technical note TN306e.

65. Shang, J., Flury, M., Harsh, J.B., Zollars, R.L. (2008). "Comparison of Different Methods to Measure Contact Angles of Soil Colloids," Journal of Colloid and Interface Science, Vol. 328, Issue 2, pp. 299-307.

66. Sharfrin, E., Zisman, William A. (1960). "Constitutive relations in the wetting of low energy surfaces and the theory of the retraction method of preparing monolayers," The Journal of Physical Chemistry, Vol. 64, No. 5, pp. 519–524.

67. Tarrer, A. R., and Wagh, V. (1991). "The Effect of the Physical and Chemical Characteristics of the Aggregate on Bonding," Strategic Highway Research Program, SHRP-A/UIR-91-507.

68. U.S. Department of Transportation, Federal Highway Administration, Highway Statistics, Washington, D.C. http://www.bts.gov/publications/national_transportation_statistics. Accessed October 14, 2012.

69. van Oss, C.J. (2002). "Use of the Combined Lifshitz-van der Waals and Lewis Acid-base Approaches in Determining the Apolar Contributions to Surface and Interfacial Tensions and Free Energies," Journal of Adhesion Science and Technology, Vol. 16, pp. 669-677.

70. Van Oss, C.J., Chaudhury, M.K, Good, R.J. (1988). "Interfacial Lifshitz-van der Waals and Polar Interactions in Macroscopic Systems," Chemical Reviews, Vol. 88, pp. 927-941.

71. van Oss, C.J., Chaudhury, M.K., and Good, R.J. (1987). "Monopolar surfaces," Journal of Protein Chemistry, Vol. 5, pp. 385-405.

72. van Oss, C.J. (1994). "Interfacial Forces in Aqueous Media," Marcel Dekker, Inc., New York.

73. van Oss, C.J. (2002). "Use of the Combined Lifshitz-van der Waals and Lewis Acid-base Approaches in Determining the Apolar Contributions to Surface and

Interfacial Tensions and Free Energies," Journal of Adhesion Science and Technology, Vol. 16, pp. 669-677.

74. Wasiuddin, N. M. (2007) "Effect of Additives on Surface Free Energy Characteristics of Aggregate and Binders in Hot Mix Asphalt," Ph.D. Dissertation, University of Oklahoma, Norman, OK.

75. Wasiuddin, N. M., Fogle, C. M., Zaman, M. M., and O'Rear, E. A. (2007). "Effectof Anti-Strip Additives on Surface Free Energy Characteristics of Asphalt Binders for Moisture-Induced Damage Potential," Journal of Testing and Evaluation, Vol. 35, No. 1, pp. 36-44.

76. Wasiuddin, N. M., Zaman, M. M., and O'Rear, E. A. (2008). "Effect of Sasobit® and Aspha-Min® on wettability and adhesion between asphalt binders and aggregates," Transportation Research Record, No. 2051, pp. 80–89.

77. WSDOT (2008). "Standard Specifications for Road, Bridge, and Municipal Construction 2008," Online, Wisconsin State Department of transportation, http://www.wsdot.wa.gov/publications/manuals/fulltext/M41-10/SS2008.pdf, Last Accessed: Feb. 2012.

78. Wu, S., (1982). "Interfacial Thermodynamics in Polymer Interface and Adhesion." Marcel Dekker, New York.

79. Xiao, F., Jordan, J., and Amirkhanian, S. N. (2009). "Laboratory investigation of moisture damage in warm-mix asphalt containing moist aggregate," Transportation Research Record: Journal of the Transportation Research Board, Vol. 2126, pp. 115-124.

80. Xiao, F., Amirkhanian, S. N., and Putman, B. (2010). "Evaluation of rutting resistance in warm mix asphalts containing moist aggregate," Transportation Research Record, Vol. 2180, No. 2, Transportation Research Board, Washington, DC, pp. 75-84.

81. Yildirim, I. (2001). "Surface Free Energy Characterization of Powders," Ph.D. Dissertation, Virginia Polytechnic Institute and State University, Blacksburg, Virginia.

82. Yildirim, I., Jayawickrama, P. W., Hossain, M. S., Alhabshi, A., Yildirim, C., Smit, A. D. F., and Little, D. (2007). "Hamburg wheel-tracking database analysis" (No. FHWA/TX-05/0-1707-7). Texas Transportation Institute, The Texas A&M University System.

83. You, Z., Goh, S. W., and Dai, Q. (2011). "Laboratory Evaluation of Warm Mix Asphalt," Report No. RC-1556, Michigan Department of Transpiration Construction Paving Unit – C&T Secondary Governmental Complex, 8885 Ricks Road, Lansing, MI 48909.

84. Zettlemoyer, A. C. (1969). "Hydrophobic surfaces: in Hydro- phobic Surfaces," Academic Press, New York, NY, pp. 1-26.
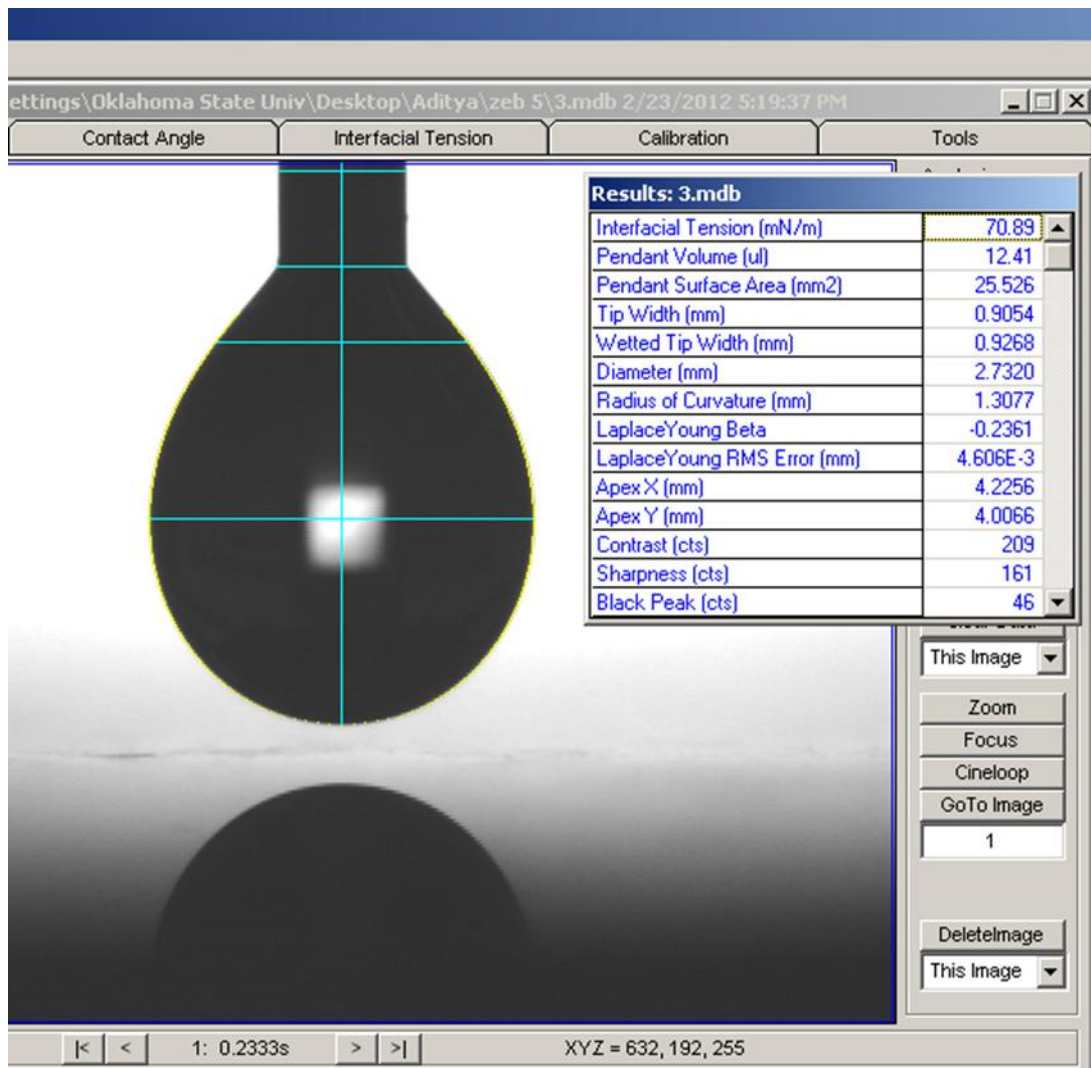
APPENDIX A

Calibration of Sessile Drop Device

The FTA 1000 was employed to measure contact angles on both aggregates and asphalt binder. The device includes a high resolution camera which takes pictures of the samples with the sessile drop dispensed from the needle and sends them to the software in order to be processed. The magnification has to be adjusted to get better snapshots of liquid-solid interface. The qualities of these pictures directly affect the precision of the contact angles calculated by the FTA software. Focus, image clarity, and isolation from mechanical vibration can cause inaccurate contact angle results. To achieve more precise results, the device was calibrated by the procedure given below.

In this example, distilled water was used as the probe liquid. About 12 µL of distilled water was dispensed as pendant drop. The snapshots of the drop were taken and sent to the software. Certain physical parameters of the drop such as volume, diameter, radius of curvature, and interfacial tension were measured by the software. The actual value of interfacial tension (IFT) of the water is 72.00 mN/m at the room temperature. However as it can be seen in Figure A.1, the device measured 70.89 mN/m before the calibration.

The calibration can be done in three different ways (see Figure A.2). In this study, the calibration of the device was done by matching the actual and measured IFT values. Once these values are entered, the calibration is done by clicking the apply button. The differences in the results are shown in Figure A.3. The physical parameters of the pendant drop are now closer to the actual values. To illustrate it quantitatively, the pendant volume has increased from 12.41 µL to 12.70 µL after the magnification of the FTA device was calibrated. These differences in the readings of physical parameters of the pendant drop have a direct impact on contact angle values.

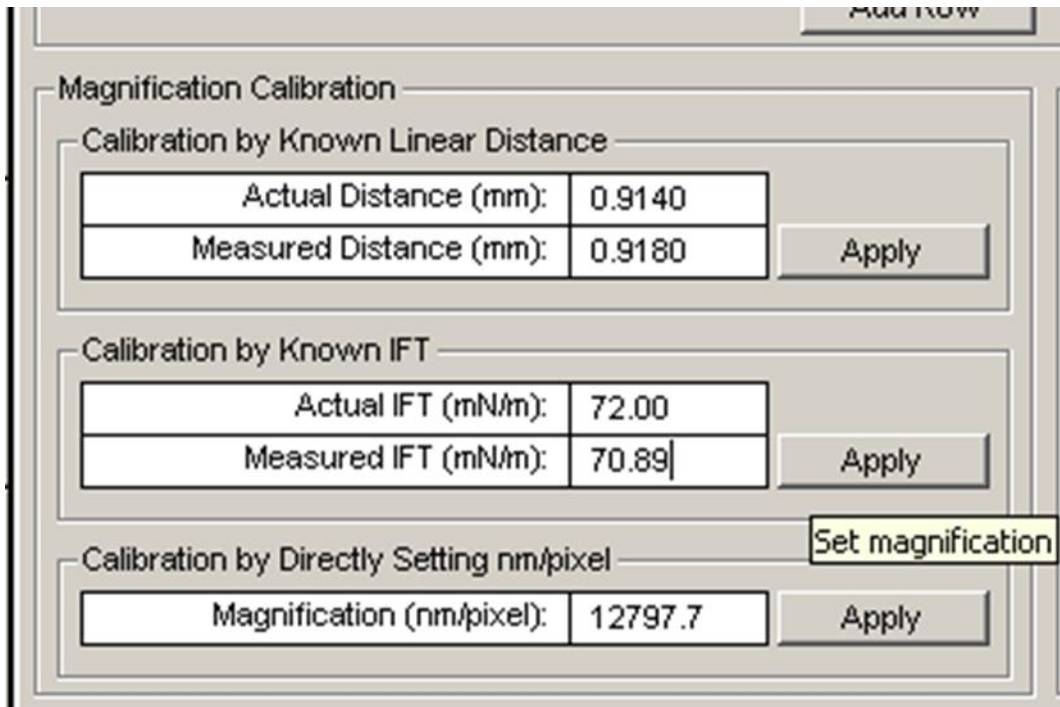**Figure A. 1 IFT Results Before Calibration**
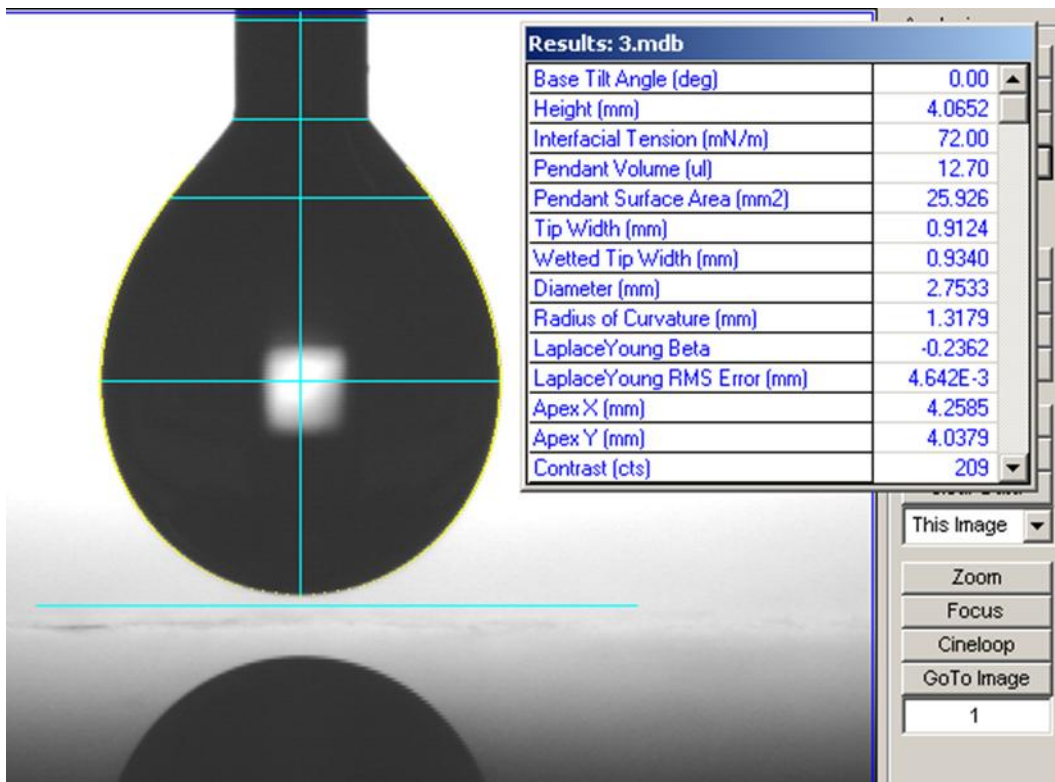
Figure A. 2 IFT Calibration Software Dialog Box

Figure A. 3 IFT Results After Calibration

APPENDIX B

Contact Angle Test Results with the Final Testing Protocol

Table B. 1 Final Contact Angle Results with PG 64-22 Neat Asphalt Binder

PG 64-22	Contact Angle (Deg)		
Trial Number	Ethylene Glycol	DIM	Water
1	68.5	48.0	93.0
2	70.5	47.5	92.0
3	69.0	46.0	94.0
4	73.5	49.0	94.5
5	73.5	50.0	91.5
6	68.0	47.5	93.0
Std. Dev.	2.5	1.4	1.1
Average	70.5	48.0	93.0

Table B. 2 Final Contact Angle Results on Aggregate Samples with Distilled Water

Distilled Water	Contact Angle (Deg)			
Sample	Set-1	Set-2	Set-3	Average
Davis Limestone	79.6	78.1	80.4	79.4
Snyder Granite	74.5	73.5	75.8	74.6

Table B. 3 Final Contact Angle Results on Aggregate Samples with Diiodomethane

Diiodomethane	Contact Angle (Deg)			
Sample	Set-1	Set-2	Set-3	Average
Davis Limestone	47.1	47.7	44.5	46.4
Snyder Granite	50.4	49.5	49.5	49.8

Table B. 4 Final Contact Angle Results on Aggregate Samples with Ethylene Glycol

Ethylene Glycol	Contact Angle (Deg)			
Sample	Set-1	Set-2	Set-3	Average
Davis Limestone	60.5	63.4	61.3	61.7
Snyder Granite	56.8	59.6	59.5	58.6

Table B. 5 Contact angle results on PG 64-22 neat binder with Distilled Water

Distilled Water	Contact Angle (Deg)		
Trial Number	Set-1	Set-2	Set-3
1	93.0	94.5	95.0
2	88.0	92.0	94.5
3	92.0	95.0	93.0
4	91.5	93.0	94.0
5	89.5	91.5	91.5
6	92.5	93.0	93.5
7	88.0	92.5	90.0
8	85.0	89.0	89.5
9	87.5	92.5	90.5
10	81.0	94.0	91.0
11	86.5	95.5	91.5
12	82.0	94.0	88.0
13	87.5	92.5	92.5
14	90.0	93.0	93.0
Std. Dev.	3.7	1.6	2.0
Average	88.1	93.0	92.0

Table B. 6 Contact Angle Results on PG 64-22 Neat Binder with Diiodomethane

Diiodomethane	Contact Angle (Deg)		
Trial Number	Set-1	Set-2	Set-3
1	46.0	48.0	47.0
2	46.0	47.5	49.5
3	44.5	46.0	50.0
4	47.0	49.0	51.0
5	48.0	50.0	47.5
6	45.0	47.5	45.5
7	47.0	48.0	48.0
8	44.0	47.0	50.5
9	43.5	47.5	51.0
10	43.0	46.5	51.0
11	46.0	47.0	49.0
12	44.0	49.5	48.5
13	42.0	50.5	50.0
14	41.0	51.0	52.0
Std. Dev.	2.0	1.5	1.8
Average	44.8	48.2	49.3

Table B. 7 Contact Angle Results on PG 64-22 Neat Binder with Ethylene Glycol

Ethylene Glycol	Contact Angle (Deg)		
Trial Number	Set-1	Set-2	Set-3
1	78.5	68.5	76.5
2	83.5	70.5	76.5
3	79.5	69.0	74.0
4	85.0	73.5	72.5
5	84.0	73.5	75.5
6	80.0	68.0	77.0
7	75.5	70.0	78.0
8	75.0	72.5	79.5
9	76.0	70.5	76.0
10	74.5	73.0	75.0
11	75.5	71.0	73.5
12	73.5	68.0	72.0
13	71.0	68.5	71.0
14	66.0	70.0	69.0
Std. Dev.	5.2	2.0	2.9
Average	77.0	70.5	74.7